Drivers of root and fungal litter decomposition: implications for soil carbon cycling

A DISSERTATION

SUBMITTED TO THE FACULTY OF THE

UNIVERSITY OF MINNESOTA

BY

Craig Robert See

IN PARTIAL FULFILLMENT OF THE REQUIREMENTS

FOR THE DEGREE OF

DOCTOR OF PHILOSOPHY

Dr. Sarah E. Hobbie and Dr. Peter G. Kennedy

May 2021

Acknowledgments

This work would not be possible without the emotional support, dedication, and mentorship of an incredibly large group of people. The following is an abbreviated list.

I would like to thank my advisors Sarah Hobbie and Peter Kennedy for providing me with all I needed to flourish as a graduate student (advice, resources, patience). Additionally, I would like to thank my committee members Jess Gutknecht and Peter Reich. I am beyond grateful for the sheer volume off science conversations I had with my extended lab family: Adrienne Keller, Lotus Lofgren, Chris Fernandez, Luke McCormack, Lang Delancey, Allison Gill, Melissa Pastore, Erin Mittag, Chris Walter, Tao Sun, Megan Wilcots, Rachel King, Claire Kazanski, Lauren Cline, Ashley Keiser, Francois Maillard, Talia Michaud, Eduardo Perez-Pazos, Nishia Nieves, YueHua Hu.

I owe a lot to the wonderful and unique group of individuals in my cohort: Amod Zambre, Sarah Hammarlund, Sam Weaver, Tony Massaro, Saumya Gupta, Sarah Huebner, Erin Mittag, Amanda Muelbauer, Naomi Rushing. I am also deeply indebted to the individuals at Cedar Creek, who I have known now for over 10 years: Troy, Kally, Mark, Pam, John and Jim.

Additional thanks to a number of mentors/collaborators/friends: Jennifer Pett-Ridge, Hanan Farah, Alex Strauss, Ruth Yanai, John Campbell, Mark Green, Jennifer Knoepp, Tim Fahey, Laura Toro-Gonzalez, German Vargas, Kate Heckman, Shinjini Goswami, Matt Vadeboncoeur Jake Grossman, Reb Bryant, Leno Smith, Shan Kothari, Cristy Portales, Steve Blazewicz, Anita Krause, Tom Ramoski, George Furey, Mayank Kohli, Kaitlin Kimmel, Kaitlin Troung, Anna Conley, Rachel Hestrin, Sue Pierre

A sincere thank you to my funding sources: EEB, Department of Energy SCGSR, Geri Nelson Grant, UMN Doctoral Dissertation Fellowship, the Carolyn Crosby Grant, the Minnesota Mycological Society, and the Sitka Center for Art and Ecology for providing me with a wonderful workspace.

Dedication

To my parents Bob See and Arlene Craig. Thanks for everything.

Table of Contents

List of Tables

List of Figures

Introduction

Humans have drastically altered the world's carbon (C) cycle through the consumption of fossil fuels and changes in land use. Since the start of the industrial revolution, anthropogenic emissions have more than doubled the concentration of CO_2 in the atmosphere, which has destabilized the earth's climate system. Importantly, the earth's ecosystems have acted as a C sink during this time, removing approximately half of human emissions from the atmosphere on an annual basis (Le Quéré et al., 2016). Soils are a particularly important to C storage terrestrial systems, and globally contain more C than vegetation and the atmosphere combined. Thus, relatively small changes to the rate of C exchange between soils and the atmosphere have the potential to substantially impact the earth's climate. Despite its clear importance, estimates of soil C storage, as well as the rate of C inputs and losses to this pool remain highly uncertain in the global C budget.

Carbon dioxide (CO_2) release due to decomposition is the dominant form by which C is lost from soils, though some losses also occur due to leaching of dissolved and particulate C in soil solution (Fahey et al., 2005; Kindler et al., 2011). Plant litter is the dominant input of new carbon to soils, where it is subsequently decomposed by fungi, bacteria, and soil animals. These initial litter grazers form the second tier of an incredibly complex food web (Wardle, 2002). With every trophic interaction in this food web, some organic matter is converted into new biomolecules (i.e. retained in the soil), and some is lost from the system as CO_2. Predicting rates of soil C sequestration will require a deeper

understanding of the functional ecology of how these soil communities transform and decompose organic matter (Anthony et al., 2020a; Crowther et al., 2019; Romero-Olivares et al., 2021). This is a daunting task due to the methodological challenges associated with studying microbial communities in the field (Philippot et al., 2012), as well as the ever-present uncertainties associated with studying soil processes in general (Yanai et al., 2017). Currently, much more is known about the factors affecting plant litter decomposition than the decomposition of tissues produced by other soil organisms.

The vast majority of studies of plant litter decomposition studies have focused on leaves, with thousands of papers published on the topic in last 40 years (Prescott, 2010). Decomposition of leaf litter occurs primarily due to consumption by soil heterotrophs, though abiotic processes (e.g. photodegradation, freeze-thaw cycles) play an important role in some systems. Temperature and moisture are important regulators of decomposer activities. The ectothermic organisms which feed on litter are more active at higher temperatures. Fungi and bacteria rely on extracellular digestion, and the efficiency of the enzymes they produce are temperature dependent (Fierer et al., 2005). Similarly, these organisms require water to function, and decomposer activity is often moisture limited (Manzoni et al., 2012). Thus, climatic controls over litter decomposition are common at both local and global scales, due to temperature and moisture effects on decomposer physiology (Bradford et al., 2016; Y. Chen et al., 2018; Djukic et al., 2018; Keiser & Bradford, 2017).

In addition to climatic factors, the chemical composition of plant litter has strong effects on decomposer communities, and ultimately the rate of litter decomposition. In general, litters that are richer in mineral nutrients (e.g. N, P, Ca) decompose faster than those of lower nutritional quality (Cornwell et al., 2008; X. Zhang & Wang, 2015). In contrast, litter decomposition rate tends to decrease with increasing C complexity of the substrate (i.e. increasing lignin, cellulose; Cornwell et al., 2008), presumably due to the increased costs associated with enzymatic degradation. Complex aromatic structures such as lignins must be degraded oxidatively, and litter manganese (Mn) has also been found to limit decomposition because it is required for fungal production of Mn peroxidase enzymes (Whalen et al., 2018).

Emerging evidence suggests that the chemical traits affecting leaf litter decomposition are predictable based on carbon and nutrient economies (i.e. resource acquisition strategies) of individual plant species. For instance, carbon and nutrient-acquisitive plants have higher leaf N contents (Wright et al., 2004), which results in higher litter N concentrations, and faster decomposition (Cornwell et al., 2008). These afterlife effects of plant traits on litter decay are likely present in other litter types besides leaves (Freschet et al., 2010; Reich, 2014), but species-level datasets of root decomposition have only recently become large enough to make these comparisons. Furthermore, mycorrhizal symbioses with fungi are an integral part of the nutrient economy of plants (Averill et al., 2019), and their effects on root decomposition have not been explored across systems.

While understanding of belowground plant litter decomposition lags far behind that of leaf litter, even less is known about how other (non-plant) belowground litters decompose. Fungal litter (necromass) constitutes a significant quantity of total soil C across systems (Angst et al., 2021), and recent research has shown clear parallels between the chemical drivers of decomposition in plant and fungal substrates. Like plant tissues, fungal necromass tends to decompose faster when it contains higher concentrations of N (Fernandez et al., 2016a). Additionally, fungal melanins appear to play a similar role to plant lignins in terms of inhibiting decomposition rates (Fernandez & Koide, 2014a). This is intriguing, because melanin is costly to produce, and melanization is inversely related to fungal growth rate (Siletti et al., 2017), suggesting that slow growing species may also be slow decomposers.

As knowledge of litter decomposition has continued to grow, so has the concept of soil organic matter. Traditionally, soil C was thought to consist primarily of complex plant-derived molecules that are resistant to decomposition. More recently however, evidence suggests that much of the soil C with long residence times exists as relatively simple organic molecules that become physically or chemically protected from decomposition via association with soil minerals (Schmidt et al., 2011). Importantly, many of these simple organic molecules are derived from microbes, not plant tissues (Grandy & Neff, 2008; Kleber et al., 2015). This leads to the counterintuitive hypothesis that more labile (fast-decomposing) plant litters can lead to a faster accumulation of stable soil carbon, if it leads to greater microbial C use efficiency (Cotrufo et al., 2013a). This growing

recognition of microbes as an input of stable soil C highlights the importance of quantifying the rate and spatial extent of microbial exploration in soils, as well as a need to better understand how microbial community function influences the residence time of soil organic matter.

In this dissertation, I focus on understanding of the drivers of belowground litter decomposition and its implications for soil C sequestration. My first chapter focusses on how climatic factors, substrate chemistry, and species traits affect rates of fine root decomposition across the globe (See, McCormack, et al., 2019). My second chapter focuses on how variations in substate chemistry across taxa affect the decomposition of fungal necromass, a less commonly studied form of belowground litter (See et al., 2020). Finally, my third chapter reviews literature exploring the extent of fungal hyphal exploration in soil, and its resulting implications for microbial necromass deposition and rates of mineral-associated organic matter formation.

Chapter 1

Global patterns in fine-root decomposition: climate, chemistry, mycorrhizal association and woodiness

Summary

Fine-root decomposition constitutes a critical yet poorly understood flux of carbon and nutrients in terrestrial ecosystems. Here we present the first large-scale synthesis of species trait effects on the early stages of fine-root decomposition at both global and local scales. Based on decomposition rates for 279 plant species across 105 studies and 176 sites we found that mycorrhizal association and woodiness are the best categorical traits for predicting rates of fine-root decomposition. Consistent positive effects of nitrogen and phosphorus concentrations, and negative effects of lignin concentration emerged on decomposition rates within sites. Similar relationships were present across sites, along with positive effects of temperature and moisture. Calcium was not consistently related to decomposition rate at either scale. While the chemical drivers of fine-root decomposition parallel those of leaf decomposition, our results indicate that the best plant functional groups for predicting fine-root decomposition differ from those predicting leaf decomposition.

Introduction

Plant litter decomposition in terrestrial systems constitutes one of the largest annual fluxes in global carbon (C) and nutrient cycling, but the role of fine-root (diameter ≤ 2 mm) traits is poorly understood relative to aboveground litter (Bardgett *et al.* 2014). Fine-root turnover accounts for approximately 14-27% of net primary production (NPP) globally (McCormack *et al.* 2015a) and is estimated to contribute 33% of the annual litter inputs in forests and 48% of the inputs in grasslands (Freschet *et al.* 2013). Recent evidence also suggests that the plant and microbial byproducts of root decomposition contribute disproportionately to soil C stores relative to

aboveground litter (e.g. Rasse *et al.* 2005; Clemmensen *et al.* 2013; Austin *et al.* 2017). Faster

fine-root decomposition rates reflect more labile litter inputs, which in turn are thought to control

microbial inputs to stabilized soil organic matter (Cotrufo *et al.* 2013). Since fine-roots represent a substantial nutrient pool in soils, their decomposition also represents an important release of nutrients to the rhizosphere, with implications for soil nutrient availability. Thus, a comprehensive understanding of the rates and drivers of fine-root decomposition is crucial to reducing uncertainty in ecosystem carbon and nutrient

budgets ranging from landscape to global scales (Fahey *et al.* 2005; Le Quéré *et al.* 2016).

Fine-roots are functionally similar to leaves in that they are the local site of resource exchange between plants and their environment, exhibit diverse morphologies (Ma *et al.* 2018) and chemical composition (Iversen *et al.* 2017), and are ephemeral in comparison to structural tissues (Eissenstat & Yanai 1997; McCormack *et al.* 2012). Globally, plant tissue decomposition rates are positively correlated with mean annual temperature (MAT) and precipitation (MAP) (Parton *et al.* 2007; Zhang *et al.* 2008), but there remains considerable unexplained variation both globally and locally (Prescott 2010; Bradford *et al.* 2016). At local scales, substrate chemistry is a dominant factor controlling leaf litter decomposition (Djukic *et al.* 2018), with the early stages of decomposition being positively correlated with nutritional quality, and negatively correlated with substrate complexity (Melillo *et al.* 1982; Hobbie 2015). Tradeoffs involving the speed of return on investment largely dictate plant species' leaf chemistry (Wright *et al.* 2004), which in turn controls leaf litter decomposition worldwide (Cornwell *et al.* 2008). A similar global relationship may exist between plant species' traits and fine-root decomposition, since fine-root chemistry correlates with the water and nutrient economies of plants (Reich 2014). However, only one study thus far has addressed the effects of plant species' acquisition strategy on fine-root decomposition (Freschet *et al.* 2012), and the generality of those findings across ecosystems remains unexplored.

Fine-root decomposition might be expected to vary at the species level based on traits relating to aspects of the plant economics spectrum such as growth form (e.g. woody vs. herbaceous, broadleaf vs. conifer), nutrient acquisition strategy (i.e. mycorrhizal association), leaf lifespan of woody plants (i.e. deciduous vs. evergreen), or plant life cycle of herbaceous plants (i.e. annual vs. perennial). Although some plant traits are correlated across organs (Freschet *et al.* 2010), which could be advantageous at the whole-plant scale (Reich 2014), fundamental differences exist between above- and belowground organs. Different environmental stressors, different resources acquired, and the presence of mycorrhizal symbionts complicate the application of a one-dimensional plant economics spectrum to fine-roots (Weemstra *et al.* 2016). Thus, the best way to functionally categorize species to predict rates of litter decomposition may differ between fine-roots and leaves. For example, while fine-root decomposition likely varies with root lifespan, aboveground traits controlling leaf decomposition (e.g. deciduousness) may be less important to fine-roots. Conversely, leaf decomposition rates in woody plants do not differ from non-woody plants (Cornwell *et al.* 2008), but higher lignin content in the fine-roots of woody plants likely results in slower decomposition (Zhang *et al.* 2008). Furthermore, the presence of an ectomycorrhizal (EcM) fungal mantle can slow the decomposition of some woody roots (Langley *et al.* 2006; but see Koide *et al.* 2011), whereas effects of ericoid (ErM) or arbuscular (AM) mycorrhizal colonization on fine-root decomposition have not yet been explored. Thus, it remains unknown whether fine-roots with contrasting mycorrhizal associations differ in their decomposition rates.

An earlier global analysis of species-specific fine-root decomposition rates indicates that fine-roots of conifers decompose more slowly than those of broadleaved plants, which in turn decompose more slowly than those of graminoids (Silver and Miya 2001). Underlying these results were relationships between decomposition rate and root nutrient concentration, most notably a strong positive effect of calcium (Ca) and a negative effect of the C:nitrogen (N) ratio. Although these results helped to identify a set of potential drivers of fine-root decomposition at the global scale, they were based on a relatively small number of studies. The number of published studies on fine-root decomposition has increased more than three-fold over the last two decades, and the number of individual species and observations has increased by an order of magnitude. Despite recent attempts to synthesize this growing literature in terms of climate and litter-quality effects on decomposition (Zhang & Wang 2015), no study since Silver and Miya (2001) has examined differences among plant growth forms. Furthermore, previous syntheses have not looked for consistent within-site patterns, nor how fine-root decomposition is influenced by other plant traits affecting nutrient cycling in ecosystems (e.g. mycorrhizal association, leaf lifespan of woody plants, plant life cycle of herbaceous species).

To address these knowledge gaps, we compiled a dataset of decomposition rates (*k*-values from single exponential decay models) for fine-roots of 279 species across 105 studies, with the goal of co-analyzing global- and local-scale drivers of fine-root

decomposition. Our specific objectives were: 1) to elucidate effects of litter chemistry, specifically concentrations of phosphorus (P), N, Ca, and lignin on decomposition rates both within and across sites; and 2) to compare fine-root decomposition rates across plant growth forms (woody broadleaf, woody conifer, herbaceous graminoid, and herbaceous forb, as well as a broader comparison of all woody vs. all herbaceous plants); types of mycorrhizal association (arbuscular mycorrhizal, ectomycorrhizal, and ericoid mycorrhizal); leaf lifespan of woody species (deciduous vs evergreen); and plant life cycle of herbaceous species (annual vs perennial). We hypothesized that fine-root chemistry would be a strong predictor of decomposition rate both within and among sites, and that the best categorical predictors would be nutrient acquisition strategy (i.e. mycorrhizal association) and woodiness. Additionally, we sought to update previously identified decomposition-climate relationships based on a significantly expanded dataset.

Methods

Data collection and compilation

We conducted a literature search in December 2017 for all papers containing fine-root decomposition values by species. For each species in each study, we retrieved simple exponential decay rate constants (k-values) based on the model $M = e^{-kt}$, where M is equal to the proportion of dry mass remaining at time t (in years), and k is the exponential rate of decomposition (Olson 1963). When papers did not report k-values, or reported them based on a different model, we re-calculated the exponential rate constant using non-linear regression (Adair *et al.* 2010), based on the data reported in the paper.

Although models including additional terms often better describe the later stages of decomposition (Adair *et al.* 2008), our approach allowed us to most effectively leverage existing data, as the vast majority of studies fit a single exponential decay model (Adair *et al.* 2010). The reported diameter cutoffs for fine-roots ranged from 0.5-3 mm, with 85% of the observations between 1-2 mm. Studies ranged in duration from 0.3-10 years, with the exception of one 20-day study (representing 4 data points).

In addition to *k*-values, we collected available information on species identity, root chemistry and climate as predictor variables. When litter chemistry was reported for multiple time points, we only used initial root concentrations of C, N, P, Ca, and lignin. We used MAT and MAP values for sites as reported, and, if unavailable, we used Worldclim projections based on reported latitude and longitude (Fick & Hijmans 2017). We also assembled a moisture index (MI) for each location, calculated as the ratio of MAP to potential evapotranspiration. Since most studies do not report potential evapotranspiration, we matched the latitude and longitude coordinates in our dataset to an existing global climate dataset (Butler *et al.* 2017). All woody plant species were assigned a mycorrhizal association (AM, EcM, ErM), either according to the original description by the authors or, if not given, based on species characteristics according to Maherali *et al.* (2016). Further description of our publication selection criteria and data compilation methods is available in the supplementary material (Appendix S1.1).

Statistical analyses

Addressing our objectives required different statistical models applied to different subsets of the data. For example, we included greenhouse-based studies when comparing the effects of plant traits on local decomposition, but excluded these when assessing global-scale relationships with climate. A table summarizing which studies were included in the different analyses is given in the supplementary material (Appendix S1.2).

To assess the global (i.e. across-site) effects of climate on fine-root decomposition we fit multiple mixed-effects linear models, with natural logarithm (ln) transformed *k*-values as the response variable, and a random intercept fit to each study. The fixed effects included study duration, along with all combinations of MAT, MAP, MI, and their interactions (Appendix S1.3). We compared all possible models based on the corrected Akaike Information Criterion (AICc) to select the most parsimonious model. A full comparison of candidate models is reported in the supplementary material (Appendix 3).

For global comparisons of the effects of tissue chemistry on fine-root decomposition, we controlled for climatic differences using mixed-effects linear models, with study duration, MAT, MAP and the chemical predictor of interest (N, P, Ca or lignin, fit separately for each) as fixed effects, a random intercept for study, and the ln-transformed *k*-value as dependent variable. Predictor variables were ln-transformed when needed to better conform to variance assumptions. To assess the effects of initial chemistry on fine-root decomposition at local scales, we calculated standardized slopes for the relationship between each chemical constituent and *k*-value for all studies

containing at least 5 observations (i.e. 5 *k*-values with associated initial chemistry values). We then calculated the mean standardized slope across all studies for each variable.

To examine the effects of different plant functional groups on fine-root decomposition, we used a set of mixed-effects linear models following the general form: ln(*k*) = group + ln(duration) + (1|study), where ln(*k*) is the natural log of the *k*-value, ln(duration) is the natural log of study length, group is the functional group of interest, and (1|study) represents a random effect for the study-level mean of ln(*k*). We used ln-response ratios to compare the effect sizes between the various functional groups mentioned above, and constructed bootstrap confidence intervals for each ratio. To assess the robustness of our findings, we ran these analyses on both the complete and a conservative dataset. The complete dataset contained all available observations (n = 703). The conservative dataset (n = 356) included data averaged over all species-level observations by site to avoid potential pseudoreplication. It also had more stringent requirements for including studies (e.g. rejecting methods other than the buried bag approach, rejecting studies that categorize roots by order rather than diameter, and restricting the location of litterbag deployment to the top 0-20 cm mineral soil). Full criteria for inclusion in the conservative dataset and a comparison of sample sizes by category can be found in the supplementary material (Appendix S1.1). To further test the robustness of our findings, we analyzed both datasets using equivalent models that also included a random coefficient (analogous to a random slope, but for categorical data) which assumes that the size of each group effect (i.e. response ratio) is randomly

distributed among studies. All of the mixed-effects linear models were conducted using the 'lme4' package in R (Bates *et al.* 2015).

Results

Globally, fine-root decomposition increased with MAT, MAP, and MI (Figure 1.1, Appendix S1.3). The most parsimonious model (lowest AICc) for climatic factors included only MAT and MAP as main effects with no interactions, along with study duration as a covariate (Appendix S1.3). Our regression analyses of litter chemistry showed that, after accounting for MAT, MAP and study duration, initial stoichiometry explains a small but significant portion of the variation in global decomposition rates. Decomposition increased globally with initial N concentration (partial R^2 = 0.03, p = 0.02, Figure 1.2a) and decreased with initial lignin concentration (partial R^2 = 0.11, p < 0.001, Figure 1.2b). While modest, the effects of N and lignin on fine-root decomposition appeared to be independent, as the two predictors were poorly correlated (r = -0.05; Appendix S1.4). In contrast, there was no significant global relationship between decomposition rate and fine-root Ca (Figure 1,2c) and only a marginally significant positive relationship with initial P concentration (p = 0.054, Figure 1.2d), which was correlated with N concentrations in this dataset (r = 0.58, Appendix S1.4), making it difficult to partition the independent effects of N and P.

Within sites, tissue chemistry effects showed similar trends to the global-scale analysis, with fine-root decomposition rates positively related to root N concentrations,

negatively related to lignin concentration, and unrelated to Ca concentration (Figure 1.2e). Root P concentrations were, on average, positively associated with fine-root decomposition rate within sites. While fewer studies included root P than N concentration data, the average within-site effect size on fine-root decomposition rates was 39% stronger for P than N concentration (Figure 1.2e). Similar effects on fine-root decomposition rates were evident for ratios of C:N, C:P, and lignin:N, but not for lignin:P, though few studies reported both P and lignin (Appendix S1.5).

Fine-root decomposition rates differed both among mycorrhizal associations and plant growth forms based on comparisons of 95% bootstrap confidence intervals of the random intercept model (Figure 1.3). Among growth forms, fine-roots of woody plants decomposed more slowly than fine-roots of non-woody plants, and within woody plants, fine-roots of conifers decomposed more slowly than those of broadleaved plants. Within herbaceous species, fine-roots of forbs decomposed faster than those of graminoids. Within woody plants, fine-roots of both ErM and EcM plants decomposed more slowly than those of AM plants. This finding is unaffected by how species associating with both EcM and AM (e.g. *Eucalyptus* and *Populus*) were categorized. While ErM fine-roots decomposed slower than EcM fine-roots on average, these two groups did not differ significantly from one another (possibly due to low representation of ErM roots in the dataset, n = 31). The growth form and mycorrhizal type results were robust to our choice of the dataset (i.e. complete vs. conservative). In contrast, fine-roots of perennial plants decomposed slower than those of annuals among herbaceous species,

and roots of evergreen trees decomposed slower than those of deciduous trees based on the complete dataset (Figure 1.3), but these differences were not significant at 95% for the conservative dataset when using the same models (Appendix S1.6). Finally, under our most conservative scenario (i.e. a random coefficient model run on the conservative dataset), the only significant differences remaining were those between woody and herbaceous plants, and between EcM and AM trees (Appendix S1.6).

Discussion

There is growing consensus on the need to better understand variation in root decomposition to improve terrestrial biosphere models (Smithwick *et al.* 2014; Warren *et al.* 2015). Our results demonstrate that species-level traits relate to fine-root decomposition, both within and across ecosystems, and that aggregating species into functional groups provides a means to capture broad patterns of fine-root decomposition. Importantly, the best explanatory variables of fine-root decomposition (i.e. woodiness and mycorrhizal association) did not mirror those previously identified for leaf decomposition (e.g. deciduousness; Cornwell *et al.* 2008), even though the litter chemistry drivers (N, P, lignin) appear to be similar. Though previous studies have found effects of initial litter chemistry on decomposition at the global scale (Zhang *et al.* 2008), global relationships do not necessarily reflect locally important drivers of decomposition (Bradford *et al.* 2017). In the case of fine-roots, however, the chemical

traits identified to account for differences in decomposition rates across sites were good local predictors as well.

Previous syntheses that have pooled fine-root decomposition data across sites (Silver and Miya 2001; Zhang and Wang 2015) found no significant relationships with N or P, and mixed relationships with lignin concentration. While neither of these variables explained more than 11% of variation in decomposition rates, in our study we found fine-root decomposition to be negatively related to lignin and positively related to N and P concentrations across sites. We suspect these discrepancies between past and current syntheses are due to our larger dataset, and analyses accounting for differences in climate and study in the global analyses. More compelling are the consistent within-site relationships we observed between these chemical constituents and fine-root decomposition, which mirror the results of a similar global synthesis of within-site drivers of leaf decomposition (Cornwell *et al*. 2008).

A surprising result was the lack of any consistent effect of Ca on decomposition rate at either local or global scales, as Ca has long been considered an important driver of fine-root decomposition (Silver & Miya 2001; Zhang & Wang 2015; Beidler & Pritchard 2017). Our dataset, which includes a broader range of root Ca concentrations than previous syntheses, suggests that the positive relationship between Ca and fine-root decomposition observed by Silver & Miya (2001) may have been disproportionately influenced by low root Ca values. It may be that in base poor soils,

Ca is a limiting nutrient to decomposer communities (Berg *et al.* 2000), but litter Ca content likely depends on soil Ca availability (Lovett et al. 2016), which in turn may be confounded with pH effects on decomposition, at least in cross-site comparisons. Regardless of the underlying mechanisms, our results suggest the effect of Ca on fine-root decomposition is ecosystem dependent. Unlike the other chemical variables in our analyses, the effect of P on fine-root decomposition varied somewhat between scales. Despite consistent positive effects within sites, the effect of P on fine-root decomposition was weak at the global scale. This likely reflects site-specific differences in the N:P stoichiometry of microbial nutrient demand and availability (Cleveland & Liptzin 2007). We caution, however, that our inferences regarding both P and Ca effects are based on rather limited sample sizes, suggesting that more site-level studies are needed to clarify the role of these elements in fine-root decomposition.

Our analyses show that categorizing plant species by growth form or mycorrhizal association can be useful to improve our understanding of fine-root decomposition. Specifically, woody species produce fine-roots that decompose slower on average than non-woody species, likely due to their greater lignin content (Appendix S1.7). However, other systematic differences in morphology such as lower root tissue densities (Freschet *et al.* 2017) or smaller average diameters (Valverde-Barrantes *et al.* 2017) of herbaceous plants may also contribute to their faster decomposition. Within woody species, mycorrhizal association was a stronger predictor of fine-root decomposition rate than growth form (i.e. broadleaved vs. conifer), and this result

was robust across multiple models. This finding is important particularly in the context of terrestrial biosphere models, which currently categorize forests by growth form rather than mycorrhizal association (Brzostek *et al.* 2017). Additionally, the finding that fine-roots of woody EcM and ErM species decomposed slower than those of AM species adds to the growing list of biogeochemical differences observed between these two forest types (Phillips *et al.* 2013; Craig *et al.* 2018; Zhang *et al.* 2018; Zhu *et al.* 2018). Notably, however, 60% of broadleaf EcM species observations were within the order Fagales, and 90% of the conifers in our dataset were EcM. Thus, the effect of mycorrhizal association on fine-root decomposition rates is confounded with broader order-based plant traits common to Fagales and Pinales. Our dataset is biased towards temperate regions (Appendix S1.1), where these orders are most common. A recent meta-analysis of leaf litter showed that in temperate zones leaves of EcM plants decompose slower than leaves of AM plants, but this difference was not found in tropical or subtropical ecosystems (Keller & Phillips 2018); however, that dataset was subject to similar phylogenetic biases as the data we present here. Further research is needed to disentangle the confounding effects of plant phylogeny, climate, and mycorrhizal type on fine-root decomposition.

The chemical drivers of fine-root decomposition (i.e. N, P, lignin) observed in our study parallel the findings of previous work relating leaf economic strategy to afterlife effects on leaf decomposition (Cornwell *et al.* 2008). However, the plant functional groups which best predict fine-root decomposition in our study are not the same as the groups that predict leaves. For instance, woodiness (i.e. woody vs herbaceous plants) does not

consistently predict leaf decomposition rate (Cornwell *et al.* 2008), but is a strong predictor of fine-root decomposition in our dataset. Similarly, while deciduousness is a strong predictor of leaf decomposition (Cornwell *et al.* 2008), it does not consistently predict root decomposition in our dataset, which is perhaps not surprising since deciduousness is an inherent leaf trait that does not correlate with fine-root longevity (Withington *et al.* 2006; McCormack *et al.* 2015b). It is important to note that aboveground and belowground acquisition strategies are not completely unrelated, as rapid C acquisition strategies aboveground often necessitate faster acquisition of belowground resources (Reich 2014). Leaf and root litter decomposition are indeed often correlated within sites (Birouste *et al.* 2012; Freschet *et al.* 2013), though this is not always the case (e.g. Hobbie *et al.* 2010; Ma *et al.* 2016, Sun *et al.* 2018), and additional factors need to be taken into account to understand variation between fine-root and leaf decomposition across scales.

Our analysis represents considerable progress towards synthesizing effects on fine-root decomposition of fine-root litter traits analyzed at the species and functional-group level, but current data limitations leave important questions to be addressed. For example, functional differences between absorptive and transport fine-roots cause them to differ in nutrient concentration, structural development, and other traits (McCormack *et al.* 2015a; Beidler & Pritchard 2017). The most distal, first-order roots often decompose more slowly than higher order fine-roots (Goebel et al. 2011; Sun et al. 2013), which is likely an effect of differences in chemical composition (e.g. concentrations of condensed

tannins or non-structural carbohydrates; Sun *et al.* 2018). First-order roots represent only a small proportion of the total fine-root biomass in the studies we have synthesized here, but given their short lifespans, they may be disproportionately important to ecosystem C and nutrient cycling (Guo *et al.* 2008). In addition to combining higher and lower root orders, most decomposition studies are based on roots harvested live, which have not been subjected to nutrient resorption and other developmental changes during senescence. Any differences between live-harvested and naturally-senesced roots (e.g. nutrient chemistry, microbial colonization) which affect decomposition rates therefore represent a consistent and unaddressed bias in the literature. Moreover, there remains a dearth of long-term studies (>3 years) of root decomposition (Appendix Figure S2), which are needed to characterize the residence times of more recalcitrant fractions in root tissues. For instance, a 6-year study of root-tip decomposition showed that among 35 tree species, EcM species decomposed more slowly than AM species at first, but this pattern reversed after two years of decomposition (Sun *et al.* 2018). Furthermore, the effects of fine-root N concentrations on decomposition can change from positive in the early stages to negative in later stages of decomposition (Berg 2014). These findings highlight the need for long-term decomposition studies by root order to accurately describe the influence of traits and mycorrhizal type on fine-root decomposition.

Finally, there is also a need to standardize methods in future studies. Here we were able to account for broad variation in annual climate in our analysis, but in regions

experiencing strong seasonality, initial decomposition rates will be influenced by the season in which the incubations were started. This issue could be partially remedied by reporting mass loss estimates based on degree days as well as calendar days in future studies (Aulen *et al.* 2012). Fine-root decomposition rates also vary with the depth at which litterbags are deployed in the soil (Mello *et al.* 2007; Sariyildiz 2015), though we suspect this source of variation is low relative to the other factors influencing decomposition (Hicks Pries *et al.* 2013; Solly *et al.* 2015). Because fine-root distribution within the soil varies among ecosystems, it would be good practice to deploy litterbags in the zone of maximum fine-root density.

Figure 1.1: Relationship between mean annual temperature (MAT, degrees C), precipitation (MAP, mm), and fine-root decomposition rate (ln(*k*)) based on published data from globally distributed sites.

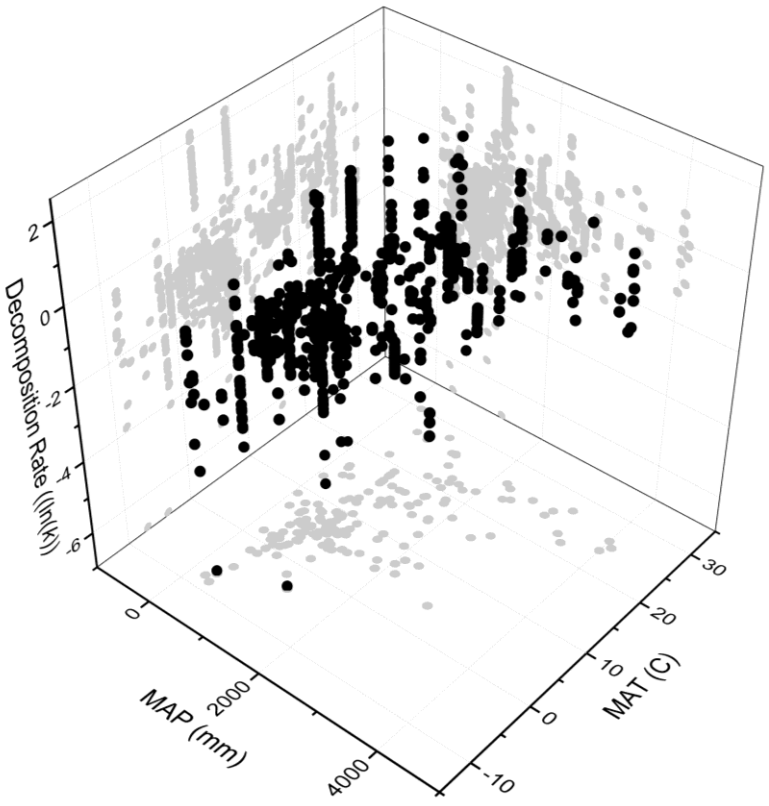

Figure 1.2: Effects of initial fine-root chemistry on fine-root decomposition rates across (a-d) and within sites (e). For the across-site comparisons, the partial effect plots show the relationship between fine-root chemistry and decomposition after accounting for climate (MAT and MAP) and study duration. Solid lines denote significance at $p < 0.05$, the dashed line denotes significance at $p < 0.1$. For the within-site comparisons, values represent the mean standardized coefficient among sites containing at least 5 observations. Error bars depict 95% bootstrap confidence intervals.

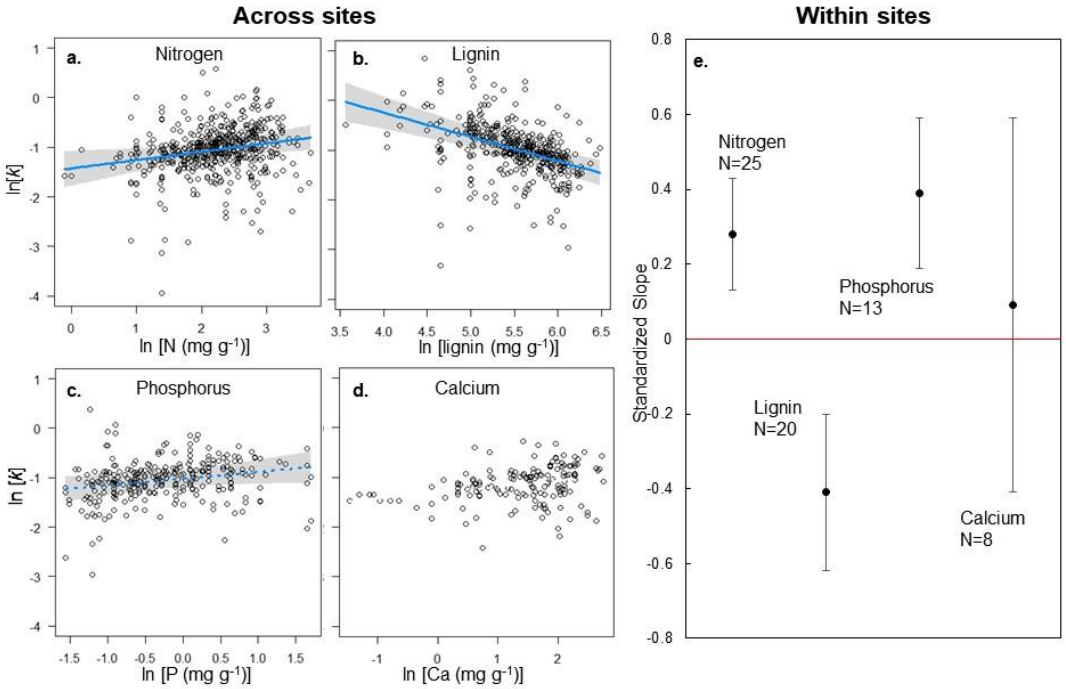

Figure 1.3: Natural logarithm of response ratios comparing fine-root decomposition across various plant functional groups based on growth form, mycorrhizal type, leaf lifespan of woody plants, and plant life cycle of herbaceous species. The red line and labels represent the reference to which other groups were compared. The dotted vertical line delineates two separate analyses within growth form. Error bars depict 95% bootstrap confidence intervals. Results shown are based on the complete dataset analyzed using mixed linear models with random intercepts.

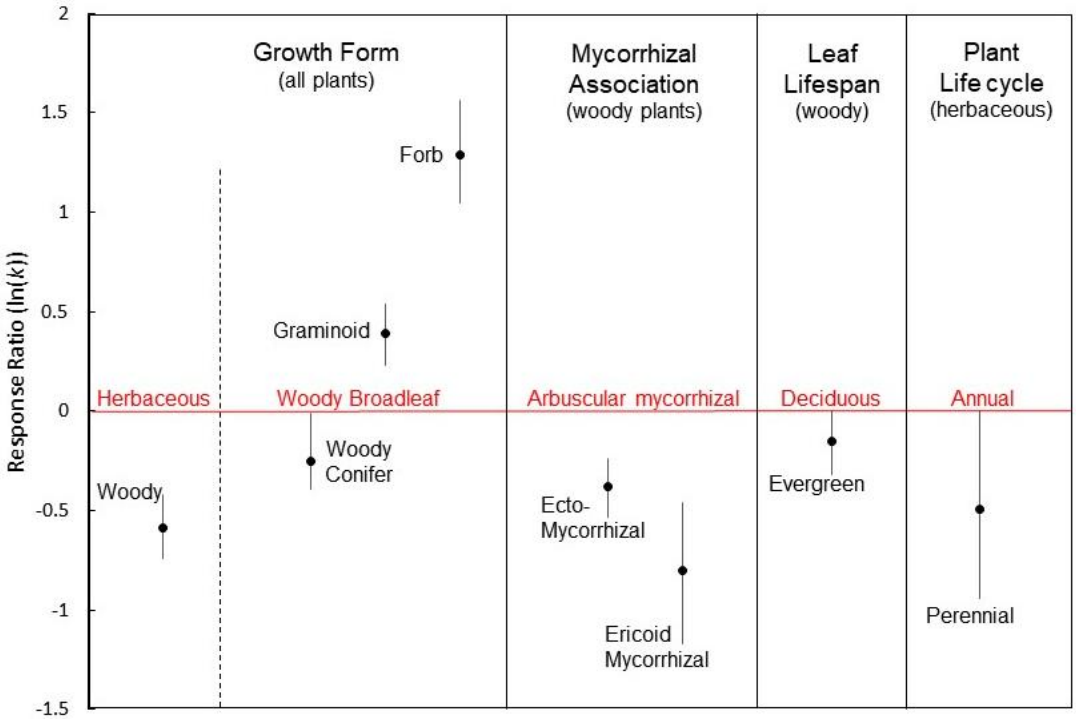

Chapter 2

Distinct carbon fractions drive a generalisable two-pool model of fungal necromass decomposition

Summary

Fungi represent a rapidly cycling pool of carbon (C) and nitrogen (N) in soils. Understanding of how this pool impacts soil nutrient availability and organic matter fluxes is hindered by uncertainty regarding the dynamics and drivers of fungal necromass decomposition. Here we assessed the generality of common models for predicting mass loss during fungal necromass decomposition and linked the resulting parameters to necromass substrate chemistry. We decomposed 28 different types of fungal necromass in laboratory microcosms over a 90-day period, measuring mass loss on all types, and N release on a subset of types. We characterised the initial chemistry of each necromass type using: 1) fiber analysis methods commonly used for plant tissues, 2) initial melanin and nitrogen (N) concentrations, and 3) Fourier transform infrared (FTIR) spectroscopy to assess the presence of bonds associated with common biomolecules. We found universal support for an asymptotic model of decomposition, which assumes that fungal necromass consists of an exponentially decomposing "fast" pool, and a "slow" pool that decomposes at a rate approaching zero. The strongest predictor of the fast pool decay rate (*k*) was the proportion of cell soluble components, though initial N concentration also predicted *k*, albeit more weakly. The size of the slow pool was best predicted by the acid non-hydrolysable fraction, which was positively correlated with melanin-associated aromatics. Nitrogen dynamics varied by necromass type, ranging from net N release to net immobilisation. The maximum quantity of N immobilised was inversely related to cell soluble contents and *k*, as positively related to FTIR spectra associated with cell wall polysaccharides. Collectively, our results indicate that the decomposition of fungal

necromass in soils can be described as having two distinct stages that are driven by different components of substrate C chemistry, with implications for rates of N availability and organic matter accumulation in soils.

Introduction

Dead microbial cells (i.e. necromass) often constitute more than half of the organic C and N in soils, with fungal necromass comprising the majority of this pool (Liang et al., 2019; Simpson, et al., 2007). On short-term time scales (e.g. days to weeks), the decomposition of fungal necromass is thus an important source of C and N to soil microbes and plants (J. Chen et al., 2019). Over longer time scales, biomolecules from decomposing microbial necromass become stabilized to mineral surfaces, increasing long-term soil C storage (Cotrufo et al., 2013; Ludwig et al., 2015) and N retention (Fuss et al., 2019; Lovett et al., 2018). Despite its clear importance to the accumulation and availability of soil C and N, knowledge of the drivers and dynamics of fungal necromass decomposition is poor relative to understanding of senesced plant tissues.

There are growing calls for the explicit inclusion of microbial necromass into ecosystem models (e.g. Simpson et al. 2007; Miltner et al. 2012; Wieder et al. 2015). Previous studies have modeled fungal necromass decomposition as a uniform substrate with a constant decay rate (i.e. single exponential decay; Fernandez & Koide, 2014), which is how it has been treated in soil C models (Sulman et al., 2017; Sulman et al., 2014). In reality, fungal necromass is a heterogeneous structure of biopolymers (e.g. polysaccharides, proteins, aromatic polymers) subject to degradation by different enzymes at different rates (Brabcova et al., 2016). This substrate heterogeneity is reflected in studies which suggest that fungal hyphae decompose in two distinct phases: an initial phase of rapid decomposition and a second phase of slow decomposition (e.g. Schweigert et al., 2015; Brabcová et al., 2016; Ryan et al. 2020). Recently, a two-year study demonstrated that an

asymptotic model of decomposition best described mass loss for four ectomycorrhizal fungal species (Fernandez et al., 2019). This model assumes that the fungal substrate consists of two distinct pools: a labile "fast" pool that decomposes exponentially, and a recalcitrant "slow" pool that decomposes at a rate approaching zero (Howard & Howard, 1974). If generalisable, this would provide useful parameters for incorporating fungal necromass into microbially-explicit biogeochemical models, since a two-pool model of necromass decomposition implies distinct biochemical fractions with distinct implications for biogeochemical cycling. However, more observations are needed to determine whether the asymptotic model can be broadly applied across diverse fungal taxa.

Accurately modeling the dynamics and drivers of the early stages of fungal necromass decomposition (i.e. the fast pool) may be particularly important to soil N availability. Modeling N release from necromass is straightforward if treated as a homogeneous pool; a simple exponential decay rate dependent solely on N concentration results in species releasing N at a rate proportional to their mass loss. However, the presence of multiple N-containing pools which decay at different rates complicates this, especially if substrate N concentration is not the only driver of decay rate. Thus, while multiple studies have demonstrated that the early stages of fungal necromass decay are controlled in part by the N concentration (e.g. Koide & Malcolm 2009; Fernandez et al. 2019), other chemical drivers (e.g. C quality) deserve further attention.

While fast pool necromass dynamics likely affect soil N availability, the size of the slow pool may affect long-term rates of C and N accumulation in particulate organic matter. This pool is thought to be composed of melanin located within the fungal cell wall (Fernandez et al., 2019). Among ectomycorrhizal fungi, melanised root tips persist longer in soil than non-melanised root tips (Fernandez et al., 2013), and melanised sclerotia can remain in soil for millennia (Scott et al., 2010). Recent field studies have linked melanized hyphae with SOM pools (Karina E. Clemmensen et al., 2015a; Lenaers et al., 2018; Siletti et al., 2017), suggesting an effect on soil C accumulation. The implications of a stable melanin-derived pool for soil N dynamics are less clear, as the chemical structure of many fungal melanin types do not contain N (Butler & Day, 1998). However, some fungal taxa produce melanin structures with N-containing indole groups (Eisenman & Casadevall, 2012), and N-containing proteins and chitin are often complexed with melanin in the cell wall (Butler & Day, 1998; Nosanchuk et al., 2015). These molecules could represent a previously overlooked pool of N immobilised in fungal necromass over long time scales.

In the present study, we decomposed 28 field-collected fungal necromass types in laboratory microcosms containing non-sterile soils further inoculated with a ubiquitous soil saprotroph. Our primary objectives were to: 1) determine which commonly applied decomposition model best describes decomposing fungal hyphae across a phylogenetically and functionally diverse suite of taxa, 2) determine the biochemical components of fungal necromass most strongly associated with its decomposition dynamics, and 3) determine how substrate chemistry and decay rate relate to the dynamics of N release during fungal necromass decomposition.

Methods

Decomposition Assay:

Fresh sporocarps of 23 species of mycorrhizal and saprotrophic fungi were field harvested and oven dried at 45°C. The stipe was separated from the pileus in all samples where the two features were distinguishable. The pileus in mushrooms contains spores and tends to have higher C and N concentrations than the stipe (E. A. Hobbie et al., 2012), which we assumed to be chemically more similar to diffuse hyphae. Therefore, we discarded the pileus in all but five samples where we analysed it separately (n = 28 total samples). Substrates were oven dried at 50ºC and ground to the consistency of fine sand in order to ensure a homogeneous sample for litterbags and chemical analyses.

We constructed five bags of each ground necromass type, each containing 85 ± 10 mg of dried fungal mycelium that was heat-sealed inside of two ~4 cm^2 squares made from 53 µm nylon mesh (Elko, Minneapolis, MN, USA). Each bag was incubated in a 120 ml microcosm filled with ~80 ml live (i.e. unsterilized) mineral soil from the Cedar Creek Ecosystem Science Reserve, MN, USA. Upland soils at Cedar Creek are sandy Entisols, classified as Udipsamments (Grigal, et al., 1974). Soils were sieved to 2mm and litterbags were deployed horizontally, with approximately 40ml of soil above and below the litterbag. Microcosms were covered in clear plastic film, incubated in the dark at 20 ºC, aerated every 4-6 days, and soil moisture levels maintained at 60% of field capacity until harvest. One bag of each necromass type was harvested after 2, 5, 8, 43, and 90 days of incubation.

Because a primary objective of this research was to compare the early stages of decomposition across substrates, we wanted to minimise differences due to the timing of saprotroph colonisation. Accordingly, we surface-inoculated all bags with a 50 µl slurry of water and hyphae from laboratory-cultured *Mortierella elongata* prior to incubation. *M. elongata* is a common saprotroph in soils globally (Li et al., 2018), plays a dominant role in microbial substrate decomposition (López-Mondéjar et al., 2018a), and is an early coloniser of fungal necromass incubated in soils at Cedar Creek (Fernandez & Kennedy, 2018).

Chemical Analyses:

We conducted a series of biochemical analyses to assess the initial substrate composition of all samples. We used forage fiber analysis, consisting of sequential extractions with neutral detergent, acid detergent, and concentrated acid, to assess proximate carbon fractions of each fungal residue (ANKOM Technology, Macedon, New York, USA). This procedure is commonly used in ecosystem studies to analyse plant tissues for decomposition studies (e.g. Wieder et al., 2009; Hobbie et al., 2010). To our knowledge this procedure has not yet been applied to fungal substrates, however the carbon fractions it is meant to quantify in plants (e.g. cross-linked polysaccharide chains, proteins, amorphous aromatic polymers) are all present in fungi, and likely subject to degradation by similar classes of enzymes in soils (e.g. hydrolytic, proteolytic, oxidative). Briefly, cell soluble contents (e.g. simple carbohydrates, lipids, soluble proteins and non-protein N)

were assessed as the amount of mass loss from each sample after gentle agitation in a neutral detergent for 75 minutes at 100℃. The residual material was agitated in an acid detergent (1N H_2SO_4) at 100℃ for 75 minutes to quantify the mass of amorphous glucan polymers (analogous to hemicellulose in plants) and bound proteins within the cell wall. Finally, the contents of acid hydrolysable cell wall components—likely crystalline glucans and chitin (Jang et al., 2004; analogous to cellulose in plants)—were determined with a 3-hour extraction in concentrated (72%) H_2SO_4 at room temperature with intermittent agitation. The remaining, acid unhydrolysable residues are thought to contain cell wall melanins (analogous to lignin) and other molecules complexed within them (Nosanchuk et al., 2015).

We quantified the relative proportion of various biochemical bonds present in the initial substrates using Fourier-transform infrared (FTIR) spectroscopy. Two mg subsamples of each necromass sample were ground into a homogeneous powder with 100 mg KBr. Samples were pressed into a disc, and 64 transmission spectra scans were averaged across the 4000-400 cm^{-1} range, at a resolution of 4 cm^{-1} using a Nicolet iS5 spectrometer fitted with an iD1 Transmission accessory (Thermo Fisher Scientific, Waltham, Massachusetts, USA). Background subtraction was applied based on pure KBr spectrum, and a baseline correction factor was applied using OMNIC, version 9 (Thermo Fisher Scientific, Waltham, Massachusetts, USA). Peak heights were z-score transformed prior to use in final analyses, and peaks corresponding to bonds in common biomolecules were identified based on previous characterisation (Table S2.1, Margenot et al., 2015; Hribljan et al., 2017).

In addition to the fiber fraction and FTIR spectral analyses, we measured total C and N concentrations and total melanin content. Percent C and N were measured via dry combustion (Costech Analytical Technologies Inc., Valencia, CA, USA). Substrate melanin content was quantified using the commonly applied Azure A colourimetric assay (Fernandez & Koide, 2014). Briefly, 15 mg of ground sample was placed in 3 ml of Azure A solution (0.1M HCl mixed with Azure A dye to a 610 nm absorbance of 0.665) and incubated overnight. Melanin content was estimated as the decrease in 610 nm wavelength absorbance after incubation, based on a standard curve created using pure fungal melanin isolated from *Cenococcum geophilum* biomass.

We calculated net N immobilization and release during the first 43 days of decay for five of the 28 necromass types, which were representative of the range in substrate quality (i.e. N and melanin concentrations). For each collection (2, 5, 8, and 43 days), we measured the N concentration of the necromass harvested from the bags. We estimated the proportion of the initial substrate N pool remaining for each bag at each collection time (Parton et al., 2007), such that $N_{retained} = (Mass_{final} \times [N]_{final})/(Mass_{initial} \times [N]_{initial})$, where $N_{retained}$ represents the proportion of the initial N pool remaining, $[N]_{initial}$ and $[N]_{final}$ represent the respective substrate N concentrations, and $Mass_{initial}$ and $Mass_{final}$ represent the respective masses of substrate in the litterbags. Values greater than 1 indicate net immobilization whereas values less than 1 indicate net release. Due to differences in the timing of N release and the magnitude of N immobilised when N release began among substrates, we calculated the maximum level of immobilisation (across all collections) for each necromass type.

Statistical Analysis:

We compared the single exponential decomposition model of the form $X = e^{-k_s t}$, where X is the proportion of the mass remaining at time t (in days) and k_s is the decay rate, to the asymptotic model of the form $X = A + (1-A)e^{-kt}$, where k is the decay rate of the fast pool, and A is the size of the slow pool which decomposes at a rate of zero (in reality, the decay rate of the slow pool is likely very close to, but not equal to, zero). We fit these models to the proportion mass remaining for each substrate across the five harvest times (Howard & Howard, 1974; Olson, 1963). We also attempted to fit the data to a double exponential model, which assumes that both the fast and slow pools decay exponentially at different rates (Lousier & Parkinson, 1976); however, these models did not converge. We compared the fits of the single and asymptotic models based on the root sum of squares, and the corrected Akaike's Information Criterion (AICc) values. We used ANOVA to compare the differences in decomposition parameters for the substrates categorised by trophic mode (mycorrhizal, soil saprotroph, wood saprotroph), taxonomic order, and sporocarp component (stipe vs spore-bearing).

To assess the effects of substrate chemistry on decomposition dynamics, we used the parameters from the decomposition models (decay rate k and slow pool size A) as dependent variables in multiple linear regression analyses, with substrate chemical concentrations as explanatory variables. Because the fiber fractions sum to 100%, using multiple fractions as predictors would violate the assumption of independence required for

multiple regression. To avoid issues of collinearity among predictors, we compared these fractions to the dependent variables separately using simple linear regression, and then included only the best predictor in the larger model. For similar reasons, we chose to include substrate N concentration, but not C:N ratio in our pool of explanatory variables—substrate C:N was highly correlated with percent N, but less correlated than N with our dependent variables (Table S2.2). Starting with a model that included N concentration, melanin concentration N , one fiber fraction, and all possible interactions, we used a backward-selection stepwise procedure to select the best model based on AIC. We qualitatively described the biochemical bonds associated with the C and N fractions using Pearson correlations with the peaks obtained from FTIR spectra. Finally, we used *k* and the chemical variables found to predict it as explanatory variables in simple linear regressions to predict immobilization (calculated as the maximum proportion of initial N remaining across collections).

Results

The asymptotic model of decomposition consistently fit the mass loss data better than the commonly used single exponential model, as evidenced by a lower residual sum of squares in all 28 models (Table 2.1). The AIC values were also lower for the asymptotic models than the single exponential models in all but one time series (*Laetiporus sulphureus*; Table 2.1). We found considerable variation in the fast pool decay rate across substrates (*CV*=34%), with *k*-values ranging from 0.07-0.35 per day. We found even higher variation in the asymptotic fraction (*CV*=41%), with *A*-values ranging from 0.04-0.26. These parameters appeared to be independent from each other, as *A*-values and *k*-values were not

significantly correlated in this dataset (R^2= 0.06, P = 0.20, Table 2.2). Variation in *k* and *A*-values was not well explained by trophic mode or sporocarp component, though we found differences between taxonomic orders (Figure S2.3).

Variation in the *k*-values associated with the fast pool from the asymptotic model was explained by initial substrate chemistry. The most parsimonious model based on stepwise AIC selection contained only the soluble cell contents and N concentration as explanatory variables with no interaction (*k*-value = -0.1417 + 0.0043* CellSolubles + 0.0088*PercentN; Table S2.4). Cell soluble components, acid detergent, and acid hydrolysable fractions all predicted *k* when considered independently (Figure 1). Of these, the strongest predictor of decomposition rate was cell soluble components, which increased with *k* (R^2=0.56, P<0.001; Figure 2.1). Initial N concentration also predicted the decomposition rate of the fast pool (R^2=0.19, P=0.02; Figure 2.1), and was not correlated with cell soluble components or any other fiber fraction (Table S2.2).

The *A*-values representing the size of the slow pool from the asymptotic model were explained by melanin concentration and the acid non-hydrolysable fraction. The most parsimonious model based on the stepwise AIC procedure contained only these two variables with no interaction (*A*-value = 0.1378 + 0.0056*Melanin + 0.0055*Non-hydrolysable; Table S2.4). Melanin and the non-hydrolysable fraction also significantly predicted the *A*-value in simple linear regression (Figure 2.2), however these relationships were driven by the upper half of these substrate concentrations (Figure S2.5).

Peaks from the FTIR spectra corresponded to substrate chemistry measurements and decomposition model parameters (Table 2.2). The two alcohol (R-OH) peaks (1080 cm^{-1} and 1160 cm^{-1}) had strong negative correlations with the two best predictors of fast pool decay rate: peak 1080 cm^{-1} was inversely correlated with N concentration, and peak 1160 cm^{-1} was inversely correlated with cell soluble contents. Consequently, these R-OH peaks were associated with lower *k* values in the fast decomposing pool (Table 2.2). Both amide bond peaks (1550 cm^{-1} and 1650 cm^{-1}) were highly indicative of N concentration, and also correlated with the fast pool decomposition rate. The two peaks thought to be associated with fungal melanins (840 cm^{-1} and 1234 cm^{-1}), however corresponded to different biochemical fractions. The 1234 cm^{-1} ester peak was associated with the non-hydrolysable fraction and melanin contents, which in turn were correlated with the size of the slow pool (*A*-value). Surprisingly, the 840 cm^{-1} aromatic peak was negatively related to total C, and was not associated with melanins, but rather was positively related with cell-soluble contents. Aliphatic peaks were positively correlated with the non-hydrolysable fraction and melanin contents (Table 2.2), but these relationships were strongly driven by a single point (Figure S2.6).

Nitrogen release during decomposition differed among the 5 necromass types examined (Figure 3a). Necromass types with the lowest initial N concentrations (3.2% N in both *Camarops petersii* and *Grifola fondosa*) both displayed net immobilisation of N by the second day of decomposition (Figure S2.7). Notably, *C. petersii* necromass more than

doubled its N content during the first 48 hours of decomposition. Similarly, *G. fondosa* N content increased 30% after losing 40% of its mass (Figure 3a). In contrast, necromass types with the highest initial N concentrations exhibited immediate declines in N content. Nitrogen immobilisation (measured as the maximum proportion of initial N) was negatively related to decay rate of the fast pool (R^2=0.81, *P=0.04*, Figure 2.3b). As cell soluble contents increased, the maximum proportion of N immobilised decreased (R^2=0.91, *P=0.01*), with necromass types with the highest concentrations of cell solubles releasing N immediately (Figure 2.3c). Conversely, we found a strong positive relationship between the maximum quantity of N immobilised and the R-OH bond contents of the initial substrate (R^2=0.96, *P=0.003*, Figure 2.3d).

DISCUSSION:

A generalisable two-pool model of fungal necromass decay

Our results demonstrate broad support for the asymptotic model in describing the decomposition of fungal necromass in soils. In this model, a fast pool decomposes exponentially on the order of days to weeks, followed by a slow pool that decomposes at a rate approaching zero. This model has been used extensively to characterise plant tissue decomposition (Berg, 2000; Wieder & Lang, 1982), but with the fast pool in plants decomposing orders of magnitude more slowly than fungal necromass (i.e. measured in years, not days). The size of the slow pool across fungal species (7-35%, mean = 18%) was smaller and less variable than those observed in leaf litter (e.g. 5-49%, mean = 29%; Berg 2000). The length of our study did not allow us to quantify the long-term decomposition

dynamics of the slowly decomposing necromass pool. Moving forward, multi-year studies are needed to better characterise the decay rate of the slow fraction of fungal necromass.

Our study examined the dynamics and drivers of the fast pool across phylogenetically diverse fungi. We found a wide range in C and N fractions among the necromass types analysed (Table S2.8), corresponding to different bonds in the FTIR spectra (Table 2.2). Prior studies have related N concentration to early stages of necromass decomposition (e.g. Koide & Malcolm 2009; Fernandez & Koide 2014; Maillard et al. 2020; Ryan et al. 2020), but have largely overlooked the importance of carbon fractions in these substrates. We found cell-soluble contents to be the strongest predictor of *k*, independent of substrate N concentration. This observation, along with the negative relationships observed between *k* and the more recalcitrant fractions of our assay, supports the idea that the size and C chemistry of the fungal cell wall determines *k* for the fast pool (Fernandez et al., 2016). This is further supported by the strong inverse correlation between *k* and R-OH functional groups from the FTIR analyses, as these groups are present in high quantities in the polysaccharides (β-glucan, chitin) composing the cell wall (Table 2.2). While the fast fraction represented the majority of the initial substrate across our dataset (65-93% by mass), our use of freshly-killed hyphae may overestimate the relative proportion of the fast pool *in situ*, since some of it is likely reabsorbed by the fungi as hypha senesce (Boberg et al., 2014). Importantly, the half-life of the fast pool fraction varied by a factor of 6 (range = 3-18 days) across these species, suggesting that differences in fungal community composition can result in important differences in C and nutrient availability to soil.

Drivers of N retention during necromass decomposition

Our results highlight considerable variation in N release among fungal necromass types during the early stages of decomposition. Despite substantial mass loss from all necromass types in the first 8 days of decomposition, N dynamics ranged from net release to net immobilisation of N during this time (Figure 2.3a). Substrates with the highest initial N began losing N immediately, while lower-N substrates remained a net sink for N until the majority of mass loss had occurred (Figure S7). This pattern mirrors observations in plant litter in many ecosystems (Parton et al., 2007), but over a much shorter time scale. Interestingly, initial N concentrations were not the best predictors of initial N release, and did not significantly correlate with the rates of immobilization (Figure S2.7), though the limited sample size of this analysis only allowed for detection of strong trends. Instead we found that N retention in fungal necromass was well predicted by *k*, and the substrate C chemistry driving *k* (Figure 2.3b,c,d).

Differences in N release among necromass types likely reflect variation in the size and composition of the cell wall, with more N immobilization in taxa with more cell wall polysaccharides (i.e. R-OH groups; Figure 2.3d). In contrast to N contained within the cell soluble fraction, N complexed as proteins within the cell wall or contained within acetylglucosamine monomers of chitin require enzymatic attack to be released. Both cell wall components and R-OH bond content were inversely correlated with *k* (Figure 1, Table 2.2), reflecting rate limitation of the hydrolytic enzymes responsible for degrading the

polysaccharides within this pool (Sinsabaugh et al., 2002). This is consistent with the findings of Fernandez & Koide (2012), who found that chitin losses from decomposing necromass were much greater during the second half of a one-month incubation. This suggests that rates of N release from the fast decomposing pool of fungal necromass will be determined by the ratio of N contained in the cell-soluble fraction to N incorporated within the cell wall. Fungal cell walls vary considerably in size, and contents of chitin and glycoproteins (Bowman & Free, 2006). Ecologically, this implies that factors affecting the cell wall traits of soil fungi (e.g. environmental stress, species turnover) may have considerable afterlife effects on rates of soil N availability. Future field studies are needed to confirm this hypothesis.

Implications of a two-pool model for soil carbon storage

Both fast and slow decomposing pools of fungal necromass are likely to affect rates of SOM accumulation, but through different mechanisms. The fast fraction will directly contribute to mineral-stabilised SOM formation insomuch as low-molecular weight components (e.g. amino sugars, lipids) released during decomposition are directly sorbed to mineral surfaces (Miltner et al., 2012; Shao et al., 2019). This pool may also affect rates of C stabilisation by altering the carbon use efficiency of the microbial communities that feed upon it (Cotrufo et al., 2013). Regardless of the mechanism, it is worth noting that the higher proportion of fast decomposing mass in fungal necromass relative to plant litter suggests that these substrates may play a disproportionate role in building stable soil C.

The role of the slow necromass pool in SOM accumulation is less clear, as its residence time has not been well quantified. Fernandez et al. (2019) found that the recalcitrant pool remained largely unchanged in litterbags for at least two years in a peat bog, with only negligible effects of temperature under oxic conditions. Since the litterbags in that study (53µm mesh, placed 5cm into *Sphagnum* spp.) prevented direct interactions with soil minerals, this pool persisted as particulate organic matter. While recent research has focused on the role of mineral associated organic matter in SOM accumulation (Lavallee et al., 2019), fungal byproducts physically stabilised as particulate matter can constitute a large proportion of SOM (Frey, Elliott, & Paustian, 1999; Six et al., 2006). Melanin may be especially important to this pool, as fungal-derived melanin is prevalent in soils across systems (Van Der Wal et al., 2009), correlates with soil C stocks (Siletti et al., 2017), and has the potential to accumulate rapidly (Kallenbach et al., 2016). Because melanin is unhydrolysable even by strong acids (Bull, 1970), it is worth noting that fungal melanin is likely included in estimates of pyrogenic or "slow-moving" soil C pools determined via acid hydrolysis (Paul et al., 2006).

Study limitations and future directions

This study advances understanding of fungal necromass decay as it relates to substrate chemistry, but many limitations exist due to it being conducted under laboratory conditions. The soils used in our microcosms contained an intact community of soil saprotrophs, but not active mycorrhizal fungi, which influence decomposition in the field (Frey, 2019). It is also possible that inoculating with *M. elongata* biased our results towards the enzymatic capabilities of this fungi. However, *M. elongata* is an early colonizer of

necromass and is quickly outcompeted (Beidler et al., 2020; Fernandez & Kennedy, 2018), and prior work suggests it can decompose both chitin (De Boer et al., 1999) and β-glucans (Li et al., 2018), the major polysaccharides present in fungal cell walls. Finally, our results reflect decomposition dynamics from a single soil type. Biotic and abiotic differences across systems will likely to affect fungal necromass decomposition as they do plant tissues (Prescott, 2010; Veen et al., 2015). Currently, the only cross-system study of necromass decomposition found relatively small effects of edaphic factors and plant communities on the rate of fungal necromass decay, concluding that substrate chemistry was the largest driver (Beidler et al., 2020). Future field studies across a wide range of soil conditions are needed to confirm this pattern.

Conclusions

Here we demonstrate strong generality of the asymptotic decomposition model for describing mass loss in fungal necromass, which occurs in two stages driven by distinctly different chemical fractions of the substrate. The fast pool constitutes the majority of fungal dry mass, and decomposes exponentially at a rate that is positively related to the mass of cell soluble contents and negatively to the mass of cell wall constituents. The size of the cell wall fraction (relative to cell soluble components) determines the rate of N release during the early stages of decomposition, and whether the necromass acts as a net source or a net sink of N during this time. The residence time of the slow decomposing fungal necromass pool remains unknown, but is composed of melanins and other aromatic, acid-unhydrolysable compounds. Beyond empirically fitting the data, the asymptotic model of decomposition implicitly acknowledges the variation in biochemistry across this diverse

kingdom, allowing for better characterisation of the effects of fungal traits (e.g. melanisation, cell wall structure) on rates of soil C and N cycling.

Table 2.1

Model parameters and fit statistics for two decomposition models describing mass loss for 28 types of fungal necromass. k_s = exponential decay rate form single pool model, k = exponential decay rate from asymptotic model, A = size of remaining "slow pool" after exponential phase (asymptotic model only), AIC= corrected Akaike Information Criterion score, RSS= Root sum of square error for model.

Necromass type				Single exponential model			Asymptotic model			
Species	Tissue	Order	Trophic Mode	k_s	AIC	RSS	A	k	AIC	RSS
Lactarius vinaceorufescens	Stipe	Russulales	Mycorrhizal	0.03	−15.24	0.014	0.15	0.04	−21.17	0.004
Laetiporus sulphureus	Sporocarp	Polyporales	Wood rotter	0.03	−10.52	0.031	0.07	0.04	−8.85	0.029
Camarops petersii	Sporocarp	Boliniales	Wood rotter	0.02	−7.50	0.052	0.35	0.06	−31.89	0.001
Laccaria laccata	Stipe	Russulales	Mycorrhizal	0.03	−4.15	0.090	0.22	0.08	−4.38	0.062
Lactarius chelodonius	Stipe	Russulales	Mycorrhizal	0.05	−6.10	0.065	0.19	0.09	−8.88	0.029
Scleroderma citrinum	Sporocarp	Boletales	Mycorrhizal	0.04	−2.74	0.114	0.29	0.09	−14.98	0.011
Russula emetica	Cap	Russulales	Mycorrhizal	0.06	−4.70	0.082	0.22	0.11	−16.24	0.009
Rhizopogon ochraceorubens	Sporocarp	Boletales	Mycorrhizal	0.08	−4.37	0.087	0.14	0.11	−4.81	0.058
Macrolepiota procera	Cap	Agaricales	Soil saprotroph	0.10	−6.61	0.060	0.13	0.12	−8.76	0.030
Suillus grisellus	Stipe	Boletales	Mycorrhizal	0.06	−3.61	0.099	0.23	0.12	−9.51	0.026
Boletus pseudosensibilis	Stipe	Boletales	Mycorrhizal	0.06	−3.13	0.107	0.23	0.12	−8.09	0.034
Gomphidius glutinosus	Stipe	Boletales	Soil saprotroph	0.07	−3.16	0.107	0.21	0.12	−7.02	0.040
Russula emetica	Stipe	Russulales	Mycorrhizal	0.07	−3.64	0.098	0.24	0.12	−14.45	0.012
Suillus viscidus	Stipe	Boletales	Mycorrhizal	0.09	−4.96	0.079	0.15	0.13	−6.76	0.042
Tricholoma spp	Stipe	Agaricales	Mycorrhizal	0.05	−2.40	0.121	0.25	0.13	−8.42	0.032
Hygrophorus paludosoides	Stipe	Agaricales	Soil saprotroph	0.07	−2.38	0.121	0.20	0.13	−4.31	0.063
Lactarius chelodonius	Cap	Russulales	Mycorrhizal	0.07	−3.83	0.095	0.21	0.13	−9.91	0.025
Leccinum aurantiacum	Stipe	Boletales	Mycorrhizal	0.09	−0.73	0.160	0.19	0.15	−1.35	0.103
Grifola frondosa	Sporocarp	Polyporales	Wood rotter	0.13	−5.54	0.072	0.11	0.16	−5.86	0.049
Suillus spectabilis	Stipe	Boletales	Mycorrhizal	0.12	−8.36	0.045	0.13	0.16	−14.80	0.011
Macrolepiota procera	Stipe	Agaricales	Soil saprotroph	0.13	−2.62	0.117	0.13	0.17	−2.68	0.083
Hygrocybe punicea	Stipe	Agaricales	Soil saprotroph	0.13	−5.73	0.069	0.15	0.19	−9.41	0.027
Boletus pseudosensibilis	Cap	Boletales	Mycorrhizal	0.15	−7.26	0.054	0.13	0.19	−10.73	0.022
Polyporus squamosus	Sporocarp	Polyporales	Wood rotter	0.17	−8.22	0.046	0.08	0.20	−8.25	0.033
Boletus campestris	Stipe	Boletales	Mycorrhizal	0.15	−4.38	0.087	0.18	0.22	−9.73	0.026
Chlorophyllum molybdites	Stipe	Agaricales	Soil saprotroph	0.14	−3.26	0.105	0.22	0.23	−13.23	0.014
Suillus spectabilis	Cap	Boletales	Mycorrhizal	0.17	−7.17	0.055	0.14	0.24	−12.23	0.017
Chlorophyllum molybdites	Cap	Agaricales	Soil saprotroph	0.17	−3.85	0.095	0.18	0.26	−8.04	0.034

Table 2.2

Pearson's correlation coefficients between chemical fractions and normalized FTIR peaks for 28 fungal necromass types. Columns reflect FTIR wavenumber and the corresponding organic functional group. *A* and *k* are parameters from an asymptotic decomposition model. All chemical and fiber fractions were calculated as a percentage of dry mass. Bold, italicised values denote statistical significance at $P<0.10$, "*" denotes $P<0.05$, "**" denotes $P<0.01$, and "***" denotes $P<0.001$.

	Aromatic		Amide		Alcohol		Aliphatic		Alkene
	840	1,234	1,650	1,550	1,080	1,160	2,850	2,924	920
A	−0.21	***0.35***	−0.07	0.02	0.18	0.13	***0.33***	***0.35***	−0.02
K	0.23	−0.16	***0.47****	***0.45****	***−0.40****	***−0.69*****	−0.16	−0.20	−0.11
Total N (%)	−0.13	***0.33***	***0.83*****	***0.80*****	***−0.70*****	−0.28	***0.37***	***0.34***	***−0.32***
Melanin (%)	0.07	***0.37****	−0.10	−0.03	0.01	0.02	***0.30***	***0.39****	−0.09
Total C (%)	***−0.41****	***0.56*****	0.27	0.21	***−0.58*****	−0.18	***0.72*****	***0.78*****	***−0.53*****
Cell soluble components (%)	***0.44****	−0.17	0.22	0.26	−0.23	***−0.63*****	−0.27	−0.22	0.06
Acid detergent fraction (%)	−0.21	−0.16	−0.28	−0.33	***0.34***	***0.42****	−0.13	−0.20	0.16
Acid hydrolysable fraction (%)	***−0.44****	−0.05	−0.22	−0.24	0.18	***0.45****	0.15	−0.01	−0.15
Non-hydrolysable fraction (%)	−0.14	***0.5*****	0.11	0.13	−0.12	0.27	***0.50*****	***0.65*****	−0.13

Figure 2.1

Relationships between fast pool decay rates (i.e. *k*-values from the asymptotic models) and initial substrate chemistry for the 28 fungal necromass types.

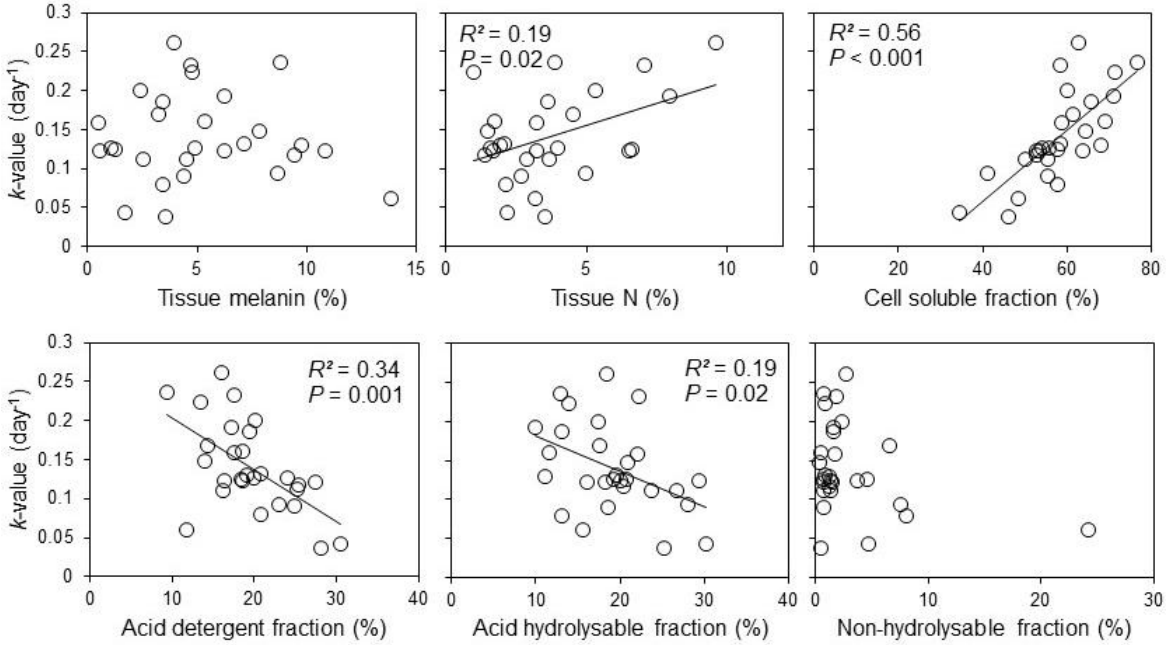

Figure 2.2

Relationships between slow pool size (i.e. *A*-values from the asymptotic models) and initial substrate chemistry for the 28 fungal necromass types.

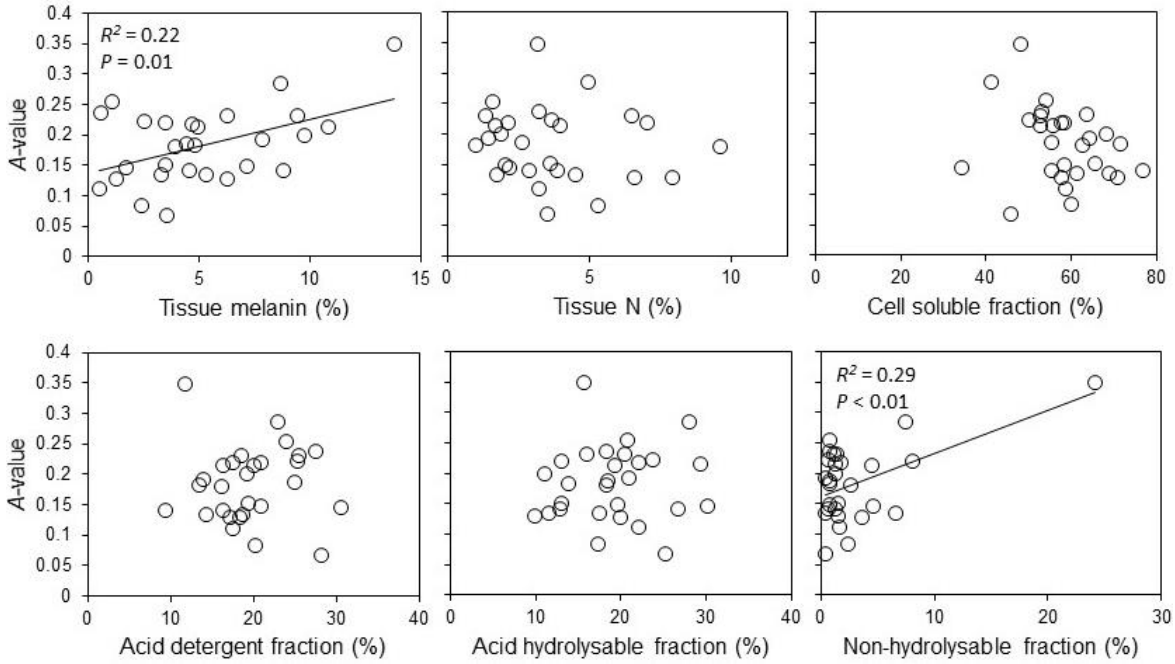

Figure 2.3

(a) Patterns of N release from decomposing fungal necromass over a 43-day period, calculated for five substrates as the proportion of the initial N pool. **(b)** The maximum proportion of N immobilised for each substrate over the course of decomposition declined as the decomposition rate *k* of the fast pool increased. **(c)** The maximum proportion of N immobilised was lower in substrates with high initial cell soluble contents. **(d)** Normalized R-OH bond contents (reflecting cell wall polysaccharides) estimated using peak intensity at 1160 cm^{-1} on FTIR spectrum linearly predicted the maximum proportion of initial substrate N immobilised.

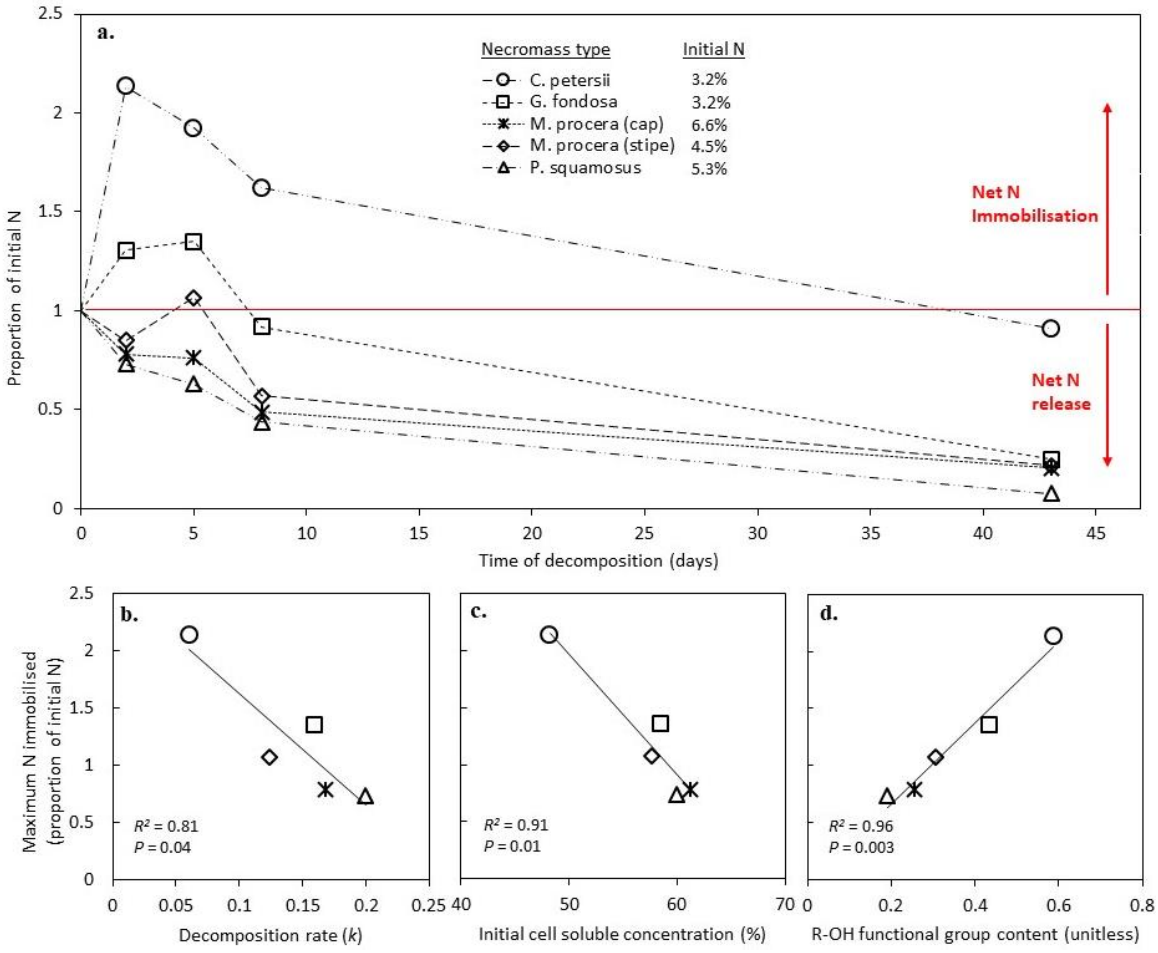

Chapter 3

Hyphae move matter and microbes to mineral microsites: integrating the hyphosphere into conceptual models of soil organic matter stabilization

Summary

Recent work has highlighted the importance of microbially-derived organic matter in association with soil minerals (MAOM) as a pool of slow cycling soil carbon (C). The rhizosphere, defined as the zone of influence proximate to roots, is thought to control the spatial extent of MAOM formation because it is the dominant entrypoint of new C inputs to soil. However, this implicitly assumes that microbial redistribution of C into bulk (non-rhizosphere) soils is minimal. We question this assumption, arguing that the fungal redistribution of soil C from the rhizosphere to bulk soil minerals is common, and encourages MAOM formation. First, we summarize published estimates of fungal hyphal length density and turnover rates to argue that fungal C inputs are high throughout the rhizosphere-bulk soil continuum. Second, because colonization of hyphal surfaces is a common dispersal mechanism for soil bacteria, we argue that hyphal exploration allows for the non-random colonization of mineral surfaces by hyphae-associated taxa. These bacterial communities and their fungal host will determine the chemical form of organic matter deposited on the colonized mineral surface. Collectively, this work demonstrates that omission of the hyphosphere from conceptual models of soil C flow overlooks a key mechanism for MAOM formation in bulk soils. There is an urgent need for quantitative research characterizing the environmental drivers of hyphal exploration and hyphosphere community composition across systems, as these traits represent dominant controls over the deposition rate and organic chemistry of C deposited on minerals.

Introduction

Soils store the majority of terrestrial carbon (C), and a mechanistic understanding of the formation of soil organic matter (SOM) with a long residence time will be crucial to predicting future atmospheric C concentrations (Sulman et al., 2018). Recent work has focused extensively on the formation of mineral-associated organic matter (MAOM) due to its potential to persist at for millenia (Dungait et al., 2012; Schmidt et al., 2011). Broadly defined, MAOM consists of low molecular weight organic molecules that are chemically bonded to soil mineral surfaces (Lavallee et al., 2019), although both the molecular species and bond types can vary considerably (Kögel-Knabner et al., 2008). While plant-derived compounds represent the ultimate source of new C inputs to soils, there is growing recognition that the majority of MAOM in many soils likely originates from microbial byproducts (Grandy & Neff 2008; Miltner *et al.* 2012; Cotrufo *et al.* 2013a; Sokol *et al.* 2019a; but see Castellano *et al.* 2015; Angst *et al.* 2021).

The rhizosphere, defined as the zone of biological influence surrounding the root, serves as a spatially explicit point of entry for newly fixed C into mineral soils and a locus of microbial activity (Kuzyakov & Blagodatskaya, 2015). Accordingly, the spatial extent of the rhizosphere has been proposed as a dominant control point for the formation of new microbially-derived MAOM (Figure 3.1a, Rasse *et al.* 2005; Sokol & Bradford 2019). While conceptually attractive, focus on the rhizosphere as the dominant location of new microbially-derived MAOM is hard to reconcile with observations from CO_2 pulse-labeling studies, which often recover large proportions (c.a. 30-50%) of belowground plant

C allocation outside of the rhizosphere within days of adding the label (e.g. Norton *et al.* 1990; Leake *et al.* 2001). This non-rhizosphere C flux occurs via mycorrhizal fungal hyphae, which can explore soil centimeters away from the root (Agerer, 2001; Friese & Allen, 1991). Similarly, saprotrophic soil fungi redistribute C from high-to-low organic matter soil regions while searching for patchily-distributed nutrients (S. D. Frey et al., 2003). Despite representing a ubiquitous and dynamic network of labile C in soil, fungal hyphae and the zone they influence (the "hyphosphere", Figure 3.1b,c) are not explicitly included in conceptual models of MAOM formation, which implicitly assume that the rhizosphere is the point of conversion of plant C to MAOM (Miltner et al., 2012; Schmidt et al., 2011; Sokol et al., 2019b). While the rhizosphere is undoubtedly the point of entry for newly fixed C to soils, we argue that conceptual omission of the hyphosphere from these models hinders our understanding of the microbial processes that ultimately control the rate and spatial extent of MAOM formation in soils (Anthony et al., 2020b).

Mycorrhizal fungi are increasingly recognized as an important SOM input (Cairney, 2012; K. E. Clemmensen et al., 2013; Ekblad et al., 2013; Serita D. Frey, 2019; Godbold et al., 2006a; J. Leake et al., 2004). Estimates of ectomycorrhizal (EcM) fungal hyphal production range from 40-1000 kg ha yr^{-1} in the top 10 cm of soil (Ekblad et al., 2013), while one study found hyphal production by arbuscular mycorrhizal fungi (AM) to be 339-457 kg ha yr^{-1} (Miller et al., 1995), making hyphal production potentially comparable to fine root production (ca. 400-1500 kg ha yr^{-1}; Jackson *et al.* 1996, 1997; McCormack *et al.* 2015) in some systems. Due to their microscopic diameters, hyphae explore tens to thousands of meters of pore space within a single cubic centimeter of soil, representing a

large flux of labile organic matter at spatial scales relevant to MAOM formation (Godbold et al., 2006a). While hyphal densities are typically assumed to be higher inside of the rhizosphere, rhizosphere and non-rhizosphere soils often have similar fluxes of newly-fixed C into fungal biomass (Huang et al., 2020). As such, the existence of a hyphosphere which moves plant-derived C well beyond rhizosphere soils suggests that considering fungal dynamics will be critical to the underlying processes driving MAOM formation.

Here, we summarize disparate areas of research to demonstrate that fungal hyphae are crucial to the transport and subsequent stabilization of organic matter throughout the soil matrix. First, we contend that because of the high density, rapid turnover, and rapid decomposition of hyphae, the majority of organo-mineral interactions originate from hyphosphere, not rhizosphere derived C. Second, we describe mounting evidence suggesting that hyphae act as "highways" upon which unicellular microbes travel or are transported, helping disperse these organisms to mineral binding sites of MAOM formation beyond the rhizosphere. Third, we identify three distinct mechanisms by which organic matter is transferred from hyphae to mineral surfaces upon colonization. Collectively, these properties of the hyphosphere suggest that hyphal movement of matter to mineral microsites drive rates of MAOM formation in soil. We discuss predictions for how fungal traits might affect rates MAOM formation and conclude with a set of research priorities that will be crucial to integrating the hyphosphere into conceptual and process-based models of MAOM formation. Although our focus is on drivers of MAOM formation, the hyphosphere properties reviewed here have clear implications for particulate organic C accumulation as well.

Hyphae distribute carbon to minerals

Soil hyphal dynamics are difficult to accurately quantify *in situ* (Fernandez, 2021), but existing estimates of hyphal exploration clearly demonstrate their importance relative to roots in distributing C throughout the soil matrix. We conducted Based on a literature search, we found that field-based estimates of hyphal length density in EcM-dominated systems averaged 137,700 cm cm^{-3} across sites and soil depths ≤ 30 cm, with the lowest study reporting a density of 1,800 cm cm^{-3} (Table 3.1, Appendix S3.1 for calculation methods). When considering studies that measured only AMF hyphae (i.e. excluded other fungi), global densities still averaged 1,553 cm cm^{-3} (Table 3.1). These values stand in stark contrast to global estimates of root length density, which average just 6.8 cm cm^{-3} (Jackson *et al.* 1997). Although there is wide variation in both root and hyphal density estimates it is safe to assume that the surface area of potential mineral binding sites in contact with standing stocks of soil hyphae outnumber those in direct contact with root surfaces by multiple orders of magnitude.

In addition to the spatial extent of standing hyphal biomass, the ephemeral nature of fungal hyphae means that they explore more soil volume than roots per unit time. Although published estimates of hyphal turnover rate are sparse, methodologically inconsistent, and largely focused on mycorrhizal fungi, some patterns have begun to emerge. For example, the turnover rates of AM hyphae appear to be much faster than those of EcM hyphae (Table 3.2). Multiple studies suggest that the lifespan of absorbent AMF hypha is less than one

week (Table 3.2), implying potential turnover rates as rapid as 60 yr^{-1} in systems with year-round growing seasons, though in seasonal systems turnover rate appears to be much slower during the dormant season (Treseder et al., 2010). Turnover rates of AMF have been assessed either by visually following individual hyphae through time (using a soil window or minirhizotron) or by repeated measurements of hyphal C isotopes following a pulse labeling of CO_2. Conveniently, these two methods have largely yielded similar turnover estimates. In contrast, EcM hyphal turnover rates have generally been assessed less directly, by combining hyphal production rates from ingrowth cores with estimates of standing hyphal biomass from ergosterol extractions. These studies assume that the sand substrate within the ingrowth cores limits the presence of saprotrophic fungi and therefore makes the estimate representative of EcM fungal turnover, but this assumption may be problematic (Branco et al., 2013; Fernandez, 2021). These studies have all been conducted in the field, with estimated turnover rates ranging from 3.2-13 yr^{-1}. Regardless of these differences by mycorrhizal type, even low estimates of hyphal turnover rates from these studies stand in stark contrast to estimates of fine root turnover, which has a global average of 0.82 ± 1.11 yr^{-1} (mean, s.d.) based on estimates using the Fine Root Ecology Database (Iversen *et al.* 2017; Appendix S3.2).

Although we recognize that the summary estimates of both hyphal density and turnover are poorly constrained, their magnitude in relation to fine roots clearly demonstrates the importance of hyphae to the frequency of organo-mineral interactions in soil. Assuming an annual EcM hyphal turnover rate of 7.6 yr^{-1} (mean across studies in Table 3.2) and average hyphal density of 137,700 cm cm^{-3} (average of woody systems, Table 3.1), the product of

these numbers would suggest that EcM fungi have the potential to explore more than 1,000,000 cm of pore space per cm^3 annually. The same calculation for AM fungi (mean hyphal turnover = 62 yr^{-1} during active season, average density in grasslands = 1,973 cm cm^{-3}) suggests the potential of these hyphae to explore over 120,000 cm cm^{-3} annually. These estimates stand in stark contrast to comparable estimates of annual root exploration. Using the global averages of fine root density in table 3.1, and turnover rates from the FRED database, a similar calculation for annual root exploration averages only 2.1 cm cm^{-3} yr^{-1} in woody systems and 11.7 cm cm^{-3} in grassland systems (Appendix S3.2). Even with the high uncertainty associated with each of these values, they strongly signal the importance of hyphae for distributing new C through soil across time and space.

Ultimately, relating the soil volume explored by hyphae to potential C stabilization will e depend on interactions between fungal community traits and soil physiochemical properties. Research to date has focused primarily on mycorrhizal fungi, and these are arguably more important than saprotrophs since they represent new inputs of gross primary productivity to soils. However, all hyphae have the potential to distribute C spatially through soils, and are thus important in the context of MAOM formation. More accurate estimates of the hyphal length density and turnover rates for entire fungal communities are needed across systems, as well as a better understanding of the factors influencing these dynamics. Soil structure influences the extent of hyphal exploration (Ritz & Young, 2004), more quantitative data on these effects are greatly needed. Importantly, while hyphal exploration determines the potential for hyphosphere-derived MAOM formation, the proportion and reactivity of available mineral binding sites and the surface area of soil particles within a given soil volume (i.e. porosity) are ultimately just as important for C

stabilization (X. Wang et al., 2019). Moreover, the affinity of organo-mineral bonds varies by both mineral-type and organic molecule species (Jilling et al., 2018; Kleber et al., 2015), implying complex interactions between soil mineralogy and the hyphosphere communities responsible for depositing organic substrates.

Hyphae distribute other microbes through soil

As hyphae redistribute organic matter through soils, they provide a physical structure which allows for the transport and establishment of microbial communities to microsites (Guennoc et al., 2018; Junier et al., 2013; Nazir et al., 2010; Warmink et al., 2011). Soils are one of the most heterogeneous environments on Earth (Vos et al., 2013). To account for the spatial and temporal patchiness in water and resource availability, the vast majority of unicellular microbes in soil exist as colonies anchored to surface particles by extracellular polymeric substances (EPS) (Costa et al., 2018). The physical dispersal of these organisms through the soil matrix is prevented by air pockets, with motility largely restricted along the water films connecting particles (Dechesne et al., 2010), and subsequent establishment after colonization determined by resource availability (Or et al., 2007). Hyphae-forming fungi move freely through soil pores and provide both a trail of available C and a physical substrate upon which unicellular microbes can travel. Bacterial migration along these "fungal highways" is well documented. Flagellated bacteria are able to swim along the water films on hyphal surfaces (Yuanchen Zhang et al., 2018), and biofilms of non-motile bacteria enmeshed in EPS have been observed on the hyphae of AM, EcM, saprotrophic, and plant pathogen fungi (Guennoc et al., 2018; Hover et al.,

2016; Nazir et al., 2014; Scheublin et al., 2010). Importantly, these biofilms occur on both live and dead hyphae (Guennoc et al., 2018), but tend to concentrate along the leading edge of hyphal exploration (Guennoc et al., 2018; Nazir et al., 2014; Otto et al., 2017), underscoring the importance of fungal exploration to new colony establishment of soil microsites (Warmink et al., 2011).

Bacterial assemblages on hyphae are not random, and relationships among these taxa and their host fungi span the full range ecological interactions (Deveau et al., 2018). Hyphosphere communities are diverse, and community composition (on a single species of hyphae) varies with nutritional demand in both mycorrizal (Gorka et al., 2019; F. Wang et al., 2019) and saprotropic fungi (Yuan Zhang et al., 2020). Bacterial community assembly on AMF hyphae appears to be relatively conserved across time and soil, and similar across two genera of AMF species (Emmett et al., 2021). Both field and laboratory studies suggest that the presence of individual fungal taxa can structure the composition and function of soil bacterial communities (e.g. Zagryadskaya *et al.* 2011; Nuccio *et al.* 2013; Liu *et al.* 2018). Moreover, a recent AMF mesocosm study demonstrated different bacterial assemblages colonizing different minerals, and concluded that assembly was dispersal limited (Whitman et al., 2018). In this way, the fungal community composition of the hyphosphere directly impacts the functional diversity of the bacterial communities which establish on soil minerals.

Hyphal establishment on mineral surfaces encourages MAOM formation

There is growing consensus that a large proportion of MAOM consists of common microbial biomolecules such as polysaccharides, lipids, organic acids, and enzymes (Grandy & Neff, 2008; Heckman et al., 2018; Miltner et al., 2012). As fungi comprise the majority of soil microbial biomass (He et al., 2020) and necromass (Liang et al., 2019; Simpson et al., 2007) in terrestrial systems, they likely contribute disproportionately to microbially derived MAOM. Hyphal proliferation along soil mineral surfaces leads to the production and subsequent stabilization of microbial compounds via three distinct mechanisms (Figure 2): (1) live hyphae and their associated microbes produce exudates (organic acids, enzymes, sugars) which can become sorbed, (2) when hyphae die, the direct decomposition products of the fungal necromass can become sorbed, and (3) as decomposition of the original fungal necromass proceeds, molecules originating from processes of microbial succession (e.g. EPS, exudates, bacterial necromass products) can become sorbed. The relative importance of these mechanisms will depend on both the hyphosphere community composition (Anthony et al., 2020a) and mineralogy (Creamer et al., 2019; Heckman et al., 2018).

Both hyphae and their associated microbes release a suite of organic exudates into their surrounding environment which have the potential to interact with minerals (Fig. 3.2a). The simplest of these molecules are sugars exuded by hyphae to stimulate growth of unicellular symbionts to increase nutrient acquisition (L. Zhang et al., 2016). Many of the exudates produced by hyphosphere microbes are meant to degrade existing SOM for resource acquisition, but may end up forming MAOM. For instance, extracellular enzymes intended to liberate organic matter or nutrients can form stable bonds with clay minerals (Olagoke et al., 2019), and may represent an underappreciated source of MAOM in some

systems. Indeed, a recent comparison across Critical Zone Observatory sites found that 80% of the enzymes present in the whole soil column were sorbed to clays in deeper mineral soils (Dove et al., 2020). Similarly, mineral-sorbed organic acids are thought to originate from root exudates and leaching from organic horizons (Sokol et al., 2019a), but may be fungal in origin, since hyphae produce large quantities of these acids to accelerate the weathering of minerals (Blum et al., 2002a; Hoffland et al., 2004; Smits & Wallander, 2017). Given the close proximity to mineral surfaces and the high sorptive affinity of these acids, hyphosphere exudates likely contribute substantially to this MAOM pool in mineral soils.

As hyphae senesce, the decomposition products of fungal necromass provide a wide range of organic molecules for sorption (Fig 3.2b). When fungal cells lyse, soluble components within the cell such as amino acids and sugars are made immediately available to the surrounding environment and can sorb to mineral surfaces or be consumed by decomposers for further transformation (see next paragraph). Depolymerization of B-glucans and chitin, the main components of the cell wall, occurs over the course of days to weeks (Fernandez et al., 2016b; See et al., 2020), providing opportunities for sorption of amino sugar monomers or polysaccharide chains. As hyphal necromass decomposition proceeds, more slowly decomposing cell wall components yield more complex molecules for organo-mineral interactions. For example, much has been written about the positive relationship between the AMF-produced glycoprotein glomalin and SOM formation in soils (Rillig & Mummey, 2006). Similarly, many dikaryotic fungi (including many EcM species) contain melanins within their cell walls, which can persist in soils for millennia (Scott et al., 2010).

A recent decomposition experiment demonstrated that the melanized fraction of fungal hyphae persisted for two years as particulate matter in litterbags (Fernandez et al., 2019). The extent to which melanin-derived molecules form organo-mineral complexes remains poorly characterized, but such complexes are likely important given the ubiquity of melanized fungi (Siletti et al., 2017) and the fact that other complex aromatic molecules (i.e. lignins) contribute substantially to mineral-bound SOM (Angst et al., 2021; Rasse et al., 2005). Indeed, increases mineral-associated phenolic and aromatic compounds were observed after 18 months of microbial growth in lignin-free model soils (Kallenbach et al., 2016), suggesting the accumulation of fungal melanins.

Fungal necromass contains a higher proportion of labile C (e.g. cell soluble sugars, polysaccharide chains) than root litter, and hyphal decomposition rates are commonly measured in days, while fine root decomposition commonly occurs over the course of years (See *et al.* 2019, 2020). As hyphal necromass decomposes, it forms the base of a complex food web of microbial decomposers dominated by bacterial taxa (López-Mondéjar et al., 2018b) which anchor themselves to the hyphal remnants and adjacent mineral surfaces with EPS (Fig. 3.2c). This biofilm production is thought to be a dominant source of MAOM in many soils (Kleber et al., 2015). Many of the bacterial taxa present on living mineral-associated hyphae are likely some of the earliest necromass decomposers when the hyphae senesces. For instance, biofilms of *Pseudomonas* species are common on EcM genus *Laccaria*, and thought to be beneficial to the fungi (Duponnois & Garbaye 1991; Labbe *et al.* 2014; Guennoc *et al.* 2018), and these taxa have also observed in high numbers during the first weeks of fungal necromass decomposition in field studies (Beidler et al., 2020;

Brabcová et al., 2016b; Fernandez & Kennedy, 2018). As microbial succession proceeds other decomposer taxa establish, likely arriving via other hyphae or by traveling along EPS pathways established on the decomposing hyphae. Within days to weeks, little of the original hyphal necromass remains, but the C deposited by the hyphae on the microsite will constitute the majority of the microbial residues replacing it (Fig 3.3).

Drivers of hyphosphere function related MAOM formation

The work summarized above highlights and urgent need to understand the factors controlling the variability of hyphosphere spatiotemporal dynamics and microbial community composition across systems. Collectively, these two factors will exert strong controls over the rate and molecular composition of MAOM formation in soil (Fig. 3.4). Current understanding of these traits and environmental factors influencing their variability is still nascent, but some general principles have started to emerge.

The dominant trophic mode (i.e. mycorrhizal vs saprotrophic) will affect the spatial extent of the hyphosphere throughout the soil profile (Fig. 3.2a). Saprotrophic fungi are limited by the availability of both C and nutrients in soil, and their exploration will be higher in regions of higher soil organic matter where these resources are coupled. In contrast, mycorrhizal fungi are not limited by soil C availability, and their hyphal exploration is dictated instead by the nutrient demands of the plant host (Han et al., 2020; Smith & Read, 2008), suggesting they may play a disproportionate role in distributing newly fixed carbon to mineral soil (Ekblad et al., 2013; Godbold et al., 2006b). Indeed, the proportion of

mycorrhizal hyphae relative to saprotrophic fungi increases with decreasing SOM:mineral content in soils (Carteron et al., 2020; Lindahl et al., 2007; Schlatter et al., 2018). It was recently demonstrated that the contribution of AMF-associated glomalin to soil C pools increases with depth of mineral soil (W. Wang et al., 2017); similar patterns with depth have been observed with EcM-associated melanins (Karina E. Clemmensen et al., 2015b), though this study was conducted in a highly organic soil. It appears that EcM hyphae may be more extensive than AM hyphae in their spatial exploration, suggesting greater rates of deposition on minerals, (Table 3.1), but this may be partially offset by the fact that AMF hyphae turn over more rapidly (Table 3.2). These differences support the idea of alternative nutrient foraging strategies among mycorrhizal guilds (i.e. tradeoffs between root and hyphal foraging precision; Chen *et al.* 2016). However, both EcM and AM fungal taxa vary considerably in the extent of their hyphal exploration (Agerer, 2001; Jakobsen et al., 1992; Joner & Jakobsen, 1995; Schnepf et al., 2008), and species composition within both of these guilds varies with soil depth and organic matter content (Bahram et al., 2015; Rosling et al., 2003). This fungal diversity also structures hyphosphere bacterial diversity (*sensu* section 3), and therefore affects not only the rate of C accumulation in mineral soils, but the organic chemistry of the C deposited (Fig. 3.4).

Environmental stressors play an important role in structuring the composition and function of hyphosphere fungal and bacterial communities (Lustenhouwer et al., 2020; Moore et al., 2021), which will have cascading effects on the rate and chemistry of MAOM formation (J. Schimel et al., 2007; J. P. Schimel & Schaeffer, 2012). A full review of these stressors is beyond the scope of this paper, but examples include baseline edaphic factors such as

soil water availability, pH, and salinity (Rath & Rousk, 2015; J. P. Schimel, 2018; Tedersoo et al., 2020), as well as the natural and anthropogenic disturbances that affect these factors (Hopkins et al., 2021; Kane et al., 2020; Querejeta et al., 2009). Importantly, environmental stressors will not only alter the microbial community composition of the hyphosphere, but also the physiology of individual taxa as it relates to C use and MAOM formation (e.g. allocation to EPS production, Schimel & Schaeffer 2012). For instance, melanized structures in fungi are energetically expensive to produce, and protect from environmental stressors ranging from desiccation to metal toxicity (Koide et al., 2014). Melanization of the hyphosphere has been shown to occur during periods of drought (Querejeta et al., 2009), and effects the chemistry of C deposition directly by increasing the aromatic complexity of hyphal necromass, and indirectly by structuring the community composition of bacterial decomposers present (Fernandez & Kennedy, 2018). Similarly, cell walls composed of ß-glucans may be more resistant to decomposition than those composed of chitin alone, and may be more prevalent in more stressful environments (Treseder & Lennon, 2015). Thus, environmental stressors with play a large role in controlling the functional composition of hyphosphere communities, and ultimately the rate and chemistry of MAOM formation (Koide et al., 2014).

In addition to environmental stressors and trophic mode, the stoichiometry of biotic resource limitation in relation to resource availability will dictate the extent of hyphal exploration along mineral surfaces. The hyphal growth form evolved in part as an adaptation to account for heterogeneous distribution of the multiple resources required for life (Nagy *et al.* 2020). Fungal "mining" of mineral-derived nutrients is well documented

(Burford et al., 2003; Hoffland et al., 2004), and can represent a significant input of rock-derived nutrients to ecosystem budgets (Blum et al., 2002b). Similarly, mycorrhizal fungal exploitation of soil water in mineral soils is common in water stressed systems (Augé, 2001; Lehto & Zwiazek, 2011). It stands to reason then, that soils where mineral resources (e.g. Ca, P, K, Mg, water) are in high demand will have greater hyphal exploration (and subsequent rates of C deposition) on mineral surfaces. This hypothesis further points to the relative importance of mycorrhizal fungi in rates of MAOM formation, as their relative lack of C limitation should allow them increased access to these regions of lower organic matter. A comprehensive understanding of multiple resource limitation by fungi and their associated plants and microbes across systems remains elusive, but is an active area of research (Van de Waal et al., 2018) with clear implications for the rate of C distribution through mineral soils.

Conclusions:

We contend that although plant detritus and exudates are the source of new C inputs to soil, fungal hyphae are the dominant mechanism by which this C is distributed through the soil matrix. Hyphae explore many orders of magnitude more pore space than roots (Tables 3.1, Table 3.2), and in the process come into contact with orders of magnitude more mineral surfaces. Furthermore, hyphae shape the organic chemistry of C deposited on mineral surfaces through differences in hyphal chemistry and through their influence on bacterial community composition. Mycorrhizal hyphae are of particular importance because they represent a flux of newly-fixed atmospheric C, and are more likely to explore areas of low

organic matter. A better understanding the drivers of MOAM formation rates will thus require better characterization of the extent and functional diversity of the hyphosphere in mineral soils.

The task of integrating the hyphosphere into conceptual and process-based models of MAOM formation will require research across scales and disciplines. There is an urgent need for fine-scale estimates of hyphal exploration and functional community composition within and across mineral soils. Such estimates will require the use of laboratory and field-based mesocosms to provide spatially explicit measurements of hyphal length density, turnover, and microbial community composition. Incorporating buried mineral substrates and stable isotope probing approaches into these experiments would provide invaluable data relating hyphosphere function to rates of MAOM formation (Pett-Ridge & Firestone, 2017). As understanding of hyphosphere function relating to MOAM formation matures, a better understanding of the dominant controls of this functional diversity across systems will be crucial to its incorporation into global models (Sulman et al., 2018). The use of "omics"-based approaches will be invaluable in characterizing the response of hyphosphere functional traits to environmental conditions (Romero-Olivares et al., 2021), but will require validation with trait measurements (Malik et al., 2020). Focusing these tools on genes related to hyphal proliferation, fungal cell wall composition (e.g. melanization, glomalin production), and EPS production by hyphae-associated bacteria would be potentially valuable in linking environmental conditions to MAOM formation.

The purpose of this paper is to call attention to the importance of the hyphosphere as an input of new MAOM. Conversely, many studies have focused the importance of the hyphosphere in the decomposition of soil C, including MAOM (Averill et al., 2014; Frey, 2019; Read et al., 2004; Terrer et al., 2021; T. Wang et al., 2020; Zak et al., 2019). The net effect of soil fungi on soil C stocks will ultimately be determined by difference between these opposing effects. Moving forward, explicit consideration of the hyphosphere as a separate entity from the rhizosphere will be crucial to improving conceptual models belowground C dynamics.

Table 3.1

Global estimates of hyphal length density (mean, standard deviation) and fine root length density averaged by vegetation type in the top 30 cm of soil. Total hyphal estimates reflect studies where length of all fungal hyphae was quantified. Estimates of all hyphae in woody systems are dominated by studies that used sand ingrowth cores intended to quantify EcM fungi, and thus underestimate the contribution of saprotrophs. AMF only estimates reflect studies where AMF were measured using AMF-specific protocols. Fine root length density estimates were derived from Jackson et al. (1997). Data and calculation methods available in appendix S31.

Density in soil	Woody systems	Non-Woody Systems	Croplands	Global Mean
All hyphae (cm cm^{-3})	137,700 ± 318,332 (EcM-dominated)	23,990 ± 26,741	3,300 ± 1,411	76,400 ± 225,900
AMF only (cm cm^{-3})	2,059 ± 3,948	1,973 ± 3,178	292 ± 196	1,553 ± 2,903
Fine roots (cm cm^{-3})*	1.6	19.2	3.1	6.8

Table 3.2

Estimates of mycorrhizal hyphal turnover rates reported in the literature along with plant-host community and method of estimation.

Host species or community	Hyphal Type	Turnover Rate	Method	Source	Study location
Plantago lanceolata	AMF	52-60 yr^{-1} (5-6 day lifespan)	Repeated hyphal extraction after $^{14}CO_2$ pulse label	Staddon *et al.* (2003)	Pot study
Artemisia tridentata and *Oryzopsis hymenoides*	AMF	52-75 yr^{-1} (5-7 day lifespan)	Direct observation (soil window)	Friese & Allen 1991	Pot study
Lycopersicum esculentum	AMF	69 yr^{-1} for branched structures	Direct observation (soil window)	Bago *et al.* 1998	Pot study
Prunus pennsylvania, Rubus spp. woodland	AMF and saprotrophs	15-121 yr^{-1} (majority > 52 yr^{-1})	Direct observation (soil window)	Atkinson & Watson 2000	Field study
Plantago lanceolata	AMF	69 yr^{-1} for branched structures, <11 yr^{-1} for runner hyphae	Repeated fatty acid sampling after $^{13}CO_2$ pulse label	Olsson & Johnson 2005	Pot study
Bromus diandrus, Bromus hordaceous, Avena fatua	AMF and saprotrophs	median 2.5 yr^{-1} during dormant season	Direct observation (minirhizotrons)	Treseder *et al.* 2010	Field study
Mixed *Pinus* & *Quercus* forest	EcM	7.6 yr^{-1}	Direct observation (minirhizotrons)	Allen & Kitajima 2014	Field study
Pinus sylvestris	EcM (ergosterol)	3.2 yr^{-1}	Sequential ingrowth bags	Hagenbo *et al.* 2017	Field study
Pinus taeda	EcM (ergosterol)	13 yr^{-1}	Sequential ingrowth bags	Eckblad *et al.* 2016	Field study
Pinus palustris	EcM (ergosterol)	10 yr^{-1}	Sequential ingrowth bags	Hendricks *et al.* 2017	Field study

Temperate deciduous AMF and EMF forests	EcM & saprotrophs (ergosterol)	3.5 yr^{-1}	Sequential ingrowth bags	Cheeke 2021	Field study
Pinus pinaster, *Pinus sylvestris* and *Quercus ilex*	EcM (ergosterol)	7.2-9.9 yr^{-1}	Sequential ingrowth bags	Hagenbo *et al.* 2020	Field study

Figure 3.1

Generalized soil profile showing the spatial extent of the rhizosphere in yellow (a) contrasted against the spatial extent of the hyphosphere (b), depicted as a color gradient representing the relative dominance of fungal guilds. New leaf litter inputs are dominated by saprotrophic fungi (in blue), while regions of low organic matter in deeper soils are dominated by mycorrhizal fungi (in red). Soil particles located outside of the rhizosphere are heavily colonized by fungal hyphae (saprotrophic in blue, mycorrhizal in red), which represent transport of carbon from spatially distant (i.e. mm to cm) regions of soil (c).

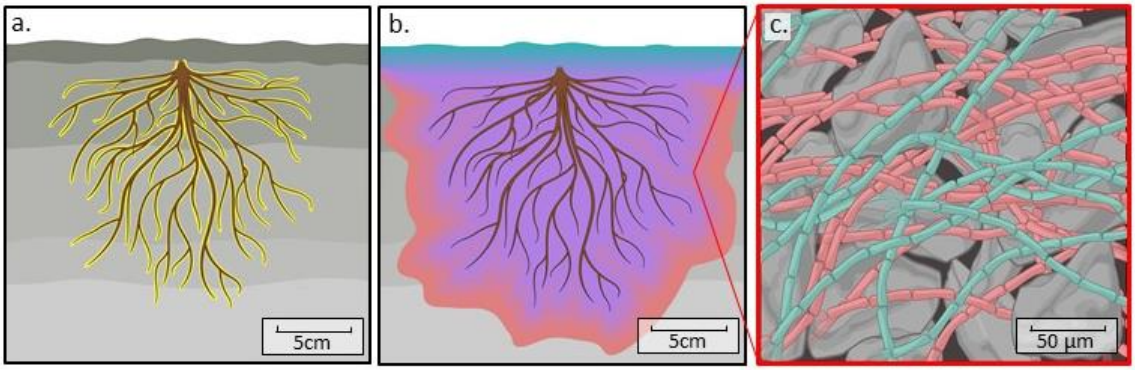

Figure 3.2

Three distinct mechanisms leading to the mineral stabilization of hyphosphere organic matter. Live hyphae and associated bacteria exude organic molecules (e.g. enzymes, sugars, organic acids, depicted by stars) into their environment (a). During the early stages of fungal necromass decomposition, hyphal cytoplasm components, cell wall polysaccharides, and lipids originating from the necromass are released (depicted as red dots) (b). As necromass decomposition proceeds, unicellular colonies of decomposers form EPS (depicted in green) along the remnants of recalcitrant cell wall structures (e.g. melanins) colonized the mineral surface.

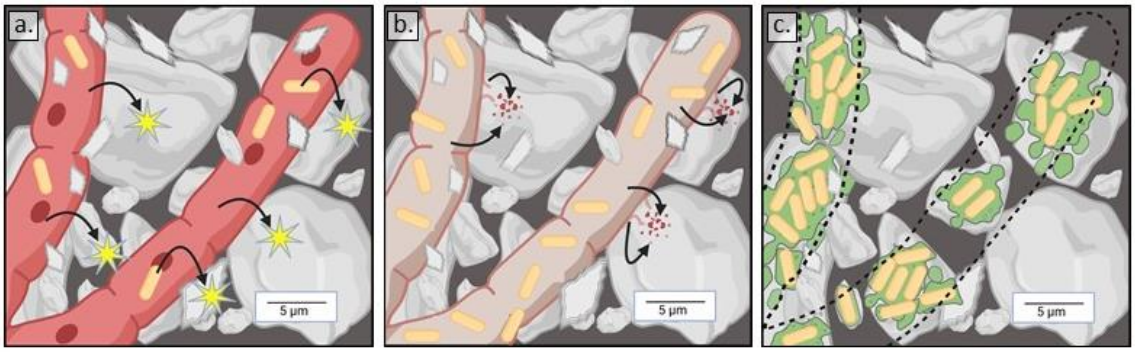

Figure 3.3

Images from an experiment in which organic matter free minerals were incubated in live soil for 35 days directly below decomposing fungal necromass isotopically enriched in 13C. A Scanning electron microscope (SEM) image of an unknown fungal saprotroph connecting fragments of vermiculite is shown in panel a. A segment of this hypha is depicted in panel b using Nano-scale secondary ion mass spectrometry (NanoSIMS), and reveals that the hypha is highly enriched in 13C, demonstrating transfer of the C from the decomposing substrate to the mineral surfaces. Panel C shows an SEM image of hyphae in various stages of decomposition along the surface of a goethite particle. A NanoSIMS image of the surface shown in panel c is depicted in panel d, and demonstrates that 13C enrichment of the surface is not randomly distributed in space, but concentrated in regions of hyphal colonization. Collectively these images suggest that the transfer of C from the decomposing substrate (located ≤ 1mm away) to the mineral surfaces occurred predominantly through hyphal exploration, and not by means of passive transport in soil solution.

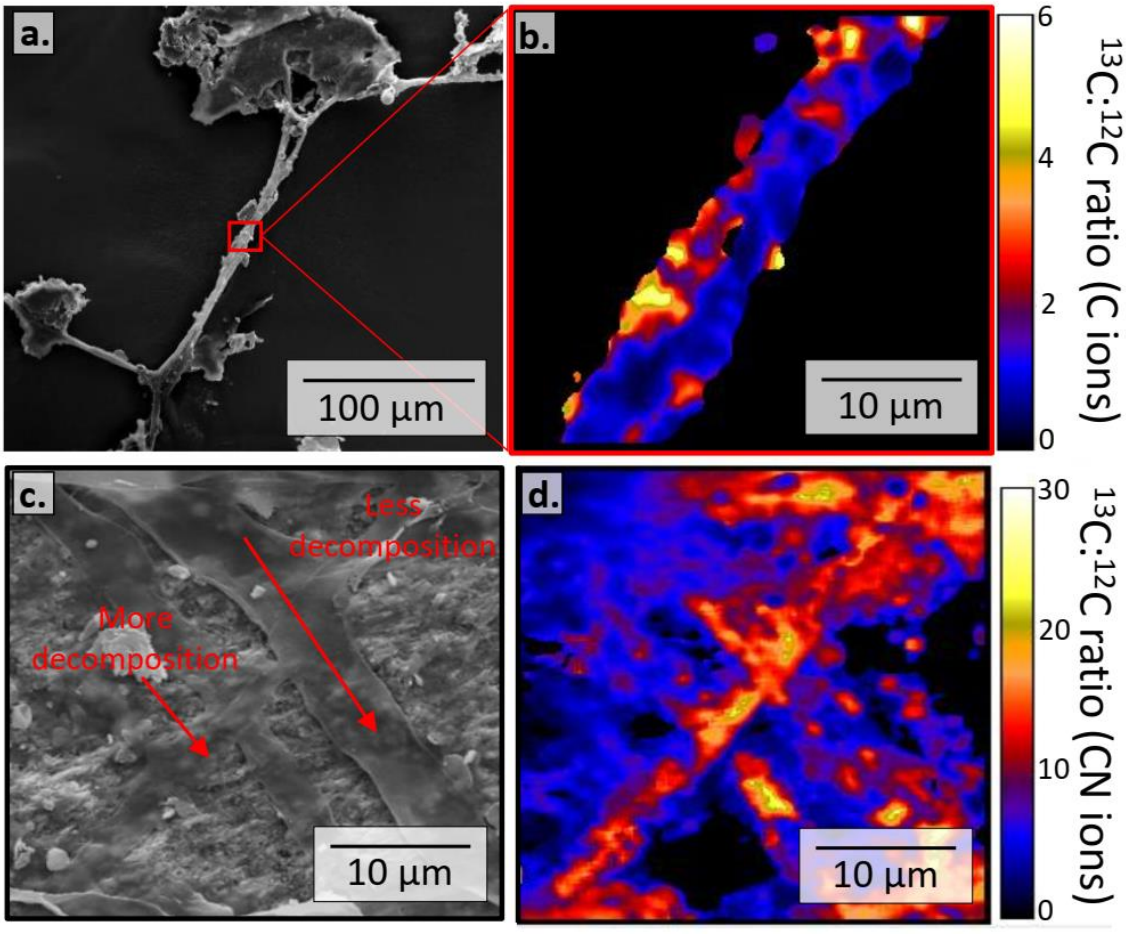

Figure 3.4

Conceptual diagram of hyphosphere function relating to MAOM formation. Hyphal exploration of soil microsites across space and time (spatioptemporal dynamics) control the rate at which C is deposited on mineral surfaces. The hyphal taxa and its associated bacterial community control the organic chemistry of C deposited on minerals though differences in exudates, cell wall composition, and EPS production. Factors affecting hyphosphere spatiotemporal dynamics and community composition include the dominant trophic mode (saprotrohic vs mycorrhizal), the spatial distribution of limiting resources, and environmental stressors.

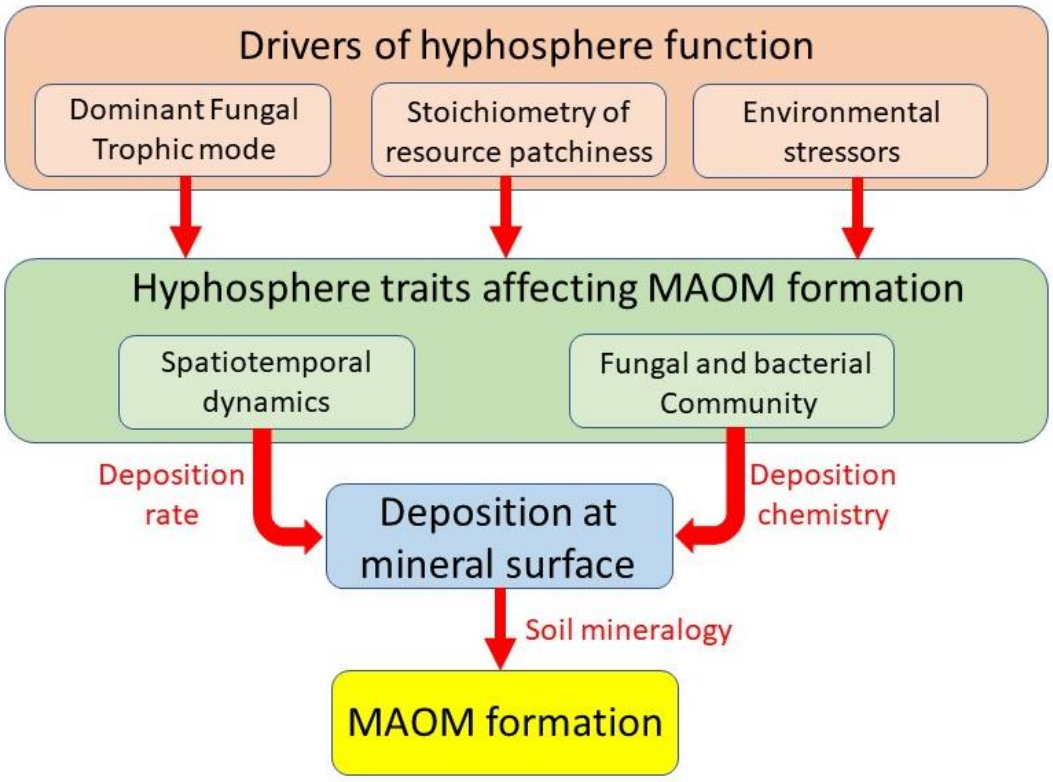

Bibliography

Agerer, R. (2001). Exploration types of ectomycorrhizae. *Mycorrhiza*, *11*(2), 107–114.

Angst, G., Mueller, K. E., Nierop, K. G. J., & Simpson, M. J. (2021). Plant- or microbial-derived ? A review on the molecular composition of stabilized soil organic matter. *Soil Biology and Biochemistry*, *156*(November 2020), 108189. https://doi.org/10.1016/j.soilbio.2021.108189

Anthony, M. A., Crowther, T. W., Maynard, D. S., van den Hoogen, J., & Averill, C. (2020a). Distinct Assembly Processes and Microbial Communities Constrain Soil Organic Carbon Formation. *One Earth*, *2*(4), 349–360. https://doi.org/10.1016/j.oneear.2020.03.006

Anthony, M. A., Crowther, T. W., Maynard, D. S., van den Hoogen, J., & Averill, C. (2020b). Distinct Assembly Processes and Microbial Communities Constrain Soil Organic Carbon Formation. *One Earth*, *2*(4), 349–360. https://doi.org/10.1016/j.oneear.2020.03.006

Augé, R. M. (2001). Water relations, drought and vesicular-arbuscular mycorrhizal symbiosis. In *Mycorrhiza* (Vol. 11, Issue 1, pp. 3–42). Springer. https://doi.org/10.1007/s005720100097

Averill, C., Bhatnagar, J. M., Dietze, M. C., Pearse, W. D., & Kivlin, S. N. (2019). Global imprint of mycorrhizal fungi on whole-plant nutrient economics. *Proceedings of the National Academy of Sciences of the United States of America*, *116*(46), 23163–23168. https://doi.org/10.1073/pnas.1906655116

Averill, C., Turner, B. L., & Finzi, A. C. (2014). Mycorrhiza-mediated competition between plants and decomposers drives soil carbon storage. *Nature*, *505*(7484), 543–545. https://doi.org/10.1038/nature12901

Bahram, M., Peay, K. G., & Tedersoo, L. (2015). Local-scale biogeography and spatiotemporal variability in communities of mycorrhizal fungi. *New Phytologist*, *205*(4), 1454–1463. https://doi.org/10.1111/nph.13206

Beidler, K. V., Phillips, R. P., Andrews, E., Maillard, F., Mushinski, R. M., & Kennedy, P. G. (2020). Substrate quality drives fungal necromass decay and decomposer community structure under contrasting vegetation types. *Journal of Ecology*, *108*(5), 1845–1859. https://doi.org/10.1111/1365-2745.13385

Berg, B. (2000). Litter decomposition and organic matter turnover in northern forest soils. *Forest Ecology and Management*, *133*(1–2), 13–22. https://doi.org/10.1016/S0378-1127(99)00294-7

Blum, J. D., Klaue, A., Nezat, C. A., Driscoll, C. T., Johnson, C. E., Siccama, T. G., Eagar, C., Fahey, T. J., & Likens, G. E. (2002a). Mycorrhizal weathering of apatite as an important calcium source in base-poor forest ecosystems. *Nature*, *417*(6890), 729–731. https://doi.org/10.1038/nature00793

Blum, J. D., Klaue, A., Nezat, C. A., Driscoll, C. T., Johnson, C. E., Siccama, T. G.,

Eagar, C., Fahey, T. J., & Likens, G. E. (2002b). Mycorrhizal weathering of apatite as an important calcium source in base-poor forest ecosystems. *Nature*, *417*(6890), 729–731. https://doi.org/10.1038/nature00793

Boberg, J. B., Finlay, R. D., Stenlid, J., Ekblad, A., & Lindahl, B. D. (2014). Nitrogen and Carbon Reallocation in Fungal Mycelia during Decomposition of Boreal Forest Litter. *PLoS ONE*, *9*(3), e92897. https://doi.org/10.1371/journal.pone.0092897

Bowman, S. M., & Free, S. J. (2006). The structure and synthesis of the fungal cell wall. In *BioEssays* (Vol. 28, Issue 8, pp. 799–808). Bioessays. https://doi.org/10.1002/bies.20441

Brabcová, V., Nováková, M., Davidová, A., & Baldrian, P. (2016a). Dead fungal mycelium in forest soil represents a decomposition hotspot and a habitat for a specific microbial community. *New Phytologist*, *210*(4), 1369–1381. https://doi.org/10.1111/nph.13849

Brabcová, V., Nováková, M., Davidová, A., & Baldrian, P. (2016b). Dead fungal mycelium in forest soil represents a decomposition hotspot and a habitat for a specific microbial community. *New Phytologist*, *210*(4), 1369–1381. https://doi.org/10.1111/nph.13849

Bradford, M. A., Berg, B., Maynard, D. S., Wieder, W. R., & Wood, S. A. (2016). Understanding the dominant controls on litter decomposition. *Journal of Ecology*, *104*(1), 229–238. https://doi.org/10.1111/1365-2745.12507

Branco, S., Bruns, T. D., & Singleton, I. (2013). Fungi at a Small Scale: Spatial Zonation of Fungal Assemblages around Single Trees. *PLoS ONE*, *8*(10), e78295. https://doi.org/10.1371/journal.pone.0078295

Bull, A. T. (1970). Chemical composition of wild-type and mutant Aspergillus nidulans cell walls. The nature of polysaccharide and melanin constituents. *Journal of General Microbiology*, *63*(1), 75–94. https://doi.org/10.1099/00221287-63-1-75

Burford, E. P., Kierans, M., & Gadd, G. M. (2003). Geomycology: Fungi in mineral substrata. In *Mycologist* (Vol. 17, Issue 3, pp. 98–107). Cambridge University Press. https://doi.org/10.1017/S0269915X03003112

Butler, M. J., & Day, A. W. (1998). Fungal melanins: a review. *Canadian Journal of Microbiology*, *44*(12), 1115–1136. https://doi.org/10.1139/w98-119

Cairney, J. W. G. (2012). Extramatrical mycelia of ectomycorrhizal fungi as moderators of carbon dynamics in forest soil. In *Soil Biology and Biochemistry* (Vol. 47, pp. 198–208). https://doi.org/10.1016/j.soilbio.2011.12.029

Carteron, A., Beigas, M., Joly, S., Turner, B. L., & Laliberté, E. (2020). Temperate Forests Dominated by Arbuscular or Ectomycorrhizal Fungi Are Characterized by Strong Shifts from Saprotrophic to Mycorrhizal Fungi with Increasing Soil Depth. *Microbial Ecology*, 1–14. https://doi.org/10.1007/s00248-020-01540-7

Castellano, M. J., Mueller, K. E., Olk, D. C., Sawyer, J. E., & Six, J. (2015). Integrating plant litter quality, soil organic matter stabilization, and the carbon saturation

concept. *Global Change Biology*, *21*(9), 3200–3209. https://doi.org/10.1111/gcb.12982

Chen, J., Seven, J., Zilla, T., Dippold, M. A., Blagodatskaya, E., & Kuzyakov, Y. (2019). Microbial C:N:P stoichiometry and turnover depend on nutrients availability in soil: A 14 C, 15 N and 33 P triple labelling study. *Soil Biology and Biochemistry*, *131*(October 2018), 206–216. https://doi.org/10.1016/j.soilbio.2019.01.017

Chen, W., Koide, R. T., Adams, T. S., Deforest, J. L., Cheng, L., & Eissenstat, D. M. (2016). Root morphology and mycorrhizal symbioses together shape nutrient foraging strategies of temperate trees. *Proceedings of the National Academy of Sciences*, *113*(31), 8741–8746. https://doi.org/10.1073/pnas.1601006113

Chen, Y., Liu, Y., Zhang, J., Yang, W., He, R., & Deng, C. (2018). Microclimate exerts greater control over litter decomposition and enzyme activity than litter quality in an alpine forest-tundra ecotone. *Scientific Reports*, *8*(1), 1–13. https://doi.org/10.1038/s41598-018-33186-4

Clemmensen, K. E., Bahr, A., Ovaskainen, O., Dahlberg, A., Ekblad, A., Wallander, H., Stenlid, J., Finlay, R. D., Wardle, D. A., & Lindahl, B. D. (2013). Roots and associated fungi drive long-term carbon sequestration in boreal forest. *Science*, *340*(6127), 1615–1618. https://doi.org/10.1126/science.1231923

Clemmensen, Karina E., Finlay, R. D., Dahlberg, A., Stenlid, J., Wardle, D. A., & Lindahl, B. D. (2015a). Carbon sequestration is related to mycorrhizal fungal community shifts during long-term succession in boreal forests. *New Phytologist*, *205*(4), 1525–1536. https://doi.org/10.1111/nph.13208

Clemmensen, Karina E., Finlay, R. D., Dahlberg, A., Stenlid, J., Wardle, D. A., & Lindahl, B. D. (2015b). Carbon sequestration is related to mycorrhizal fungal community shifts during long-term succession in boreal forests. *New Phytologist*, *205*(4), 1525–1536. https://doi.org/10.1111/NPH.13208@10.1002/(ISSN)1469-8137(CAT)SPECIALISSUES(VI)ECOLOGYANDEVOLUTIONOFMYCORRHIZAS

Cornwell, W. K., Cornelissen, J. H. C., Amatangelo, K., Dorrepaal, E., Eviner, V. T., Godoy, O., Hobbie, S. E., Hoorens, B., Kurokawa, H., Pérez-Harguindeguy, N., Quested, H. M., Santiago, L. S., Wardle, D. A., Wright, I. J., Aerts, R., Allison, S. D., Van Bodegom, P., Brovkin, V., Chatain, A., … Westoby, M. (2008). Plant species traits are the predominant control on litter decomposition rates within biomes worldwide. *Ecology Letters*, *11*(10), 1065–1071. https://doi.org/10.1111/j.1461-0248.2008.01219.x

Costa, O. Y. A., Raaijmakers, J. M., & Kuramae, E. E. (2018). Microbial extracellular polymeric substances: Ecological function and impact on soil aggregation. In *Frontiers in Microbiology* (Vol. 9, Issue JUL, p. 1636). Frontiers Media S.A. https://doi.org/10.3389/fmicb.2018.01636

Cotrufo, M. F., Wallenstein, M. D., Boot, C. M., Denef, K., & Paul, E. (2013a). The Microbial Efficiency-Matrix Stabilization (MEMS) framework integrates plant litter

decomposition with soil organic matter stabilization: Do labile plant inputs form stable soil organic matter? *Global Change Biology*, *19*(4), 988–995. https://doi.org/10.1111/gcb.12113

Cotrufo, M. F., Wallenstein, M. D., Boot, C. M., Denef, K., & Paul, E. (2013b). The Microbial Efficiency-Matrix Stabilization (MEMS) framework integrates plant litter decomposition with soil organic matter stabilization: Do labile plant inputs form stable soil organic matter? *Global Change Biology*, *19*(4), 988–995. https://doi.org/10.1111/gcb.12113

Creamer, C. A., Foster, A. L., Lawrence, C., McFarland, J., Schulz, M., & Waldrop, M. P. (2019). Mineralogy dictates the initial mechanism of microbial necromass association. *Geochimica et Cosmochimica Acta*, *260*, 161–176. https://doi.org/10.1016/j.gca.2019.06.028

Crowther, T. W., van den Hoogen, J., Wan, J., Mayes, M. A., Keiser, A. D., Mo, L., Averill, C., & Maynard, D. S. (2019). The global soil community and its influence on biogeochemistry. In *Science* (Vol. 365, Issue 6455). American Association for the Advancement of Science. https://doi.org/10.1126/science.aav0550

Dechesne, A., Wang, G., Gülez, G., Or, D., & Smets, B. F. (2010). Hydration-controlled bacterial motility and dispersal on surfaces. *Proceedings of the National Academy of Sciences of the United States of America*, *107*(32), 14369–14372. https://doi.org/10.1073/pnas.1008392107

Deveau, A., Bonito, G., Uehling, J., Paoletti, M., Becker, M., Bindschedler, S., Hacquard, S., Hervé, V., Labbé, J., Lastovetsky, O. A., Mieszkin, S., Millet, L. J., Vajna, B., Junier, P., Bonfante, P., Krom, B. P., Olsson, S., van Elsas, J. D., & Wick, L. Y. (2018). Bacterial-fungal interactions: Ecology, mechanisms and challenges. In *FEMS Microbiology Reviews* (Vol. 42, Issue 3, pp. 335–352). Oxford University Press. https://doi.org/10.1093/femsre/fuy008

Djukic, I., Kepfer-Rojas, S., Schmidt, I. K., Larsen, K. S., Beier, C., Berg, B., Verheyen, K., Caliman, A., Paquette, A., Gutiérrez-Girón, A., Humber, A., Valdecantos, A., Petraglia, A., Alexander, H., Augustaitis, A., Saillard, A., Fernández, A. C. R., Sousa, A. I., Lillebø, A. I., … Tóth, Z. (2018). Early stage litter decomposition across biomes. *Science of the Total Environment*, *628–629*(April), 1369–1394. https://doi.org/10.1016/j.scitotenv.2018.01.012

Dove, N. C., Arogyaswamy, K., Billings, S. A., Botthoff, J. K., Carey, C. J., Cisco, C., Deforest, J. L., Fairbanks, D., Fierer, N., Gallery, R. E., Kaye, J. P., Lohse, K. A., Maltz, M. R., Mayorga, E., Pett-Ridge, J., Yang, W. H., Hart, S. C., & Aronson, E. L. (2020). Continental-scale patterns of extracellular enzyme activity in the subsoil: An overlooked reservoir of microbial activity. *Environmental Research Letters*, *15*(10), 1040a1. https://doi.org/10.1088/1748-9326/abb0b3

Dungait, J. A. J., Hopkins, D. W., Gregory, A. S., & Whitmore, A. P. (2012). Soil organic matter turnover is governed by accessibility not recalcitrance. In *Global Change Biology* (Vol. 18, Issue 6, pp. 1781–1796). John Wiley & Sons, Ltd. https://doi.org/10.1111/j.1365-2486.2012.02665.x

Duponnois, R., & Garbaye, J. (1991). Effect of dual inoculation of Douglas fir with the ectomycorrhizal fungus Laccaria laccata and mycorrhization helper bacteria (MHB) in two bare-root forest nurseries. *Plant and Soil*, *138*(2), 169–176. https://doi.org/10.1007/BF00012243

Eisenman, H. C., & Casadevall, A. (2012). Synthesis and assembly of fungal melanin. In *Applied Microbiology and Biotechnology* (Vol. 93, Issue 3, pp. 931–940). NIH Public Access. https://doi.org/10.1007/s00253-011-3777-2

Ekblad, A., Wallander, H., Godbold, D. L., Cruz, C., Johnson, D., Baldrian, P., Bjork, R. G., Epron, D., Kieliszewska-Rokicka, B., Kjoller, R., Kraigher, H., Matzner, E., Neumann, J., & Plassard, C. (2013). The production and turnover of extramatrical mycelium of ectomycorrhizal fungi in forest soils: Role in carbon cycling. *Plant and Soil*, *366*(1–2), 1–27. https://doi.org/10.1007/s11104-013-1630-3

Emmett, B. D., Lévesque-Tremblay, V., & Harrison, M. J. (2021). Conserved and reproducible bacterial communities associate with extraradical hyphae of arbuscular mycorrhizal fungi. *ISME Journal*, 1–13. https://doi.org/10.1038/s41396-021-00920-2

Fahey, T. J., Siccama, T. G., Driscoll, C. T., Likens, G. E., Campbell, J. L., Johnson, C. E., Battles, J. J., Aber, J. D., Cole, J. J., Fisk, M. C., Groffman, P. M., Hamburg, S. P., Holmes, R. T., Schwarz, P. A., & Yanai, R. D. (2005). The biogeochemistry of carbon at Hubbard Brook. *Biogeochemistry*, *75*(1), 109–176. https://doi.org/10.1007/s10533-004-6321-y

Fernandez, C. W. (2021). The advancing mycelial frontier of ectomycorrhizal fungi. *New Phytologist*, *230*(4), 1296–1299. https://doi.org/10.1111/nph.17281

Fernandez, C. W., Heckman, K., Kolka, R., & Kennedy, P. G. (2019). Melanin mitigates the accelerated decay of mycorrhizal necromass with peatland warming. *Ecology Letters*, *22*, 498–505. https://doi.org/10.1111/ele.13209

Fernandez, C. W., & Kennedy, P. G. (2018). Melanization of mycorrhizal fungal necromass structures microbial decomposer communities. *Journal of Ecology*, *106*(2), 468–479. https://doi.org/10.1111/1365-2745.12920

Fernandez, C. W., & Koide, R. T. (2012). The role of chitin in the decomposition of ectomycorrhizal fungal litter. *Ecology*, *93*(1), 24–28.

Fernandez, C. W., & Koide, R. T. (2014a). Initial melanin and nitrogen concentrations control the decomposition of ectomycorrhizal fungal litter. *Soil Biology and Biochemistry*, *77*, 150–157. https://doi.org/10.1016/j.soilbio.2014.06.026

Fernandez, C. W., & Koide, R. T. (2014b). Initial melanin and nitrogen concentrations control the decomposition of ectomycorrhizal fungal litter. *Soil Biology and Biochemistry*, *77*, 150–157. https://doi.org/10.1016/j.soilbio.2014.06.026

Fernandez, C. W., Langley, J. A., Chapman, S., McCormack, M. L., & Koide, R. T. (2016a). The decomposition of ectomycorrhizal fungal necromass. *Soil Biology and Biochemistry*, *93*, 38–49. https://doi.org/10.1016/j.soilbio.2015.10.017

Fernandez, C. W., Langley, J. A., Chapman, S., McCormack, M. L., & Koide, R. T. (2016b). The decomposition of ectomycorrhizal fungal necromass. *Soil Biology and Biochemistry*, *93*, 38–49. https://doi.org/10.1016/j.soilbio.2015.10.017

Fernandez, C. W., McCormack, M. L., Hill, J. M., Pritchard, S. G., & Koide, R. T. (2013). On the persistence of Cenococcum geophilum ectomycorrhizas and its implications for forest carbon and nutrient cycles. *Soil Biology and Biochemistry*, *65*, 141–143. https://doi.org/10.1016/j.soilbio.2013.05.022

Fierer, N., Craine, J. M., McLauchlan, K., & Schimel, J. P. (2005). LITTER QUALITY AND THE TEMPERATURE SENSITIVITY OF DECOMPOSITION. *Ecology*, *86*(2), 320–326. https://doi.org/10.1890/04-1254

Freschet, G. T., Cornelissen, J. H. C., van Logtestijn, R. S. P., & Aerts, R. (2010). Evidence of the "plant economics spectrum" in a subarctic flora. *Journal of Ecology*, *98*(2), 362–373. https://doi.org/10.1111/j.1365-2745.2009.01615.x

Frey, S. D., Elliott, E. T., & Paustian, K. (1999). Bacterial and fungal abundance and biomass in conventional and no-tillage agroecosystems along two climatic gradients. *Soil Biology and Biochemistry*, *31*(4), 573–585. https://doi.org/10.1016/S0038-0717(98)00161-8

Frey, S. D., Six, J., & Elliott, E. T. (2003). Reciprocal transfer of carbon and nitrogen by decomposer fungi at the soil-litter interface. *Soil Biology and Biochemistry*, *35*(7), 1001–1004. https://doi.org/10.1016/S0038-0717(03)00155-X

Frey, Serita D. (2019). Mycorrhizal Fungi as Mediators of Soil Organic Matter Dynamics. In *Annual Review of Ecology, Evolution, and Systematics* (Vol. 50, pp. 237–259). Annual Reviews Inc. https://doi.org/10.1146/annurev-ecolsys-110617-062331

Friese, C. F., & Allen, M. F. (1991). The Spread of Va Mycorrhizal Fungal Hyphae in the Soil: Inoculum Types and External Hyphal Architecture. *Mycologia*, *83*(4), 409–418. https://doi.org/10.1080/00275514.1991.12026030

Fuss, C. B., Lovett, G. M., Goodale, C. L., Ollinger, S. V., Lang, A. K., & Ouimette, A. P. (2019). Retention of Nitrate-N in Mineral Soil Organic Matter in Different Forest Age Classes. *Ecosystems*, *22*(6), 1280–1294. https://doi.org/10.1007/s10021-018-0328-z

Godbold, D. L., Hoosbeek, M. R., Lukac, M., Cotrufo, M. F., Janssens, I. A., Ceulemans, R., Polle, A., Velthorst, E. J., Scarascia-Mugnozza, G., De Angelis, P., Miglietta, F., & Peressotti, A. (2006a). Mycorrhizal hyphal turnover as a dominant process for carbon input into soil organic matter. *Plant and Soil*, *281*(1–2), 15–24. https://doi.org/10.1007/s11104-005-3701-6

Godbold, D. L., Hoosbeek, M. R., Lukac, M., Cotrufo, M. F., Janssens, I. A., Ceulemans, R., Polle, A., Velthorst, E. J., Scarascia-Mugnozza, G., De Angelis, P., Miglietta, F., & Peressotti, A. (2006b). Mycorrhizal hyphal turnover as a dominant process for carbon input into soil organic matter. *Plant and Soil*, *281*(1–2), 15–24. https://doi.org/10.1007/s11104-005-3701-6

Gorka, S., Dietrich, M., Mayerhofer, W., Gabriel, R., Wiesenbauer, J., Martin, V., Zheng, Q., Imai, B., Prommer, J., Weidinger, M., Schweiger, P., Eichorst, S. A., Wagner, M., Richter, A., Schintlmeister, A., Woebken, D., & Kaiser, C. (2019). Rapid Transfer of Plant Photosynthates to Soil Bacteria via Ectomycorrhizal Hyphae and Its Interaction With Nitrogen Availability. *Frontiers in Microbiology*, *10*(FEB), 168. https://doi.org/10.3389/fmicb.2019.00168

Grandy, A. S., & Neff, J. C. (2008). Molecular C dynamics downstream: The biochemical decomposition sequence and its impact on soil organic matter structure and function. *Science of the Total Environment*, *404*(2–3), 297–307. https://doi.org/10.1016/j.scitotenv.2007.11.013

Grigal, D. F., Finney, H. R., Wroblewski, D. V., & Gross, E. V. (1974). *Soils of the Cedar Creek Natural History Area*. Agricultural Experiment Station, University of Minnesota.

Guennoc, C. M., Rose, C., Labbé, J., & Deveau, A. (2018). Bacterial biofilm formation on the hyphae of ectomycorrhizal fungi: A widespread ability under controls? *FEMS Microbiology Ecology*, *94*(7). https://doi.org/10.1093/femsec/fiy093

Han, Y., Feng, J., Han, M., & Zhu, B. (2020). Responses of arbuscular mycorrhizal fungi to nitrogen addition: A meta-analysis. *Global Change Biology*, *26*(12), 7229–7241. https://doi.org/10.1111/gcb.15369

He, L., Mazza Rodrigues, J. L., Soudzilovskaia, N. A., Barceló, M., Olsson, P. A., Song, C., Tedersoo, L., Yuan, F., Yuan, F., Lipson, D. A., & Xu, X. (2020). Global biogeography of fungal and bacterial biomass carbon in topsoil. *Soil Biology and Biochemistry*, *151*, 108024. https://doi.org/10.1016/j.soilbio.2020.108024

Heckman, K., Throckmorton, H., Horwath, W., Swanston, C., & Rasmussen, C. (2018). Variation in the Molecular Structure and Radiocarbon Abundance of Mineral-Associated Organic Matter across a Lithosequence of Forest Soils. *Soil Systems*, *2*(2), 36. https://doi.org/10.3390/soilsystems2020036

Hobbie, E. A., Sánchez, F. S., & Rygiewicz, P. T. (2012). Controls of isotopic patterns in saprotrophic and ectomycorrhizal fungi. *Soil Biology and Biochemistry*, *48*, 60–68. https://doi.org/10.1016/j.soilbio.2012.01.014

Hobbie, S. E., Oleksyn, J., Eissenstat, D. M., & Reich, P. B. (2010). Fine root decomposition rates do not mirror those of leaf litter among temperate tree species. *Oecologia*, *162*(2), 505–513. https://doi.org/10.1007/s00442-009-1479-6

Hoffland, E., Kuyper, T. W., Wallander, H., Plassard, C., Gorbushina, A. A., Haselwandter, K., Holmström, S., Landeweert, R., Lundström, U. S., Rosling, A., Sen, R., Smits, M. M., Hees, P. A. van, & Breemen, N. van. (2004). The role of fungi in weathering. *Frontiers in Ecology and the Environment*, *2*(5), 258–264. https://doi.org/10.1890/1540-9295(2004)002[0258:TROFIW]2.0.CO;2

Hopkins, J. R., Semenova-Nelsen, T., & Sikes, B. A. (2021). Fungal community structure and seasonal trajectories respond similarly to fire across pyrophilic ecosystems. *FEMS Microbiology Ecology*, *97*(1). https://doi.org/10.1093/femsec/fiaa219

Hover, T., Maya, T., Ron, S., Sandovsky, H., Shadkchan, Y., Kijner, N., Mitiagin, Y., Fichtman, B., Harel, A., Shanks, R. M. Q., Bruna, R. E., García-Véscovi, E., & Osherov, N. (2016). Mechanisms of bacterial (Serratia marcescens) attachment to, migration along, and killing of fungal hyphae. *Applied and Environmental Microbiology*, *82*(9), 2585–2594. https://doi.org/10.1128/AEM.04070-15

Howard, P. J. A., & Howard, D. M. (1974). Microbial Decomposition of Tree and Shrub Leaf Litter. 1. Weight Loss and Chemical Composition of Decomposing Litter. *Oikos*, *25*(3), 341. https://doi.org/10.2307/3543954

Hribljan, J. A., Kane, E. S., & Chimner, R. A. (2017). Implications of Altered Hydrology for Substrate Quality and Trace Gas Production in a Poor Fen Peatland. *Soil Science Society of America Journal*, *81*(3), 633–646. https://doi.org/10.2136/sssaj2016.10.0322

Huang, J., Liu, W., Deng, M., Wang, X., Wang, Z., Yang, L., & Liu, L. (2020). Allocation and turnover of rhizodeposited carbon in different soil microbial groups. *Soil Biology and Biochemistry*, *150*. https://doi.org/10.1016/j.soilbio.2020.107973

Iversen, C. M., Mccormack, M. L., Powell, A. S., Blackwood, C. B., Freschet, G. T., Kattge, J., Roumet, C., Stover, D. B., Soudzilovskaia, N. A., Valverde-Barrantes, O. J., van Bodegom, P. M., & Violle, C. (2017). A global Fine-Root Ecology Database to address below-ground challenges in plant ecology. *New Phytologist*, *215*(1), 15–26. https://doi.org/10.1111/nph.14486

Jackson, R. B., Canadell, J., Ehleringer, J. R., Mooney, H. A., Sala, O. E., & Schulze, E. D. (1996). A global analysis of root distributions for terrestrial biomes. In *Oecologia* (Vol. 108, Issue 3, pp. 389–411). Springer Verlag. https://doi.org/10.1007/BF00333714

Jackson, R. B., Mooney, H. A., & Schulze, E.-D. (1997). A global budget for fine root biomass, surface area, and nutrient contents. *Proceedings of the National Academy of Sciences*, *94*(14), 7362–7366. https://doi.org/10.1073/pnas.94.14.7362

Jackson, Robert B., Mooney, H. A., & Schulze, E.-D. (1997). A global budget for fine root biomass, surface area, and nutrient contents. *Proceedings of the National Academy of Sciences*, *94*(14), 7362–7366. https://doi.org/10.1073/pnas.94.14.7362

Jakobsen, I., Abbott, L. K., & Robson, A. D. (1992). External hyphae of vesicular-arbuscular mycorrhizal fungi associated with Trifolium subterraneum L.. 1. Spread of hyphae and phosphorus inflow into roots. *New Phytologist*, *120*(3), 371–380. https://doi.org/10.1111/j.1469-8137.1992.tb01077.x

Jang, M.-K., Kong, B.-G., Jeong, Y.-I., Lee, C. H., & Nah, J.-W. (2004). Physicochemical characterization of α-chitin, β-chitin, and γ-chitin separated from natural resources. *Journal of Polymer Science Part A: Polymer Chemistry*, *42*(14), 3423–3432. https://doi.org/10.1002/pola.20176

Jilling, A., Keiluweit, M., Contosta, A. R., Frey, S., Smith, R. G., Tiemann, L., Jo, J. S., & Grandy, A. S. (2018). *Minerals in the rhizosphere : overlooked mediators of soil nitrogen availability to plants and microbes*. 103–122.

https://doi.org/10.1007/s10533-018-0459-5

Joner, E. J., & Jakobsen, I. (1995). Growth and extracellular phosphatase activity of arbuscular mycorrhizal hyphae as influenced by soil organic matter. *Soil Biology and Biochemistry*, *27*(9), 1153–1159. https://doi.org/10.1016/0038-0717(95)00047-I

Junier, P., Pion, M., Spangenberg, J. E., Simon, A., Bindschedler, S., Flury, C., Chatelain, A., Bshary, R., & Job, D. (2013). Bacterial farming by the fungus Morchella crassipes. *Royalsocietypublishing.Org*, *280*(1773). https://doi.org/10.1098/rspb.2013.2242

Kallenbach, C. M., Frey, S. D., & Grandy, A. S. (2016). Direct evidence for microbial-derived soil organic matter formation and its ecophysiological controls. *Nature Communications*, *7*. https://doi.org/10.1038/ncomms13630

Kane, J. L., Morrissey, E. M., Skousen, J. G., & Freedman, Z. B. (2020). Soil microbial succession following surface mining is governed primarily by deterministic factors. *FEMS Microbiology Ecology*, *96*(11). https://doi.org/10.1093/femsec/fiaa114

Keiser, A. D., & Bradford, M. A. (2017). Climate masks decomposer influence in a cross-site litter decomposition study. *Soil Biology and Biochemistry*, *107*, 180–187. https://doi.org/10.1016/j.soilbio.2016.12.022

Kindler, R., Siemens, J., Kaiser, K., Walmsley, D. C., Bernhofer, C., Buchmann, N., Cellier, P., Eugster, W., Gleixner, G., Grunwald, T., Heim, A., Ibrom, A., Jones, S. K., Jones, M., Klumpp, K., Kutch, W., Larsen, K. S., Lehuger, S., Loubet, B., … Kaupenjohann, M. (2011). Dissolved carbon leaching from soil is a crucial component of the net ecosystem carbon balance. *Global Change Biology*, *17*(2), 1167–1185. https://doi.org/10.1111/j.1365-2486.2010.02282.x

Kleber, M., Eusterhues, K., Keiluweit, M., Mikutta, C., Mikutta, R., & Nico, P. S. (2015). Mineral-Organic Associations: Formation, Properties, and Relevance in Soil Environments. *Advances in Agronomy*, *130*, 1–140. https://doi.org/10.1016/bs.agron.2014.10.005

Kögel-Knabner, I., Guggenberger, G., Kleber, M., Kandeler, E., Kalbitz, K., Scheu, S., Eusterhues, K., & Leinweber, P. (2008). Organo-mineral associations in temperate soils: Integrating biology, mineralogy, and organic matter chemistry. *Journal of Plant Nutrition and Soil Science*, *171*(1), 61–82. https://doi.org/10.1002/jpln.200700048

Koide, R. T., Fernandez, C., & Malcolm, G. (2014). Determining place and process: Functional traits of ectomycorrhizal fungi that affect both community structure and ecosystem function. *New Phytologist*, *201*(2), 433–439. https://doi.org/10.1111/nph.12538

Koide, R. T., & Malcolm, G. M. (2009). N concentration controls decomposition rates of different strains of ectomycorrhizal fungi. *Fungal Ecology*, *2*(4), 197–202. https://doi.org/10.1016/j.funeco.2009.06.001

Kuzyakov, Y., & Blagodatskaya, E. (2015). Microbial hotspots and hot moments in soil:

Concept & review. In *Soil Biology and Biochemistry* (Vol. 83, pp. 184–199). Elsevier Ltd. https://doi.org/10.1016/j.soilbio.2015.01.025

Labbe, J. L., Weston, D. J., Dunkirk, N., Pelletier, D. A., & Tuskan, G. A. (2014). Newly identified helper bacteria stimulate ectomycorrhizal formation in Populus. *Frontiers in Plant Science*, *5*, 579. https://doi.org/10.3389/fpls.2014.00579

Lavallee, J. M., Soong, J. L., & Cotrufo, M. F. (2019). Conceptualizing soil organic matter into particulate and mineral-associated forms to address global change in the 21st century. *Global Change Biology*, gcb.14859. https://doi.org/10.1111/gcb.14859

Le Quéré, C., Andrew, R. M., Canadell, J. G., Sitch, S., Ivar Korsbakken, J., Peters, G. P., Manning, A. C., Boden, T. A., Tans, P. P., Houghton, R. A., Keeling, R. F., Alin, S., Andrews, O. D., Anthoni, P., Barbero, L., Bopp, L., Chevallier, F., Chini, L. P., Ciais, P., … Zaehle, S. (2016). Global Carbon Budget 2016. *Earth System Science Data*, *8*(2), 605–649. https://doi.org/10.5194/essd-8-605-2016

Leake, J., Johnson, D., Donnelly, D., Muckle, G., Boddy, L., & Read, D. (2004). Networks of power and influence: The role of mycorrhizal mycelium in controlling plant communities and agroecosystem functioning. *Canadian Journal of Botany*, *82*(8), 1016–1045. https://doi.org/10.1139/B04-060

Leake, J. R., Donnelly, D. P., Saunders, E. M., Boddy, L., & Read, D. J. (2001). Rates and quantities of carbon flux to ectomycorrhizal mycelium following 14C pulse labeling of Pinus sylvestris seedlings: Effects of litter patches and interaction a wood-decomposer fungus. *Tree Physiology*, *21*(2–3), 71–82. https://doi.org/10.1093/treephys/21.2-3.71

Lehto, T., & Zwiazek, J. J. (2011). Ectomycorrhizas and water relations of trees: A review. In *Mycorrhiza* (Vol. 21, Issue 2, pp. 71–90). Mycorrhiza. https://doi.org/10.1007/s00572-010-0348-9

Lenaers, M., Reyns, W., Czech, J., Carleer, R., Basak, I., Deferme, W., Krupinska, P., Yildiz, T., Saro, S., Remans, T., Vangronsveld, J., de Laender, F., & Rineau, F. (2018). Links Between Heathland Fungal Biomass Mineralization, Melanization, and Hydrophobicity. *Microbial Ecology*. https://doi.org/10.1007/s00248-018-1167-3

Li, F., Chen, L., Redmile-Gordon, M., Zhang, J., Zhang, C., Ning, Q., & Li, W. (2018). *Mortierella elongata* 's roles in organic agriculture and crop growth promotion in a mineral soil. *Land Degradation & Development*, *29*(6), 1642–1651. https://doi.org/10.1002/ldr.2965

Liang, C., Amelung, W., Lehmann, J., & Kästner, M. (2019). Quantitative assessment of microbial necromass contribution to soil organic matter. *Global Change Biology*, *25*(11), 3578–3590. https://doi.org/10.1111/gcb.14781

Lindahl, B. D., Ihrmark, K., Boberg, J., Trumbore, S. E., Högberg, P., Stenlid, J., & Finlay, R. D. (2007). Spatial separation of litter decomposition and mycorrhizal nitrogen uptake in a boreal forest. *New Phytologist*, *173*(3), 611–620. https://doi.org/10.1111/j.1469-8137.2006.01936.x

Liu, Y., Sun, Q., Li, J., & Lian, B. (2018). Bacterial diversity among the fruit bodies of ectomycorrhizal and saprophytic fungi and their corresponding hyphosphere soils. *Scientific Reports*, *8*(1), 1–10. https://doi.org/10.1038/s41598-018-30120-6

López-Mondéjar, R., Brabcová, V., Štursová, M., Davidová, A., Jansa, J., Cajthaml, T., & Baldrian, P. (2018a). Decomposer food web in a deciduous forest shows high share of generalist microorganisms and importance of microbial biomass recycling. *ISME Journal*, *12*(7), 1768–1778. https://doi.org/10.1038/s41396-018-0084-2

López-Mondéjar, R., Brabcová, V., Štursová, M., Davidová, A., Jansa, J., Cajthaml, T., & Baldrian, P. (2018b). Decomposer food web in a deciduous forest shows high share of generalist microorganisms and importance of microbial biomass recycling. *ISME Journal*, *12*(7), 1768–1778. https://doi.org/10.1038/s41396-018-0084-2

Lousier, J. D., & Parkinson, D. (1976). Litter decomposition in a cool temperate deciduous forest. *Canadian Journal of Botany*, *54*(5–6). https://digitalcommons.usu.edu/aspen_bib/4989

Lovett, G. M., Goodale, C. L., Ollinger, S. V, Fuss, C. B., Ouimette, A. P., & Likens, G. E. (2018). Nutrient retention during ecosystem succession : a revised conceptual model. *Frontiers in Ecology and the Environment*, *16*(9), 532–538. https://doi.org/10.1002/fee.1949

Ludwig, M., Achtenhagen, J., Miltner, A., Eckhardt, K. U., Leinweber, P., Emmerling, C., & Thiele-Bruhn, S. (2015). Microbial contribution to SOM quantity and quality in density fractions of temperate arable soils. *Soil Biology and Biochemistry*, *81*, 311–322. https://doi.org/10.1016/j.soilbio.2014.12.002

Lustenhouwer, N., Maynard, D. S., Bradford, M. A., Lindner, D. L., Oberle, B., Zanne, A. E., & Crowther, T. W. (2020). A trait-based understanding of wood decomposition by fungi. *Proceedings of the National Academy of Sciences of the United States of America*, *117*(21), 11551–11558. https://doi.org/10.1073/pnas.1909166117

Maillard, F., Schilling, J., Andrews, E., Schreiner, K. M., & Kennedy, P. (2020). Functional convergence in the decomposition of fungal necromass in soil and wood. *FEMS Microbiology Ecology*, *96*(2), 1–13. https://doi.org/10.1093/femsec/fiz209

Malik, A. A., Martiny, J. B. H., Brodie, E. L., Martiny, A. C., Treseder, K. K., & Allison, S. D. (2020). Defining trait-based microbial strategies with consequences for soil carbon cycling under climate change. *ISME Journal*, *14*(1), 1–9. https://doi.org/10.1038/s41396-019-0510-0

Manzoni, S., Schimel, J. P., & Porporato, A. (2012). Responses of soil microbial communities to water stress: results from a meta-analysis. *Ecology*, *93*(4), 930–938. https://doi.org/10.1890/11-0026.1

Margenot, A. J., Calderón, F. J., Bowles, T. M., Parikh, S. J., & Jackson, L. E. (2015). Soil Organic Matter Functional Group Composition in Relation to Organic Carbon, Nitrogen, and Phosphorus Fractions in Organically Managed Tomato Fields. *Soil Science Society of America Journal*, *79*(3), 772–782.

https://doi.org/10.2136/sssaj2015.02.0070

McCormack, M. L., Dickie, I. A., Eissenstat, D. M., Fahey, T. J., Fernandez, C. W., Guo, D., Helmisaari, H. S., Hobbie, E. A., Iversen, C. M., Jackson, R. B., Lepp??lammi-Kujansuu, J., Norby, R. J., Phillips, R. P., Pregitzer, K. S., Pritchard, S. G., Rewald, B., & Zadworny, M. (2015). Redefining fine roots improves understanding of below-ground contributions to terrestrial biosphere processes. *New Phytologist*, *207*(3), 505–518. https://doi.org/10.1111/nph.13363

Miller, R. M., Jastrow, J. D., & Reinhardt, D. R. (1995). External hyphal production of vesicular-arbuscular mycorrhizal fungi in pasture and tallgrass prairie communities. *Oecologia*, *103*(1), 17–23. https://doi.org/10.1007/BF00328420

Miltner, A., Bombach, P., Schmidt-Brücken, B., & Kästner, M. (2012). SOM genesis: Microbial biomass as a significant source. *Biogeochemistry*, *111*(1–3), 41–55. https://doi.org/10.1007/s10533-011-9658-z

Moore, J. A. M., Anthony, M. A., Pec, G. J., Trocha, L. K., Trzebny, A., Geyer, K. M., Diepen, L. T. A., & Frey, S. D. (2021). Fungal community structure and function shifts with atmospheric nitrogen deposition. *Global Change Biology*, *27*(7), 1349–1364. https://doi.org/10.1111/gcb.15444

Nagy, L. G., Varga, T., Csernetics, Á., & Virágh, M. (2020). Fungi took a unique evolutionary route to multicellularity: Seven key challenges for fungal multicellular life. In *Fungal Biology Reviews* (Vol. 34, Issue 4, pp. 151–169). Elsevier Ltd. https://doi.org/10.1016/j.fbr.2020.07.002

Nazir, R., Tazetdinova, D. I., & van Elsas, J. D. (2014). Burkholderia terrae BS001 migrates proficiently with diverse fungal hosts through soil and provides protection from antifungal agents. *Frontiers in Microbiology*, *5*(NOV), 598. https://doi.org/10.3389/fmicb.2014.00598

Nazir, R., Warmink, J. A., Boersma, H., & Van Elsas, J. D. (2010). Mechanisms that promote bacterial fitness in fungal-affected soil microhabitats. In *FEMS Microbiology Ecology* (Vol. 71, Issue 2, pp. 169–185). Oxford Academic. https://doi.org/10.1111/j.1574-6941.2009.00807.x

Norton, J. M., Smith, J. L., & Firestone, M. K. (1990). Carbon flow in the rhizosphere of Ponderosa pine seedlings. *Soil Biology*, *22*(4), 449–455.

Nosanchuk, J. D., Stark, R. E., & Casadevall, A. (2015). Fungal melanin: What do we know about structure? In *Frontiers in Microbiology* (Vol. 6, Issue DEC). Frontiers Media S.A. https://doi.org/10.3389/fmicb.2015.01463

Nuccio, E. E., Hodge, A., Pett-Ridge, J., Herman, D. J., Weber, P. K., & Firestone, M. K. (2013). An arbuscular mycorrhizal fungus significantly modifies the soil bacterial community and nitrogen cycling during litter decomposition. *Environmental Microbiology*, *15*(6), 1870–1881. https://doi.org/10.1111/1462-2920.12081

Olagoke, F. K., Kalbitz, K., & Vogel, C. (2019). Control of Soil Extracellular Enzyme Activities by Clay Minerals—Perspectives on Microbial Responses. *Soil Systems*,

3(4), 64. https://doi.org/10.3390/soilsystems3040064

Olson, J. S. (1963). Energy Storage and the Balance of Producers and Decomposers in Ecological Systems. *Ecology*, *44*(2), 322–331. https://doi.org/10.2307/1932179

Or, D., Smets, B. F., Wraith, J. M., Dechesne, A., & Friedman, S. P. (2007). Physical constraints affecting bacterial habitats and activity in unsaturated porous media - a review. *Advances in Water Resources*, *30*(6–7), 1505–1527. https://doi.org/10.1016/j.advwatres.2006.05.025

Otto, S., Bruni, E. P., Harms, H., & Wick, L. Y. (2017). Catch me if you can: Dispersal and foraging of Bdellovibrio bacteriovorus 109J along mycelia. *ISME Journal*, *11*(2), 386–393. https://doi.org/10.1038/ismej.2016.135

Parton, W. J., Silver, W. L., Burke, I. C., Grassens, L., Harmon, M. E., Currie, W. S., King, J. Y., Adair, E. C., Brandt, L. A., Hart, S. C., & Fasth, B. (2007). Global-scale similarities in nitrogen release patterns during long-term decomposition. *Science*, *315*(January), 361–364.

Paul, E. A., Morris, S. J., Conant, R. T., & Plante, A. F. (2006). Does the Acid Hydrolysis-Incubation Method Measure Meaningful Soil Organic Carbon Pools? *Soil Science Society of America Journal*, *70*(3), 1023–1035. https://doi.org/10.2136/sssaj2005.0103

Pett-Ridge, J., & Firestone, M. K. (2017). Using stable isotopes to explore root-microbe-mineral interactions in soil. In *Rhizosphere* (Vol. 3, pp. 244–253). Elsevier B.V. https://doi.org/10.1016/j.rhisph.2017.04.016

Philippot, L., Ritz, K., Pandard, P., Hallin, S., & Martin-Laurent, F. (2012). Standardisation of methods in soil microbiology: progress and challenges. *FEMS Microbiology Ecology*, *82*(1), 1–10. https://doi.org/10.1111/j.1574-6941.2012.01436.x

Prescott, C. E. (2010). Litter decomposition: what controls it and how can we alter it to sequester more carbon in forest soils ? *Biogeochemistry*, *101*, 133–149. https://doi.org/10.1007/s10533-010-9439-0

Querejeta, J., Egerton-Warburton, L. M., & Allen, M. F. (2009). Topographic position modulates the mycorrhizal response of oak trees to interannual rainfall variability. *Ecology*, *90*(3), 649–662. https://doi.org/10.1890/07-1696.1

Rasse, D. P., Rumpel, C., & Dignac, M. F. (2005). Is soil carbon mostly root carbon? Mechanisms for a specific stabilisation. *Plant and Soil*, *269*(1–2), 341–356. https://doi.org/10.1007/s11104-004-0907-y

Rath, K. M., & Rousk, J. (2015). Salt effects on the soil microbial decomposer community and their role in organic carbon cycling: A review. In *Soil Biology and Biochemistry* (Vol. 81, pp. 108–123). Elsevier Ltd. https://doi.org/10.1016/j.soilbio.2014.11.001

Read, D. J., Leake, J. R., & Perez-Moreno, J. (2004). Mycorrhizal fungi as drivers of ecosystem processes in heathland and boreal forest biomes. *Canadian Journal of*

Botany, *82*(8), 1243–1263. https://doi.org/10.1139/B04-123

Reich, P. B. (2014). The world-wide "fast-slow" plant economics spectrum: A traits manifesto. *Journal of Ecology*, *102*(2). https://doi.org/10.1111/1365-2745.12211

Rillig, M. C., & Mummey, D. L. (2006). *Mycorrhizas and soil structure*. 41–53.

Ritz, K., & Young, I. M. (2004). Interactions between soil structure and fungi. *Mycologist*, *18*(2), 52–59. https://doi.org/10.1017/S0269915X04002010

Romero-Olivares, A. L., Morrison, E. W., Pringle, A., & Frey, S. D. (2021). Linking Genes to Traits in Fungi. *Microbial Ecology*. https://doi.org/10.1007/s00248-021-01687-x

Rosling, A., Landeweert, R., Lindahl, B. D., Larsson, K. -H., Kuyper, T. W., Taylor, A. F. S., & Finlay, R. D. (2003). Vertical distribution of ectomycorrhizal fungal taxa in a podzol soil profile. *New Phytologist*, *159*(3), 775–783. https://doi.org/10.1046/j.1469-8137.2003.00829.x

Ryan, M. E., Schreiner, K. M., Swenson, J. T., Gagne, J., & Kennedy, P. G. (2020). Rapid changes in the chemical composition of degrading ectomycorrhizal fungal necromass. *Fungal Ecology*, *45*, 100922. https://doi.org/10.1016/j.funeco.2020.100922

Scheublin, T. R., Sanders, I. R., Keel, C., & Van Der Meer, J. R. (2010). Characterisation of microbial communities colonising the hyphal surfaces of arbuscular mycorrhizal fungi. *ISME Journal*, *4*(6), 752–763. https://doi.org/10.1038/ismej.2010.5

Schimel, J., Balser, T. C., & Wallenstein, M. (2007). MICROBIAL STRESS-RESPONSE PHYSIOLOGY AND ITS IMPLICATIONS FOR ECOSYSTEM FUNCTION. *Ecology*, *88*(6), 1386–1394. https://doi.org/10.1890/06-0219

Schimel, J. P. (2018). Life in dry soils: Effects of drought on soil microbial communities and processes. In *Annual Review of Ecology, Evolution, and Systematics* (Vol. 49, pp. 409–432). Annual Reviews Inc. https://doi.org/10.1146/annurev-ecolsys-110617-062614

Schimel, J. P., & Schaeffer, S. M. (2012). Microbial control over carbon cycling in soil. In *Frontiers in Microbiology* (Vol. 3, Issue SEP, p. 348). Frontiers Research Foundation. https://doi.org/10.3389/fmicb.2012.00348

Schlatter, D. C., Kahl, K., Carlson, B., Huggins, D. R., & Paulitz, T. (2018). Fungal community composition and diversity vary with soil depth and landscape position in a no-till wheat-based cropping system. *FEMS Microbiology Ecology*, *94*(7), 98. https://doi.org/10.1093/femsec/fiy098

Schmidt, M. W. I., Torn, M. S., Abiven, S., Dittmar, T., Guggenberger, G., Janssens, I. A., Kleber, M., Kögel-Knabner, I., Lehmann, J., Manning, D. A. C., Nannipieri, P., Rasse, D. P., Weiner, S., & Trumbore, S. E. (2011). Persistence of soil organic matter as an ecosystem property. *Nature*, *478*(7367), 49–56. https://doi.org/10.1038/nature10386

Schnepf, A., Roose, T., & Schweiger, P. (2008). Growth model for arbuscular mycorrhizal fungi. *Journal of the Royal Society Interface*, *5*(24), 773–784. https://doi.org/10.1098/rsif.2007.1250

Schweigert, M., Herrmann, S., Miltner, A., Fester, T., & Kästner, M. (2015). Fate of ectomycorrhizal fungal biomass in a soil bioreactor system and its contribution to soil organic matter formation. *Soil Biology and Biochemistry*, *88*, 120–127. https://doi.org/10.1016/j.soilbio.2015.05.012

Scott, A. C., Pinter, N., Collinson, M. E., Hardiman, M., Anderson, R. S., Brain, A. P. R., Smith, S. Y., Marone, F., & Stampanoni, M. (2010). Fungus, not comet or catastrophe, accounts for carbonaceous spherules in the Younger Dryas "impact layer." *Geophysical Research Letters*, *37*(14), n/a-n/a. https://doi.org/10.1029/2010GL043345

See, C. R., Fernandez, C. W., Conley, A. M., DeLancey, L. C., Heckman, K. A., Kennedy, P. G., & Hobbie, S. E. (2020). Distinct carbon fractions drive a generalisable two-pool model of fungal necromass decomposition. *Functional Ecology*, 1365-2435.13728. https://doi.org/10.1111/1365-2435.13728

See, C. R., McCormack, M. L., Hobbie, S. E., Flores-Moreno, H., Silver, W. L., & Kennedy, P. G. (2019). Global patterns in fine root decomposition: climate, chemistry, mycorrhizal association and woodiness. *Ecology Letters*, *22*(6), 946–953. https://doi.org/10.1111/ele.13248

See, C. R., Yanai, R. D., & Fahey, T. J. (2019). Shifting N and P concentrations and stoichiometry during autumn litterfall : Implications for ecosystem monitoring. *Ecological Indicators*, *103*, 488–492. https://doi.org/10.1016/j.ecolind.2019.04.017

Shao, P., Liang, C., Lynch, L., Xie, H., & Bao, X. (2019). Reforestation accelerates soil organic carbon accumulation: Evidence from microbial biomarkers. *Soil Biology and Biochemistry*, *131*, 182–190. https://doi.org/10.1016/j.soilbio.2019.01.012

Siletti, C. E., Zeiner, C. A., & Bhatnagar, J. M. (2017). Distributions of fungal melanin across species and soils. *Soil Biology and Biochemistry*, *113*, 285–293. https://doi.org/10.1016/j.soilbio.2017.05.030

Silver, W. L., & Miya, R. (2001). Global patterns in root decomposition: comparisons of climate and litter quality effects. *Oecologia*, *129*, 407–419. https://doi.org/10.1007/s004420100740

Simpson, A. J., Simpson, M. J., Smith, E., & Kelleher, B. P. (2007). Microbially derived inputs to soil organic matter: Are current estimates too low? *Environmental Science and Technology*, *41*(23), 8070–8076. https://doi.org/10.1021/es071217x

Sinsabaugh, R. L., Carreiro, M. M., & Repert, D. A. (2002). Allocation of Extracellular Enzymatic Activity in Relation to Litter Composition, N Deposition, and Mass Loss. In *Biogeochemistry* (Vol. 60, pp. 1–24). Springer. https://doi.org/10.2307/1469657

Six, J., Frey, S. D., Thiet, R. K., & Batten, K. M. (2006). Bacterial and Fungal Contributions to Carbon Sequestration in Agroecosystems. *Soil Science Society of*

America Journal, *70*(2), 555. https://doi.org/10.2136/sssaj2004.0347

Smith, S. E., & Read, D. J. (2008). *Mycorrhizal symbiosis*. Academic Press.

Smits, M. M., & Wallander, H. (2017). Chapter 3 – Role of Mycorrhizal Symbiosis in Mineral Weathering and Nutrient Mining from Soil Parent Material. In *Mycorrhizal Mediation of Soil* (pp. 35–46). https://doi.org/10.1016/B978-0-12-804312-7.00003-6

Sokol, N. W., & Bradford, M. A. (2019). Microbial formation of stable soil carbon is more efficient from belowground than aboveground input. *Nature Geoscience*, *12*(1), 46–53. https://doi.org/10.1038/s41561-018-0258-6

Sokol, N. W., Sanderman, J., & Bradford, M. A. (2019a). Pathways of mineral-associated soil organic matter formation: Integrating the role of plant carbon source, chemistry, and point of entry. *Global Change Biology*, *25*(1), 12–24. https://doi.org/10.1111/gcb.14482

Sokol, N. W., Sanderman, J., & Bradford, M. A. (2019b). Pathways of mineral-associated soil organic matter formation: Integrating the role of plant carbon source, chemistry, and point of entry. *Global Change Biology*, *25*(1), 12–24. https://doi.org/10.1111/gcb.14482

Sulman, B. N., Brzostek, E. R., Medici, C., Shevliakova, E., Menge, D. N. L., & Phillips, R. P. (2017). Feedbacks between plant N demand and rhizosphere priming depend on type of mycorrhizal association. *Ecology Letters*, *20*(8), 1043–1053. https://doi.org/10.1111/ele.12802

Sulman, B. N., Moore, J. A. M., Abramoff, R., Averill, C., Kivlin, S., Georgiou, K., Sridhar, B., Hartman, M. D., Wang, G., Wieder, W. R., Bradford, M. A., Luo, Y., Mayes, M. A., Morrison, E., Riley, W. J., Salazar, A., Schimel, J. P., Tang, J., & Classen, A. T. (2018). Multiple models and experiments underscore large uncertainty in soil carbon dynamics. *Biogeochemistry*, *141*(2), 109–123. https://doi.org/10.1007/s10533-018-0509-z

Sulman, B. N., Phillips, R. P., Oishi, A. C., Shevliakova, E., & Pacala, S. W. (2014). Microbe-driven turnover offsets mineral-mediated storage of soil carbon under elevated CO 2. *Nature Climate Change*, *4*(12), 1099–1102. https://doi.org/10.1038/nclimate2436

Tedersoo, L., Anslan, S., Bahram, M., Drenkhan, R., Pritsch, K., Buegger, F., Padari, A., Hagh-Doust, N., Mikryukov, V., Gohar, D., Amiri, R., Hiiesalu, I., Lutter, R., Rosenvald, R., Rähn, E., Adamson, K., Drenkhan, T., Tullus, H., Jürimaa, K., … Abarenkov, K. (2020). Regional-Scale In-Depth Analysis of Soil Fungal Diversity Reveals Strong pH and Plant Species Effects in Northern Europe. *Frontiers in Microbiology*, *11*, 1953. https://doi.org/10.3389/fmicb.2020.01953

Terrer, C., Phillips, R., Hungate, B., Rosende, J., Pett-Ridge, J., Craig, M., van Groenigen, K., Keenan, T., Sulman, B., Stocker, B., Reich, P., Pellegrini, A., Pendall, E., Zhang, H., Evans, R., Carrillo, Y., Fisher, J., Van Sundert, K., Vicca, S., & Jackson, R. (2021). A trade-off between plant and soil carbon storage under elevated CO2. *Nature 2021 591:7851*, *591*(7851), 599–603.

https://doi.org/10.1038/s41586-021-03306-8

Treseder, K. K., & Lennon, J. T. (2015). Fungal traits that drive ecosystem dynamics on Land. *Microbiology and Molecular Biology Reviews*, *79*(2), 243–262. https://doi.org/10.1128/MMBR.00001-15

Treseder, K. K., Schimel, J. P., Garcia, M. O., & Whiteside, M. D. (2010). Slow turnover and production of fungal hyphae during a Californian dry season. *Soil Biology and Biochemistry*, *42*(9), 1657–1660. https://doi.org/10.1016/j.soilbio.2010.06.005

Van de Waal, D. B., Elser, J. J., Martiny, A. C., Sterner, R. W., & Cotner, J. B. (2018). Editorial: Progress in Ecological Stoichiometry. *Frontiers in Microbiology*, *9*(SEP), 1957. https://doi.org/10.3389/fmicb.2018.01957

Van Der Wal, A., Bloem, J., Mulder, C., & Boer, W. De. (2009). Soil Biology & Biochemistry Relative abundance and activity of melanized hyphae in different soil ecosystems. *Soil Biology and Biochemistry*, *41*(2), 417–419. https://doi.org/10.1016/j.soilbio.2008.10.031

Veen, G. F. C., Freschet, G. T., Ordonez, A., & Wardle, D. A. (2015). Litter quality and environmental controls of home-field advantage effects on litter decomposition. *Oikos*, *124*(2), 187–195. https://doi.org/10.1111/oik.01374

Vos, M., Wolf, A. B., Jennings, S. J., & Kowalchuk, G. A. (2013). Micro-scale determinants of bacterial diversity in soil. In *FEMS Microbiology Reviews* (Vol. 37, Issue 6, pp. 936–954). Oxford Academic. https://doi.org/10.1111/1574-6976.12023

Wang, F., Kertesz, M. A., & Feng, G. (2019). Phosphorus forms affect the hyphosphere bacterial community involved in soil organic phosphorus turnover. *Mycorrhiza*, *29*(4), 351–362. https://doi.org/10.1007/s00572-019-00896-0

Wang, T., Tian, Z., Tunlid, A., & Persson, P. (2020). Nitrogen acquisition from mineral-associated proteins by an ectomycorrhizal fungus. *New Phytologist*, *228*(2), 697–711. https://doi.org/10.1111/nph.16596

Wang, W., Zhong, Z., Wang, Q., Wang, H., Fu, Y., & He, X. (2017). Glomalin contributed more to carbon, nutrients in deeper soils, and differently associated with climates and soil properties in vertical profiles. *Scientific Reports*, *7*(1), 1–13. https://doi.org/10.1038/s41598-017-12731-7

Wang, X., Toner, B. M., & Yoo, K. (2019). Mineral vs. organic matter supply as a limiting factor for the formation of mineral-associated organic matter in forest and agricultural soils. *Science of the Total Environment*, *692*, 344–353. https://doi.org/10.1016/j.scitotenv.2019.07.219

Wardle, D. A. (2002). *Communities and ecosystems : linking the aboveground and belowground components*. Princeton University Press.

Warmink, J. A., Nazir, R., Corten, B., & van Elsas ., J. D. (2011). Hitchhikers on the fungal highway: The helper effect for bacterial migration via fungal hyphae. *Soil Biology and Biochemistry*, *43*(4), 760–765. https://doi.org/10.1016/j.soilbio.2010.12.009

Whalen, E. D., Smith, R. G., Grandy, A. S., & Frey, S. D. (2018). Manganese limitation as a mechanism for reduced decomposition in soils under atmospheric nitrogen deposition. *Soil Biology and Biochemistry*, *127*, 252–263. https://doi.org/10.1016/j.soilbio.2018.09.025

Whitman, T., Neurath, R., Perera, A., Chu-Jacoby, I., Ning, D., Zhou, J., Nico, P., Pett-Ridge, J., & Firestone, M. (2018). Microbial community assembly differs across minerals in a rhizosphere microcosm. *Environmental Microbiology*, *20*(12), 4444–4460. https://doi.org/10.1111/1462-2920.14366

Wieder, R. K., & Lang, G. E. (1982). A critique of the analytical methods used in examining decomposition data obtained from litter bags. *Ecology*, *63*(6), 1636–1642. https://doi.org/10.2307/1940104

Wieder, W. R., Allison, S. D., Davidson, E. A., Georgiou, K., Hararuk, O., He, Y., Hopkins, F., Luo, Y., Smith, M. J., Sulman, B., Todd-Brown, K., Wang, Y. P., Xia, J., & Xu, X. (2015). Explicitly representing soil microbial processes in Earth system models. *Global Biogeochemical Cycles*, *29*(10), 1782–1800. https://doi.org/10.1002/2015GB005188

Wieder, W. R., Cleveland, C. C., Townsend, A. R., Wieder, W. R., Cleveland, C. C., & Townsend, A. R. (2009). Controls over leaf litter decomposition in wet tropical forests. *Ecology*, *90*(12), 3333–3341.

Wright, I. J., Reich, P. B., Westoby, M., Ackerly, D. D., Baruch, Z., Bongers, F., Cavender-Bares, J., Chapin, T., Cornellssen, J. H. C., Diemer, M., Flexas, J., Garnier, E., Groom, P. K., Gulias, J., Hikosaka, K., Lamont, B. B., Lee, T., Lee, W., Lusk, C., … Villar, R. (2004). The worldwide leaf economics spectrum. *Nature*, *428*(6985), 821–827. https://doi.org/10.1038/nature02403

Yanai, R. D., See, C. R., & Campbell, J. L. (2017). Current Practices in Reporting Uncertainty in Ecosystem Ecology. *Ecosystems*. https://doi.org/10.1007/s10021-017-0197-x

Zagryadskaya, Y. A., Lysak, L. V., Lapygina, E. V., Voronina, E. Y., Aleksandrova, A. V., & Sidorova, I. I. (2011). The characteristics of bacterial communities in the hyphosphere of several basidial macromycetes. *Moscow University Soil Science Bulletin*, *66*(3), 129–133. https://doi.org/10.3103/s0147687411030100

Zak, D. R., Pellitier, P. T., Argiroff, W., Castillo, B., James, T. Y., Nave, L. E., Averill, C., Beidler, K. V., Bhatnagar, J., Blesh, J., Classen, A. T., Craig, M., Fernandez, C. W., Gundersen, P., Johansen, R., Koide, R. T., Lilleskov, E. A., Lindahl, B. D., Nadelhoffer, K. J., … Tunlid, A. (2019). Exploring the role of ectomycorrhizal fungi in soil carbon dynamics. *New Phytologist*, *223*(1), 33–39. https://doi.org/10.1111/nph.15679

Zhang, D. Q., Hui, D. F., Luo, Y. Q., & Zhou, G. Y. (2008). Rates of litter decomposition in terrestrial ecosystems: global patterns and controlling factors. *Journal of Plant Ecology-Uk*, *1*(2), 85–93. https://doi.org/Doi 10.1093/Jpe/Rtn002

Zhang, L., Xu, M., Liu, Y., Zhang, F., Hodge, A., & Feng, G. (2016). Carbon and

phosphorus exchange may enable cooperation between an arbuscular mycorrhizal fungus and a phosphate-solubilizing bacterium. *New Phytologist*, *210*(3), 1022–1032. https://doi.org/10.1111/nph.13838

Zhang, X., & Wang, W. (2015). The decomposition of fine and coarse roots: Their global patterns and controlling factors. *Scientific Reports*, *5*, 1–10. https://doi.org/10.1038/srep09940

Zhang, Yuan, Hao, X., Garcia-Lemos, A. M., Nunes, I., Nicolaisen, M. H., & Nybroe, O. (2020). Different effects of soil fertilization on bacterial community composition in the penicillium canescens hyphosphere and in bulk soil. *Applied and Environmental Microbiology*, *86*(10). https://doi.org/10.1128/AEM.02969-19

Zhang, Yuanchen, Kastman, E. K., Guasto, J. S., & Wolfe, B. E. (2018). Fungal networks shape dynamics of bacterial dispersal and community assembly in cheese rind microbiomes. *Nature Communications*, *9*(1), 1–12. https://doi.org/10.1038/s41467-017-02522-z

Appendix 1.1: Dataset compilation

We first searched for studies using bibliographies compiled from previous studies of fine-root decomposition (Silver & Miya, 2001; D. Q. Zhang et al., 2008; X. Zhang & Wang, 2015). On December 10th, 2017 we conducted a Web of Science search using the following terms: "fine root decay," "fine root decomposition," "belowground litter decay," and "belowground litter decomposition". We only searched back to 1999, assuming that Silver and Miya's (2000) analysis had reported all prior studies. Our search returned over 1000 published articles. Our initial criteria for inclusion included all studies where fine roots were <3 mm in diameter and decomposed in isolation (i.e. bulk root samples were excluded) and where the species identity was known. From these studies, we retained only studies that reported fine-root decomposition rates with at least 3 time points.

For each species in each study, we retrieved simple exponential decay constants (*k*-values) based on the model $M = e^{-kt}$, where M is equal to the proportion of dry mass remaining at time t, and k is the exponential rate of decay (Olson 1963). When *k*-values for simple exponential decay were reported in the study, we used the values as calculated by the authors. If *k* values were not reported, we digitized scatterplots using xyscan software (version 4.1, Yale University) or time series with a minimum of 3 points, and calculated decay constants using the nlm function in R (R core team). For studies with experimental treatments (e.g. N addition), only control treatments were included. For studies that compared decomposition rates across successional gradients (natural or human-created) we included all *k*-values.

We recorded mean annual temperature (MAT) and mean annual precipitation (MAP) directly from the paper when it was reported. If a range was reported, we used the arithmetic mean. If these values were not available in the literature or from the study site (e.g. LTER websites or other papers), we used estimates of MAT and MAP from the Worldclim database (Fig. S1).

When available, we recorded initial root concentrations of N, P and Ca for all observations. We also recorded estimates of lignin concentrations, though methods varied by study, and we included proxies such as "acid insoluble," "acid unsoluble," and "acid resistant" fractions. We recorded nutrient ratios (e.g. C:N, lignin:N) as reported in the

papers. In cases where ratios were not reported but constituents were, we calculated the ratios based on reported values. In some cases, lignin concentrations were not reported, and were back calculated based on reported values for N concentrations and lignin:N ratios. For studies reporting nutrient concentrations and *k*-values by root order or diameter class we calculated species-level means across these values.

We categorized each species of fine root in by various relevant plant traits. Following the growth-form distinctions of Silver and Miya (2000), we categorized woody species as either broadleaf or conifer, and non-woody species as either graminoid or herbaceous. We classified species based on their phenology, separating woody plants into evergreen and deciduous (leaf lifespan), and non-woody plants into annual vs perennial life cycles. We assigned each woody species a mycotype of EcM, ErM, or AM based on the authors' designation in the original publication. When no mycotype was identified, we used the species-level designation from Maherali et al. (2016), followed by genus, then family level designations if species information was unavailable. We chose to classify species known to associate with both AM and EcM fungi as EcM in our analysis. This amounted to 38 observations, or <5% of our dataset. When these observations were treated as AM instead of EcM in our analyses the results of our mycotype analysis remained unchanged.

To assess the robustness of our species-level trait comparisons, we compiled a "conservative" dataset, which consisted of a subset of the larger dataset. Here, we restricted the *k*-values to experiments that used the buried-litter bag approach (i.e. removed studies which used sequential coring methods, soil blocks, etc.). We restricted the depth of burial to 0-20 cm mineral soil, excluding deep roots and those decomposed in the O horizons. We also removed all studies distinguishing root order. Finally, we averaged all *k*-values for each site at the species-level.

Table S1.1: Sample sizes for analyses based on plant functional groups.

Group	Sample size	
	Complete dataset	Conservative dataset
Woody	524	282
Herbaceous	173	111
Broadleaf (woody)	359	199
Conifer (woody)	165	83
Graminoid	129	85
Forb	44	26
Arbuscular Mycorrhizal (woody)	210	134
Ectomycorrhizal (woody)	282	135
Ericoid Mycorrhizal	31	12
Deciduous	223	120
Evergreen	301	162
Annual	27	18
Perennial	146	93

Figure S1.1a: Map of global mean annual temperature with approximate study locations depicted by black cross marks.

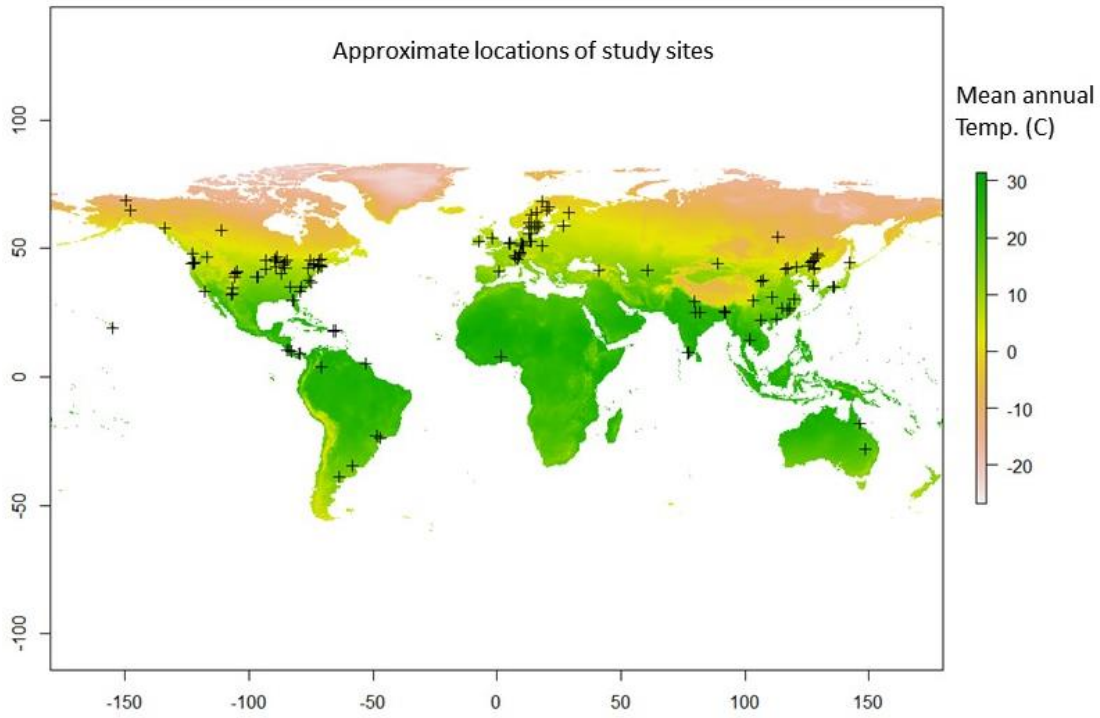

Appendix S1.1b: Histogram of study durations for the dataset. A single, 10-year study (LIDET) is not shown.

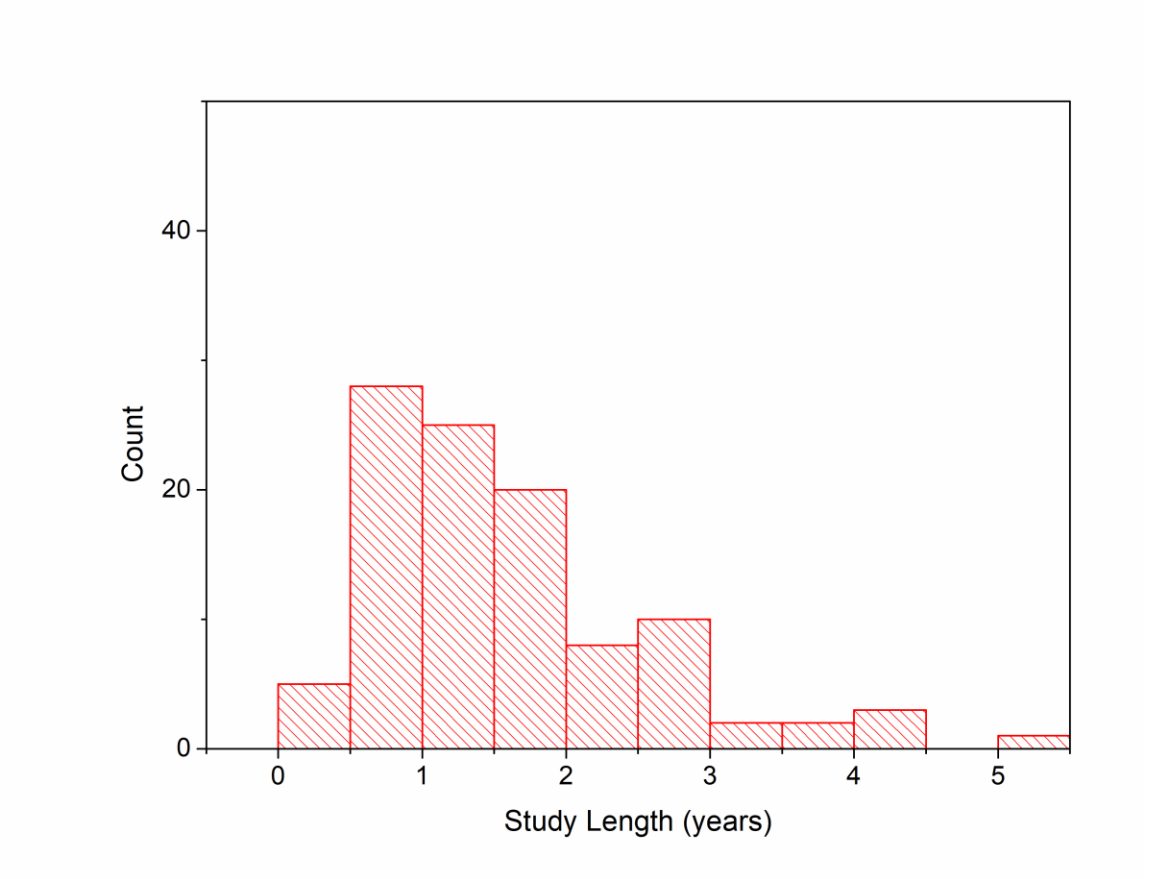

Appendix S1.1c: Scatterplot of climate characteristics at each study site where woody roots decomposed. Circles depict studies containing only AM roots, triangles indicate studies containing only EcM roots, and diamonds show studies that contain at least one of each mycotype. Studies including observations on ericoid species in addition to other species are shown as filled black circles.

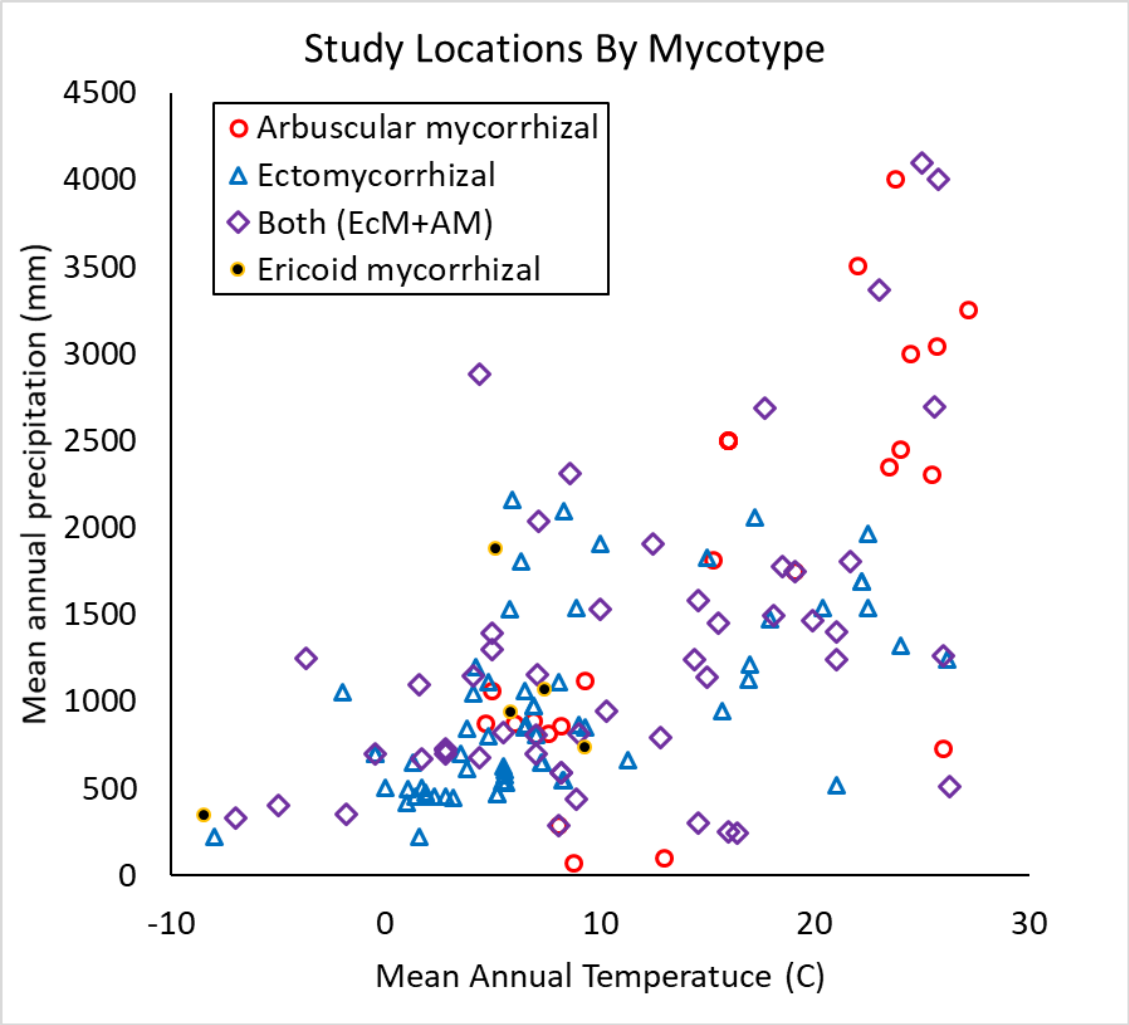

Appendix S1.2: Studies included in each analysis

Table S1.2 Studies included in our analyses. Potential biome is based on Whitaker (1975) given the MAP and MAT values for each study location.

Contributor	Species-level trait comparison		Climate and nutrient models	Within-site nutrient models				Potential biome
	Conser-vative	Com-plete		N	P	Ca	Lig-nin	
Aber et al. 1990	x	x	x					Temperate Forest
Andrén et al. 1992	x	x	x					Boreal
Arunachalam et al. 1996	x	x	x					Temperate Forest
Aulen et al. 2012		x		x			x	Temperate Forest
Bachega et al. 2016	x	x	x					Trop. Seasonal Forest
Barba et al. 2016	x	x	x	x				Shrubland/Savannah
Bauhus et al. 2004	x	x	x					Temperate Forest
Berg 1984	x	x	x		x	x		Temperate Forest
Berg et al. 1998		x	x					Temperate /Boreal
Birouste et al. 2012	x	x		x			x	Glasshouse
Bloomfield et al. 1993	x	x						Tropical Rainforest
Brechet et al. 2017	x	x	x					Tropical Rainforest
Burke and Raynal 1994	x	x	x	x	x	x		Temperate Forest
Camiré et al. 1991	x	x	x					Temperate Forest
Carrillo et al. 2014	x	x	x					Shrubland/Savannah
Chen et al. 2008	x	x	x				x	Temp. Rainforest
Chen et al. 2002	x	x	x	x				Temp. Rainforest
Conn and Day 1997	x	x	x					Shrubland/Savannah
de Miranda Mello et al. 2007	x	x	x					Trop. Seasonal Forest
Dong et al. 2016	x	x	x	x	x	x	x	Boreal
Dornbush et al. 2002	x	x	x	x			x	Temperate Forest
Fahey et al. 1988	x	x	x	x	x	x	x	Temperate Forest
Fan and Gou 2010		x	x					Boreal
Freschet et al. 2012	x	x	x					Boreal
Fujii et al. 2010	x	x	x					Temperate Forest
Fujimaki et al. 2008	x	x	x					Trop. Seasonal Forest
Gholz et al. 1986	x	x	x					Trop. Seasonal Forest
Gijsman et al. 1997	x	x	x	x		x		Trop. Seasonal Forest
Goebel et al. 2011		x	x					Shrubland/Savannah
GuerreroRamirez et al. 2016	x	x						Trop. Seas./Rainforest
Guo et al. 2006	x	x						Glasshouse
Heal et al. 1978	x	x	x					Temperate Forest

Heim and Frey 2004	x	x	x	x	x	x	x	Shrubland/Temp. For./Temp. Rainforest
Hobbie 1996	x	x		x			x	Glasshouse
Hobbie et al. 2010	x	x	x	x	x	x	x	Shrubland/Savannah
Jalota et al. 2006	x	x	x	x			x	Trop. Seasonal Forest
Jamro et al. 2015	x	x	x					Boreal
Jessy et al. 2013	x	x	x					Tropical Rainforest
Jha et al. 2014	x	x		x	x			Glasshouse
Jo et al. 2016	x	x	x	x			x	Temperate Forest
John et al. 2002	x	x	x					Temperate Forest
Jose et al. 2000	x	x	x					Shrubland/Savannah
Khamzina et al. 2015		x	x					Desert
Kou et al. 2015	x	x	x					Temperate Forest
Lai et al. 2016	x	x	x					Shrubland/Savannah
Lai et al. 2017	x	x	x					Shrubland/Savannah
Lehmann et al. 1995	x	x	x					Trop. Seasonal Forest
Li et al. 2010	x	x	x					Temperate Forest
Li et al. 2015	x	x	x					Temperate Forest
Li et al. 2016	x	x	x					Shrubland/Savannah
LIDET	x	x	x					All
Lin et al. 2011	x	x	x	x	x		x	Temperate Forest
Lin et al. 2015	x	x	x					Temperate Forest
Liu et al. 2009	x	x	x					Shrubland/Savannah
Lohmus and Ivask 1995	x	x	x					Shrubland/Savannah
Ludovici et al. 2006	x	x	x					Temperate Forest
Luo et al. 2016	x	x	x					Shrubland/Savannah
Ma et al. 2016		x						Glasshouse
Makita et al.2015	x	x	x	x	x	x	x	Temperate Forest
Fujii et al. 2015	x	x	x					Temperate Forest
McClaugherty et al. 1982		x	x					Temperate Forest
McClaugherty et al. 1984	x	x	x					Temperate Forest
McLaren et al. 2017	x	x	x					Tundra
Moore et al. 2007	x	x	x	x				Temperate Forest
Moretto et al. 2001	x	x	x					Shrubland/Savannah
Moretto et al. 2003	x	x	x					Shrubland/Savannah
Mun and Whitford 1998	x	x	x	x			x	Desert
Olajuyigbe et al. 2012	x	x	x					Shrubland/Savannah
Ostertag and Hobbie 1999	x	x	x	x	x		x	Temp. Rainforest

Palviainen et al. 2004	x	x	x					Shrubland/Savannah
Parker et al. 1984	x	x	x					Desert
Puttesepp et al. 2007	x	x	x					Temperate Forest
Raich et al. 2009		x	x					Tropical Rainforest
Robertson et al. 2015	x	x						Tropical Rainforest
Sanchez-de Leon et al. 2013	x	x	x					Shrubland/Savannah
Sariyildiz et al. 2015	x	x	x	x			x	Shrubland/Temp. Forest
Scheffer et al. 2000	X	x	x					Shrubland/Savannah
Scheu 1994		x	x					Shrubland/Savannah
Seastedt 1988	x	X	x					Shrubland/Savannah
Shen et al. 2017	x	x	x					Shrubland/Savannah
Silver and Vogt 1993	x	x						Tropical Rainforest
Singh 1989	x	x	x					Trop. Seasonal Forest
Solly et al. 2014	x	x	x					Shrubland/Temp. Forest
Solly et al. 2015	x	x	x					Shrubland/Temp. Forest
Song et al. 2017	x	x	x					Temperate Forest
Sun et al. 2013a		x	x					Boreal
Sun et al. 2013b		x	x					Boreal
Sun et al. 2015		x	x					Boreal
Sun et al. 2016		x	x	x	x	x	x	Boreal
Thormann et al. 2001	x	x	x					Temperate Forest
Tripathi and Singh 1992	x	x	x					Trop. Seasonal Forest
Tripathi et al. 2006	x	x	x					Temperate Forest
Tu et al. 2015	x	x	x					Temperate Forest
Usman et al. 2000	x	x	x					Trop. Seasonal Forest
Van Vuuren et al. 1993		x	x					Shrubland/Savannah
Vivanco et al. 2006	x	x	x	x	x			Shrubland/Savannah
Wang et al. 2010	x	x	x					Trop. Seasonal Forest
Wang et al. 2014	x	x	x					Temperate Forest
Xia et al. 2017	x	x	x					Temperate Forest
Xiong et al. 2013		x	x	x			x	Trop. Seasonal Forest
Xu et al. 2013	x	x	x					Trop. Seasonal Forest
Yang et al. 2004a	x	x	x					Temperate Forest
Yanget al. 2004b	x	x	x					Temperate Forest
Zhao et al. 2015	x	x	x					Desert
Zhou et al. 2015	x	x	x					Boreal

Appendix S1.3: Candidate models for climate effects on fine root decomposition. Parameters shown reflect fixed effects.

Formula: ln(k) ~ MAT + ln(duration) + (1 | Contributor)
AICc:1568 Marginal R^2: 0.22

Parameter	Estimate	Std Error	t value	P value
Intercept	-0.929	0.673	-1.380	0.17
MAT	0.052	0.005	9.491	<0.001
ln(duration)	-0.107	0.103	-1.035	0.30

Formula: ln(k) ~ ln(MAP) + ln(duration) + (1 | Contributor)
AICc:1609 Marginal R^2: 0.15

Parameter	Estimate	Std Error	t value	P value
Intercept	-1.797	0.848	-2.12	0.04
ln(MAP)	0.409	0.066	6.25	<0.001
ln(duration)	-0.315	0.110	-2.85	<0.01

Formula: ln(k) ~ MI + ln(duration) + (1 | Contributor)
AICc:1639 Marginal R^2: 0.10

Parameter	Estimate	Std Error	t value	P value
Intercept	0.974	0.715	1.36	0.17
MI	0.155	0.052	2.98	<0.01
ln(duration)	-0.345	0.112	-3.08	<0.01

Formula: ln(k) ~ MAT * ln(MAP) * MI + ln(duration) + (1 | Contributor)
AICc: 1599 Marginal R^2: 0.27

Parameter	Estimate	Std Error	t value	P value
Intercept	-1.26	1.406	-0.90	0.37
MAT	0.001	0.081	-0.01	0.99
ln(MAP)	0.213	0.191	0.64	0.53
MI	-1.487	1.034	-1.44	0.15
ln(duration)	-0.118	0.105	-1.12	0.27
MAT x ln(MAP)	0.004	0.012	0.35	0.73
MAT x MI	0.025	0.072	0.35	0.73

ln(MAP) x MI	0.175	0.134	1.31	0.19
MAT * ln(MAP) * MI	-0.002	0.009	-0.26	0.80

Formula: ln(k) ~ MAT * ln(MAP) + MI + ln(duration) + (1 | Contributor)
AICc: 1578 Marginal R^2: 0.24

Parameter	Estimate	Std Error	t value	P value
Intercept	-1.536	1.084	-1.42	0.16
MAT	-0.014	0.047	-0.30	0.76
Ln(MAP)	0.119	0.140	0.85	0.40
MI	-0.039	0.070	-0.55	0.58
ln(duration)	-0.121	0.104	-1.16	0.25
MAT x ln(MAP)	0.009	0.007	1.25	0.21

Formula: ln(k) ~ MAT + ln(MAP) * MI + ln(duration) + (1 | Contributor)
AICc:1572 Marginal R^2: 0.26

Parameter	Estimate	Std Error	t value	P value
Intercept	-1.833	0.913	-2.01	0.05
MAT	0.039	0.007	5.74	<0.001
ln(MAP)	0.195	0.101	1.93	0.05
MI	-1.335	0.738	-1.81	0.07
ln(duration)	-0.117	0.104	-1.12	0.26
ln(MAP) x MI	0.165	0.094	1.76	0.08

Formula: ln(k) ~ MAT *MI + ln(MAP) + ln(duration) + (1 | Contributor)
AICc: 1578 Marginal R^2: 0.25

Parameter	Estimate	Std Error	t value	P value
Intercept	-2.068	0.887	-2.33	0.02
ln(MAP)	0.220	0.098	2.23	0.03
MAT	0.033	0.009	3.48	<0.001
MI	-0.145	0.095	-1.52	0.13
ln(duration)	-0.123	0.105	-1.18	0.24

MI x ln(MAP)	0.009	0.006	1.62	0.11

Formula: ln(k) ~ MAT + MI + ln(MAP) + ln(duration) + (1 | Contributor)
AICc: 1569 Marginal R^2: 0.24

Parameter	Estimate	Std Error	t value	P value
Intercept	-2.35	0.865	-2.72	<0.01
ln(MAP)	0.245	0.097	2.53	0.01
MI	-0.040	0.070	-0.57	0.57
MAT	0.044	0.006	7.31	<0.001
ln(duration)	-0.123	0.104	-1.18	0.24

Formula: ln(k) ~ln(MAP) * MI + ln(duration) + (1 | Contributor)
AICc: 1593 Marginal R^2: 0.24

Parameter	Estimate	Std Error	t value	P value
Intercept	-1.250	0.956	-1.31	0.19
ln(MAP)	0.335	0.102	3.27	0.001
MI	-3.361	0.682	-4.93	<0.001
MI x ln(MAP)	0.413	0.087	4.74	<0.001
ln(duration)	-0.235	0.110	-2.15	0.03

Formula: ln(k) ~MAT * MI + ln(duration) + (1 | Contributor)
AICc: 1577 Marginal R^2: 0.24

Parameter	Estimate	Std Error	t value	P value
Intercept	-0.822	0.688	--1.19	0.23
MAT	0.036	0.009	3.82	<0.001
MI	-0.057	0.087	-0.66	0.51
ln(duration)	-0.113	0.104	-1.08	0.28
MI x MAT	0.011	0.006	2.01	0.05

Formula: ln(k) ~MAT * ln(MAP) + ln(duration) + (1 | Contributor)
AICc: 1573 Marginal R^2: 0.24

Parameter	Estimate	Std Error	t value	P value

Intercept	-1.332	1.017	-1.31	0.19
MAT	-0.014	0.047	-0.30	0.77
ln(MAP)	0.079	0.120	0.66	0.51
ln(duration)	-0.120	0.104	-1.16	0.25
MI x ln(MAP)	0.009	0.007	1.26	0.21

Formula: ln(k) ~MAT + ln(MAP) + ln(duration) + (1 | Contributor)
AICc: 1565 Marginal R^2: 0.24

Parameter	Estimate	Std Error	t value	P value
Intercept	-2.147	0.786	-2.73	<0.01
MAT	-0.045	0.006	7.59	<0.001
ln(MAP)	0.205	0.067	3.04	<0.01
ln(duration)	-0.122	0.103	-1.18	0.24

Formula: ln(k) ~MAT + MI + ln(duration) + (1 | Contributor)
AICc: 1572 Marginal R^2: 0.23

Parameter	Estimate	Std Error	t value	P value
Intercept	-1.000	0.675	-1.48	0.14
MAT	0.051	0.006	9.12	<0.001
MI	0.087	0.049	1.77	0.08
ln(duration)	-0.111	0.103	-1.08	0.28

Formula: log(k) ~ln(MAP) + MI + ln(duration) + (1 | Contributor)
AICc: 1610 Marginal R^2: 0.16

Parameter	Estimate	Std Error	t value	P value

Intercept	-2.605	0.940	-2.77	<0.01
ln(MAP)	0.551	0.094	5.86	<0.001
MI	0.152	0.073	-2.08	0.04
ln(duration)	-0.307	0.112	-2.74	<0.01

Appendix 1.4: Correlations among predictor variables.

Pearson correlation coefficients among mean annual temperature (MAT), mean annual precipitation (MAP), and initial fine-root chemistry in our complete dataset. Values in bold represent significance at $P \leq 0.05$.

	MAT	MAP	N	P	Ca	Lignin
MAT	1	**0.59**	**-0.16**	**-0.36**	**-0.24**	-0.03
MAP	**0.59**	1	-0.04	**-0.33**	**-0.24**	**0.17**
N	**-0.16**	-0.04	1	**0.58**	**0.58**	-0.05
P	**-0.36**	**-0.33**	**0.58**	1	**0.56**	**-0.21**
Ca	**-0.24**	**-0.24**	**0.58**	**0.56**	1	**-0.21**
Lignin	-0.03	**0.17**	-0.05	**-0.21**	**-0.21**	1

Appendix S1.5: Standardized slopes of carbon:nutrient ratios

Within sites, fine-root decomposition rates were consistently negatively correlated with the ratios of lignin:N, C:N, and C:P. There was no consistent relationship between lignin:P and the of fine-root decomposition rate; however, the sample size was limited because there were few studies reporting both lignin and P. Plot depicts the mean of the standardized coefficient (slope) among studies containing at least 5 observations. Error bars depict 95% confidence intervals.

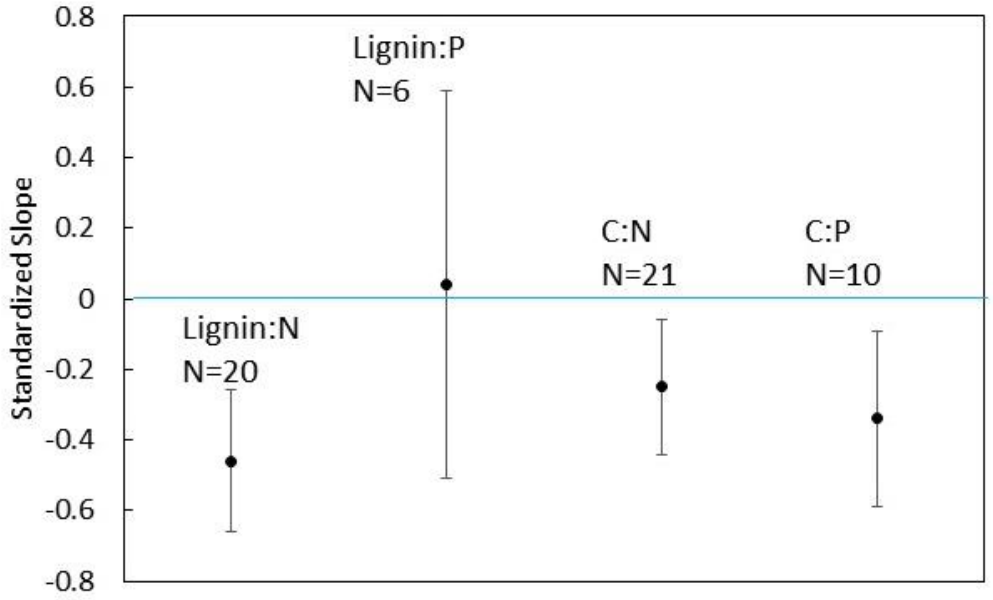

Appendix S1.6: Comparison of models and datasets

Table S1.6a: Natural log response ratios comparing the effects of various plant functional groups on fine-root decomposition rates (*k*-values). Ratios are shown for two different linear mixed-effects models, run on both the complete and conservative datasets described in Appendix 1, with results arranged from left to right corresponding to the least to the most conservative. Random intercept models contain a single random effect (intercept) for the effect of each study on mean the *k*-value. Random intercept and coefficient models contain an additional random effect (coefficient) that assumes that the magnitude of differences among categories (e.g. woody vs. herbaceous) varies randomly across studies. The ln response ratios were calculated as the difference among groups in ln-transformed *k*-values with 95% confidence intervals shown in parentheses. Asterisks signify statistical significance, with * denoting $P \leq 0.05$, ** denoting ≤ 0.01, and *** denoting $P \leq 0.001$.

		Random intercept only		**Random intercept and coefficient**	
Criterion	**Group**	**Complete dataset**	**Conservative dataset**	**Complete Dataset**	**Conservative dataset**
Woodiness (relative to herbaceous plants)	Woody	**-0.59 (0.16)*** **	**-0.58 (0.24)*** **	**-0.45 (0.30)** **	**-0.39 (0.34)***
Growth form (relative to woody broadleaf plants)	Conifer	**-0.25 (0.14)*** **	**-0.52 (0.23)*** **	-0.16 (0.18)	-0.24 (0.32)
	Graminoid	**0.39 (0.15)*** **	**0.34 (0.26)** **	0.24 (0.30)	0.18 (0.28)
	Forb	**1.29 (0.27)*** **	**0.77 (0.52)** **	**0.92 (0.42)*** **	**0.62 (0.54)***
Mycotype (relative to AM; woody species only)	EcM	**-0.38 (0.14)*** **	**-0.61 (0.24)*** **	**-0.29 (0.20)** **	**-0.47 (0.36)***
	ErM	**-0.80 (0.35)*** **	**-0.78 (0.78)***	**-0.72 (0.52)***	-0.71 (1.04)
Life cycle (relative to annuals; herbaceous plants only)	Perrenial	**-0.49 (0.48)***	-0.38 (0.40)	-0.20 (1.10)	-0.22 (0.96)
Leaf habit (relative to deciduous; woody plants only)	Evergreen	**-0.15 (0.15)***	-0.13 (0.32)	-0.15 (0.16)	-0.11 (0.34)

Table S1.6b: Mean *k*-values by functional group. Means are shown for the complete and a conservative dataset as shown in Table S2, with 95% confidence intervals given in parentheses. Note that because these are the means from the raw dataset, not the mixed-model results presented in Table S1.6a, the mean *k*-value for graminoids is lower than for broadleaf plants.

Criterion	Group	Complete dataset	Conservative dataset
Woodiness	Woody	0.83 (0.13)	1.23 (0.25)
	Herbaceous	1.27 (0.28)	1.33 (0.40)
Growth form	Forb	2.66 (0.82)	3.70 (1.28)
	Graminoid	0.80 (0.23)	0.67 (0.16)
	Broadleaf	1.05 (0.18)	1.64 (0.32)
	Conifer	0.37 (0.06)	0.29 (0.07)
Mycotype	AM	1.54 (0.28)	2.18 (0.44)
(Woody species only)	EcM	0.93 (0.06)	0.32 (0.06)
	ErM	0.17 (0.12)	0.44 (0.46)
Life cycle	Annual	2.11 (0.81)	2.88 (1.14)
	Perennial	1.07 (0.32)	1.01 (0.38)
Leaf lifespan	Deciduous	1.40 (0.28)	2.33 (0.49)
(Woody species only)	Evergreen	0.42 (0.06)	0.42 (0.08)

Appendix S1.7: Fine root chemistry by functional group

Figure S1.7a: Mean root chemical traits by growth form. Groups not sharing a letter differ significantly at $\alpha = 0.05$ based on Tukey's HSD test.

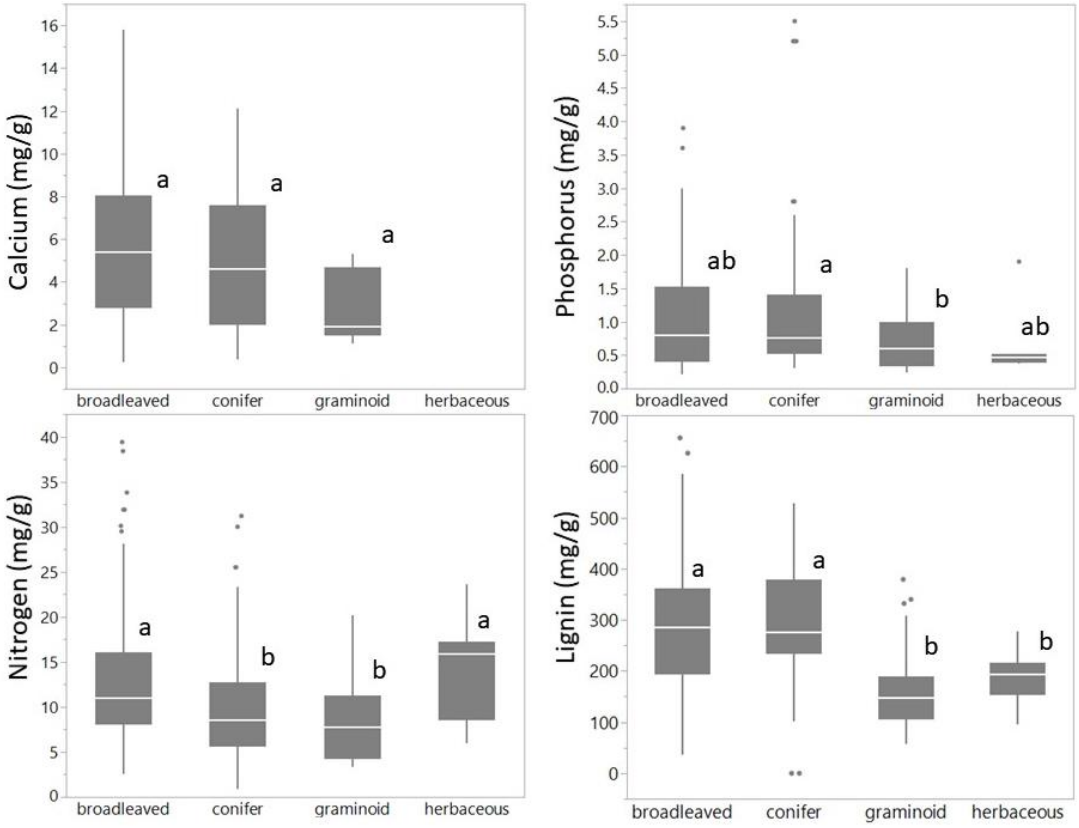

Figure S1.7b: Mean root chemical traits by mycorrhizal type. Groups not sharing a letter differ significantly at $\alpha = 0.05$ based on Tukey's HSD test.

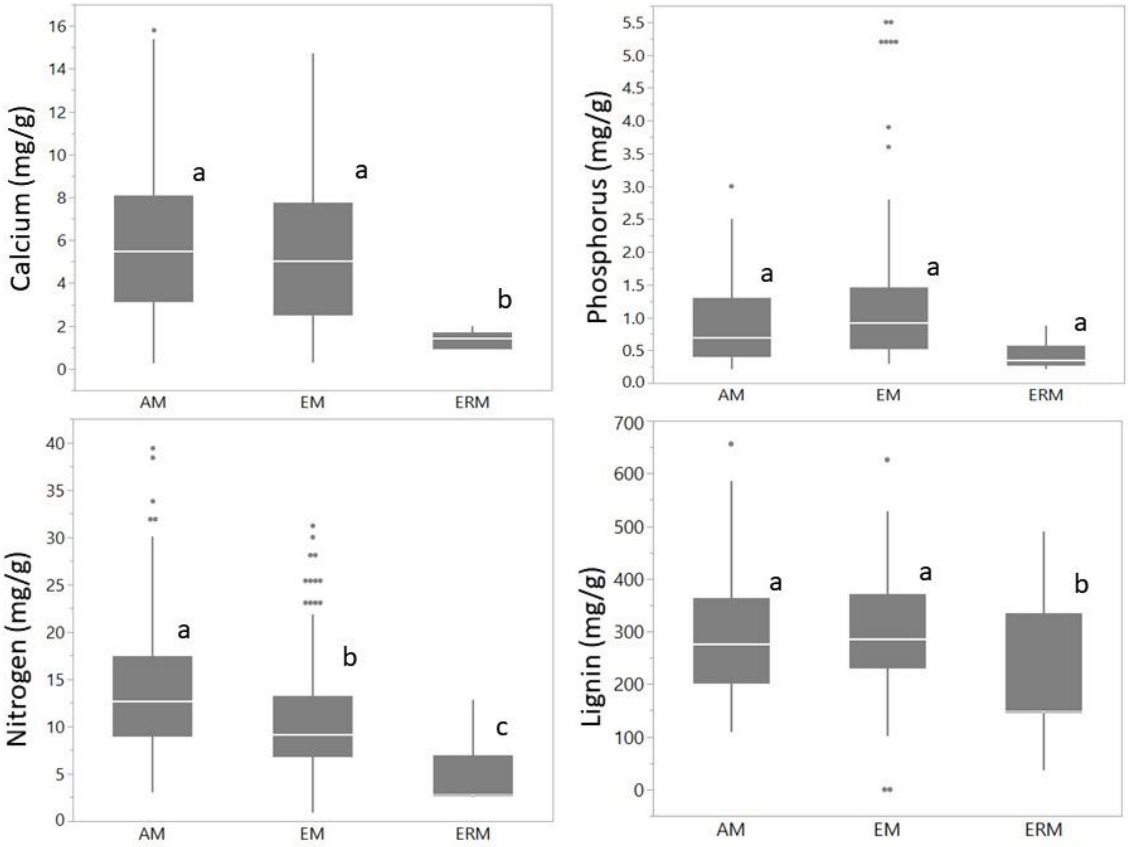

Figure S1.7c: Mean root chemical traits by woodiness. Groups not sharing a letter differ significantly at $\alpha = 0.05$ based on Tukey's HSD test.

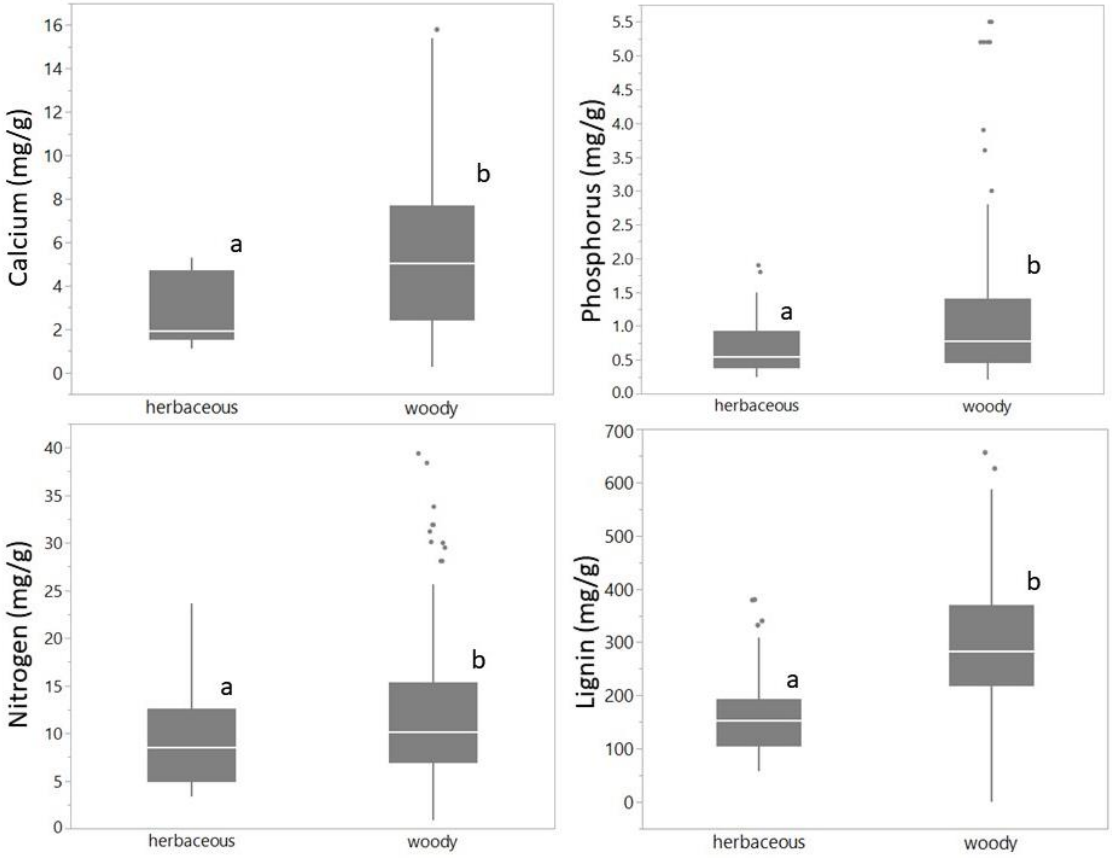

Appendix S2.1

Wavenumber, bond, chemical functional group, and fungal compound assignments for FTIR spectra.

Wavenumber (cm^{-1})	Bond	Functional group	Associated fungal compounds
840	C-H	Aromatic	Melanin
920	C-H	Alkene	Pigments; lipids
1080	C-O	Alcohol	Polysaccharides (α-glucan; β-glucan; Chitin; Glycogen)
1160	C-O	Alcohol	Polysaccharides (α-glucan; β-glucan; Chitin; Glycogen)
1234	C-O	Aromatic	Melanin
1550	N-H	Amide	Proteins
1650	C=O	Amide	Proteins
2850	C-H	Aliphatic	Lipids
2924	C-H	Aliphatic	Lipids

Appendix S2.2

Pearson correlation coefficients representing the relationship between variables. Numbers in bold represent relationships significant at $P<0.05$.

	A	K	Cell sols.	Acid Det.	Acid Hyd.	Acid Non-hyd.	%C	%N	C:N	840 Arom.	920 Alkene	1080 Alc.	1160 Alc.	1234 Ester	1550 Amide	1650 Amide	2850 Aliph.	2924 Aliph.	Mel-anin
A	1.00	-0.25	-0.29	-0.02	0.05	**0.54**	0.23	-0.13	0.16	-0.21	-0.02	0.18	0.13	0.35	0.02	-0.07	0.33	0.35	**0.47**
K		**1.00**	**0.75**	**-0.59**	**-0.44**	-0.34	0.06	**0.44**	-0.10	0.23	-0.11	**-0.40**	**-0.69**	-0.16	**0.45**	**0.47**	-0.16	-0.20	-0.07
Cell solubles			**1.00**	**-0.67**	**-0.79**	-0.34	0.05	0.14	0.09	**0.44**	0.06	-0.23	**-0.63**	-0.17	0.26	0.22	-0.27	-0.22	0.10
Acid Detergent				**1.00**	**0.42**	-0.24	-0.35	-0.18	0	-0.21	0.16	0.34	**0.42**	-0.16	-0.33	-0.28	-0.13	-0.20	**-0.43**
Acid Hyd.					**1.00**	-0.05	-0.16	-0.11	-0.03	**-0.44**	-0.15	0.18	**0.45**	-0.05	-0.24	-0.22	0.15	-0.01	-0.12
Acid Non-hyd.						**1.00**	**0.47**	0.05	-0.15	-0.14	-0.13	-0.12	0.27	**0.57**	0.13	0.11	**0.50**	**0.65**	**0.41**
%C							**1.00**	0.24	-0.18	**-0.41**	**-0.53**	**-0.58**	-0.18	**0.56**	0.21	0.27	**0.72**	**0.78**	**0.40**
%N								**1.00**	**-0.82**	-0.13	-0.32	**-0.70**	-0.28	0.33	**0.80**	**0.83**	**0.37**	0.34	-0.17
C:N									**1.00**	0.31	0.30	**0.51**	0.07	-0.21	**-0.48**	**-0.54**	**-0.46**	**-0.41**	0.23
840 Aromatic										**1.00**	**0.54**	0.31	0.08	-0.19	0.03	-0.03	**-0.73**	**-0.51**	0.07
920 Alkene											**1.00**	**0.78**	0.32	-0.21	-0.35	**-0.37**	**-0.44**	-0.32	-0.09
1080 Alcohol												**1.00**	**0.50**	-0.33	**-0.69**	**-0.73**	**-0.45**	**-0.42**	0.01
1160 Alcohol													**1.00**	0.28	-0.30	-0.24	-0.02	0.09	0.02
1234 Ester														**1.00**	**0.52**	**0.52**	**0.62**	**0.76**	**0.37**
1550 Amide															**1.00**	**0.95**	0.29	0.32	-0.03
1650 Amide																**1.00**	0.31	0.36	-0.10
2850 Aliphatic																	**1.00**	**0.93**	0.30
2924 Aliphatic																		**1.00**	**0.39**
Melanin																			**1.00**

Appendix S2.3

Comparisons of the exponential decomposition rate (*k*), and size of the recalcitrant fraction (*A*) by tissue type (spore-containing vs spore-free), trophic mode, and taxonomic order. Groups sharing a letter do not differ significantly at p<0.05. Trophic mode does not have a clear effect on *k* ($F_{2,25}$=2.08, P=0.15) or *A* ($F_{2,25}$=0.78, P=0.45). Similarly, we do not detect a difference between spore-containing and spore-free substrates in either *k* ($F_{2,25}$=0.11, P=0.74) or *A* ($F_{2,25}$=0.33, P=0.57). The size of the *A*-value differs among taxonomic orders ($F_{2,25}$=7.28, P<0.001), with members of the order Polyporales having a smaller-sized slow pool than members of Agaricales, Boletales, and Russulales. Camarops petersii, the sole member of the order Boliniales in this dataset, has the largest A-value of any sample. There are relatively weak differences in k-values across taxonomic orders ($F_{2,25}$=2.76, P=0.052), driven by slower decomposition from taxa in the Russulales than in Agaricales.

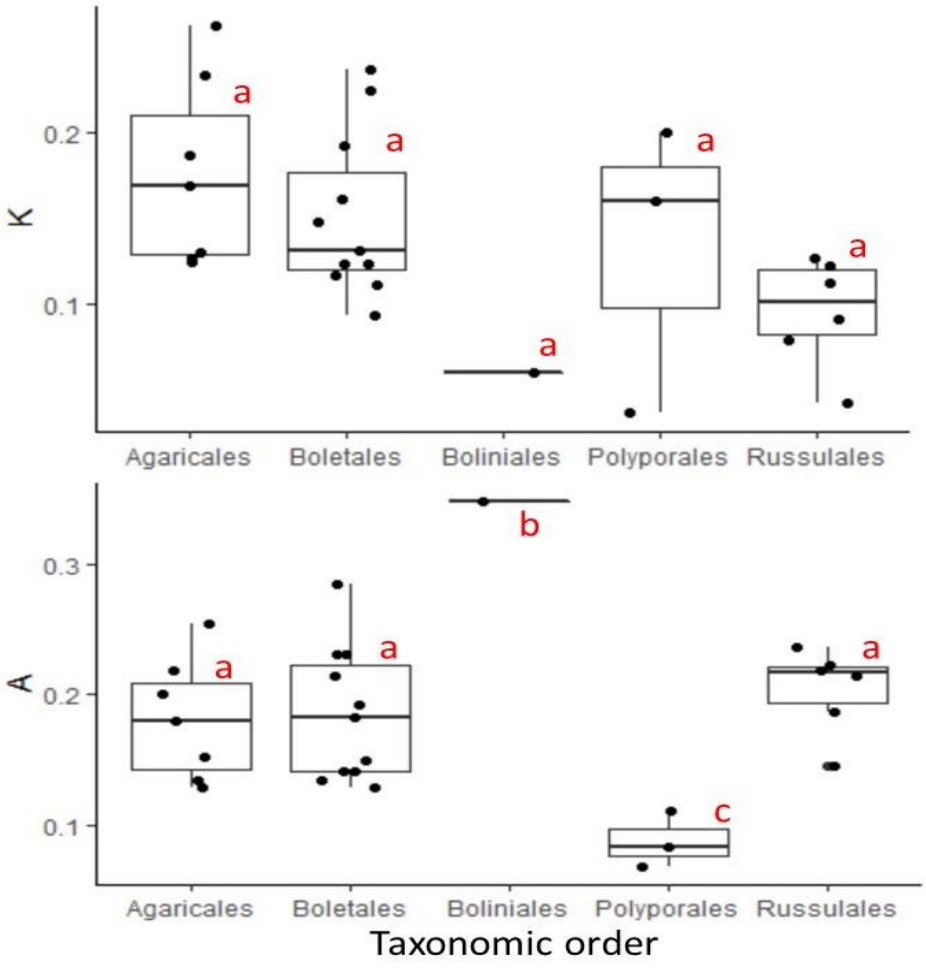

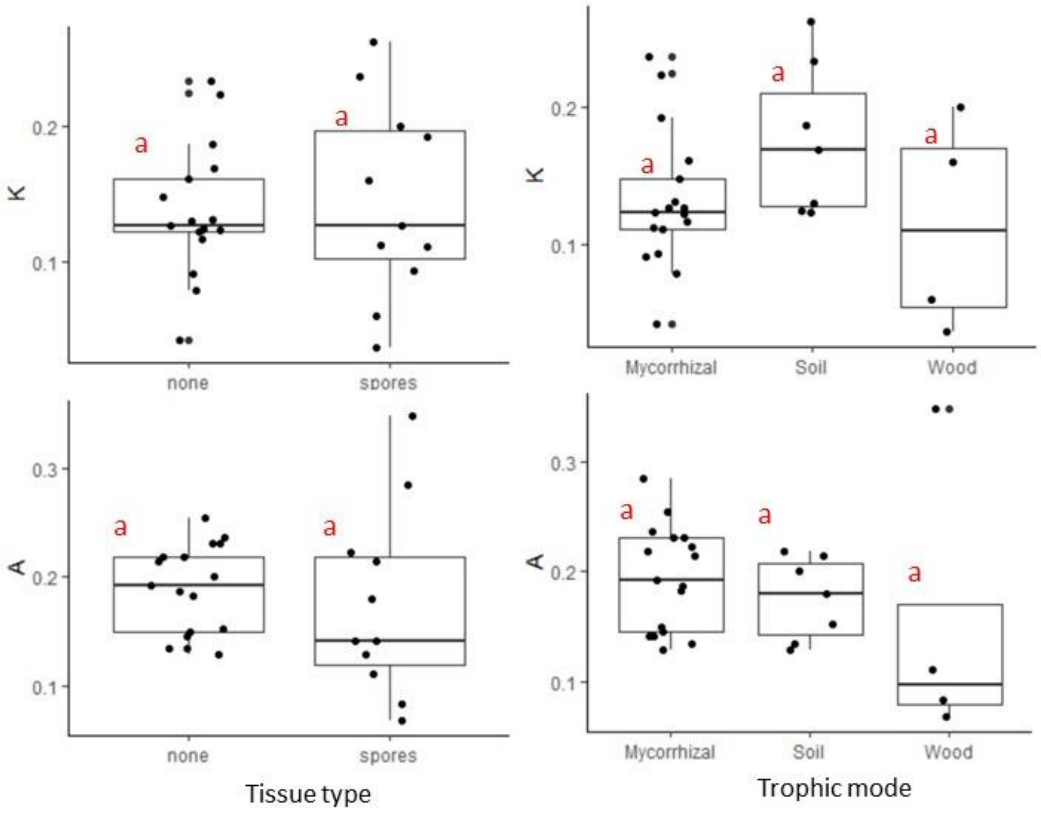
K
A
a
0.1
0.2
0.3
none
spores
Tissue type
Mycorrhizal
Soil
Wood
Trophic mode

Appendix S2.4

Final models predicting the exponential decomposition rate (*k*), and recalcitrant fraction (*A*) of fungal necromass based on initial substrate chemistry. Models were selected using AIC based on a stepwise procedure using backward selection.

```
Call:
lm(formula = A ~ Melanin + Acid.NonHyd, data = data3)

Residuals:
      Min        1Q    Median        3Q       Max
-0.091829 -0.036088  0.003349  0.026345  0.106176

Coefficients:
             Estimate Std. Error t value Pr(>|t|)
(Intercept)  0.137757   0.018071   7.623  5.6e-08 ***
Melanin      0.005608   0.003226   1.739   0.0944 .
Acid.NonHyd 0.005476   0.002304   2.377   0.0254 *
---
Signif. codes:  0 ‘***’ 0.001 ‘**’ 0.01 ‘*’ 0.05 ‘.’ 0.1 ‘ ’ 1

Residual standard error: 0.05118 on 25 degrees of freedom
Multiple R-squared:  0.3654,   Adjusted R-squared:  0.3147
F-statistic: 7.198 on 2 and 25 DF,  p-value: 0.003397


Call:
lm(formula = data4$K ~ data4$Cell.solubles + data4$X.N)

Residuals:
      Min        1Q    Median        3Q       Max
-0.066042 -0.030200  0.006635  0.020539  0.061812

Coefficients:
                       Estimate Std. Error t value Pr(>|t|)
(Intercept)           -0.1417386  0.0415566  -3.411  0.00221 **
data4$Cell.solubles    0.0042938  0.0007082   6.063 2.46e-06 ***
data4$X.N              0.0088844  0.0030226   2.939  0.00698 **
---
Signif. codes:  0 ‘***’ 0.001 ‘**’ 0.01 ‘*’ 0.05 ‘.’ 0.1 ‘ ’ 1

Residual standard error: 0.03395 on 25 degrees of freedom
Multiple R-squared:  0.6719,   Adjusted R-squared:  0.6457
F-statistic:  25.6 on 2 and 25 DF,  p-value: 8.901e-07
```

Appendix S2.5

Regressions predicting the size of the slowly decomposing necromass pool (*A*) based on initial substrate melanin concentrations and acid non-hydrolysable fractions. Regressions were calculated using the subsets of the upper and lower half of the predictor variable range. Neither melanin nor the non-hydrolysable fraction significantly predicts *A* at low concentrations.

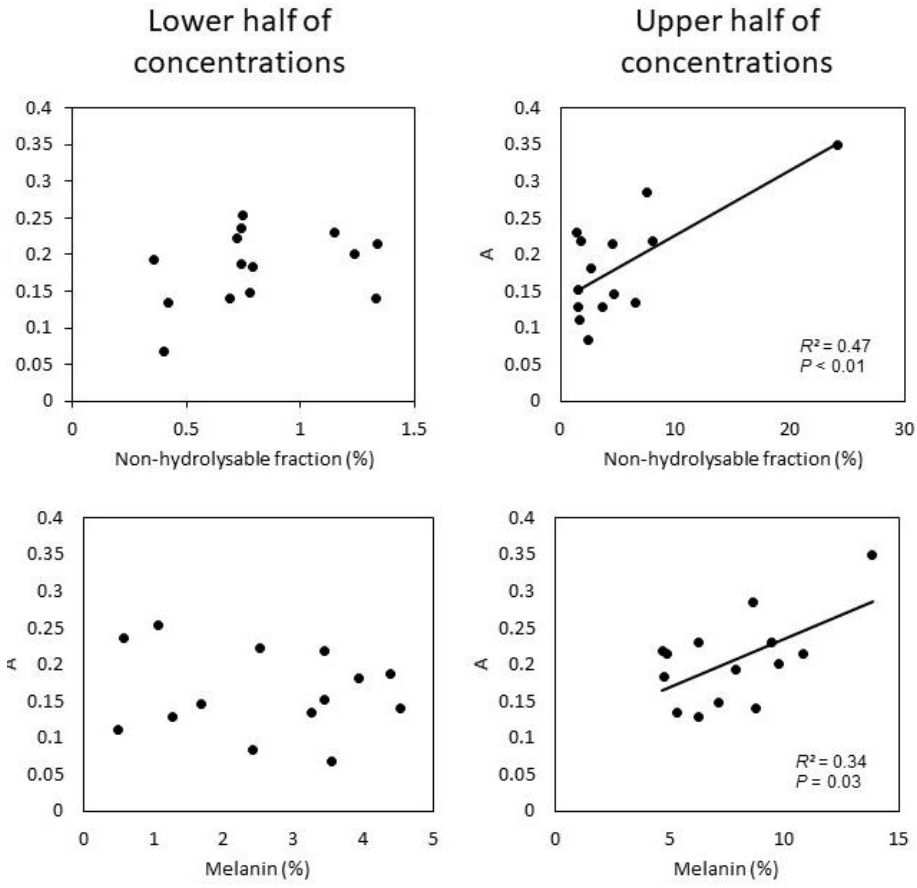

Appendix S2.6

Left: simple linear regressions predicting FTIR wavenumber 2924 cm^{-1} (aliphatic bonds) using the acid non-hydrolysable fraction and melanin content as predictor variables for 28 types of fungal necromass. Right: slopes are not statistically significant when the same regressions are conducted without a single highly leveraged point (*Camarops petersii)*.

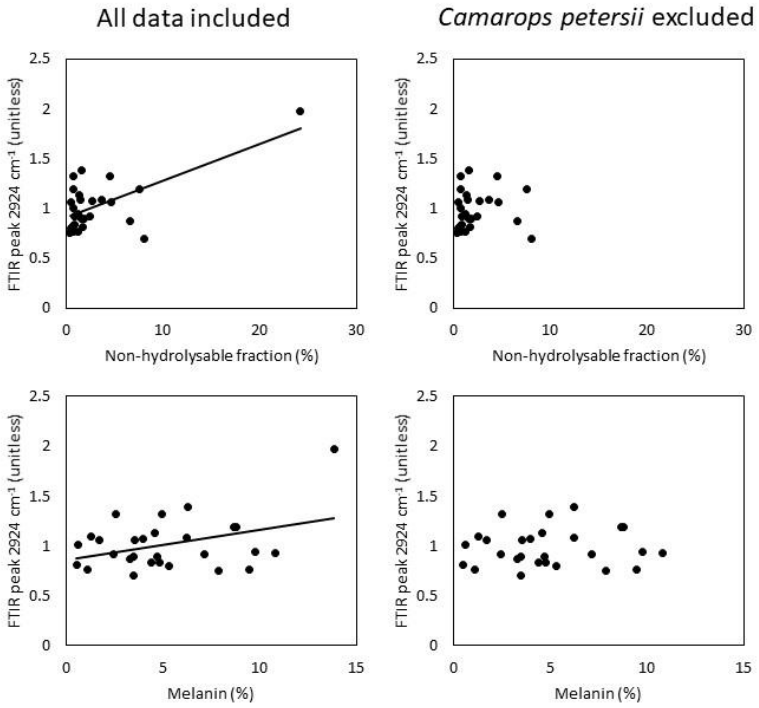

Appendix S2.7 (a) The proportion of initial N as a function of initial mass remaining for five substrates of decomposing fungal necromass. **(b)** The maximum initial N remaining for each of the five substrates as a function of the initial N concentration.

a.

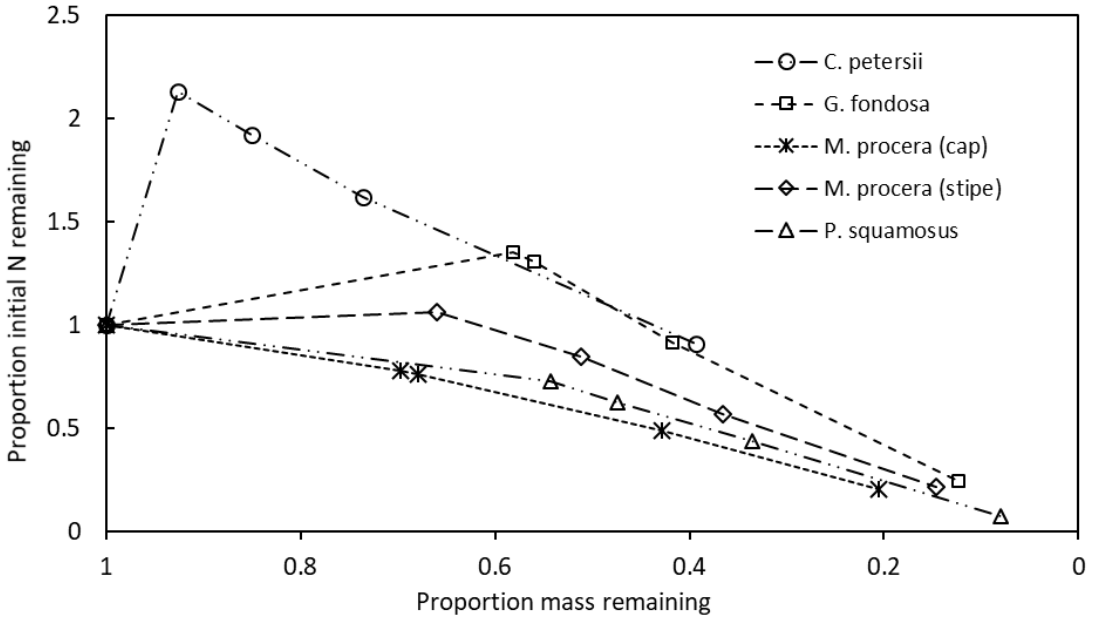

b.

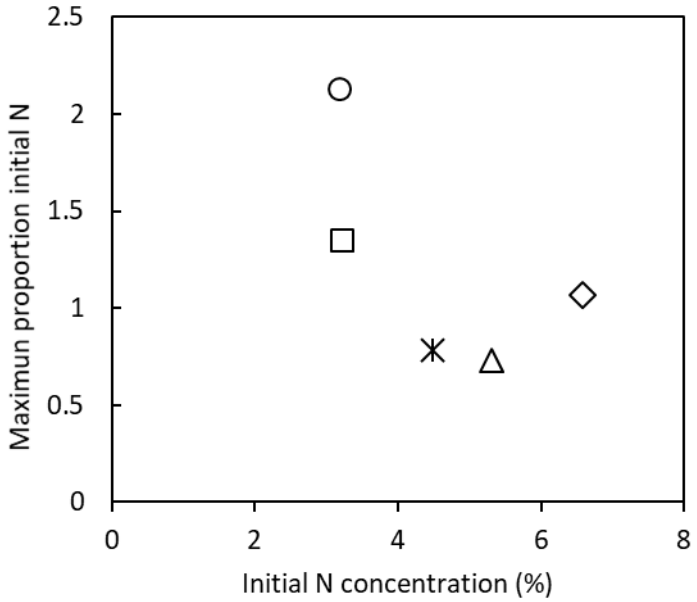

Appendix S2.8 Chemical fractions for 28 fungal necromass residues. All fractions are expressed as a percentage of dry mass.

Species	Tissue	Cell soluble	Acid Deter-gent	Acid Hydro-lysable	Non-Hydro-lysable	Total C	Total N	C:N ratio	Melanin
Boletus campestris	stipe	71.4	13.5	13.9	0.8	44.1	1	44	4.8
Boletus pseudosensibilis	stipe	63.6	18.6	16.1	1.5	43.9	6.5	7	6.2
Boletus pseudosensibilis	cap	71	17.2	9.9	1.5	45.8	7.9	6	6.2
Camarops petersii	sporocarp	48.2	11.8	15.6	24.2	49.4	3.2	16	13.8
Chlorophyllum molybdites	cap	62.5	16.1	18.4	2.7	43.9	9.6	5	3.9
Chlorophyllum molybdites	stipe	58.2	17.5	22.2	1.8	43.1	7	6	4.7
Gomphidius glutinosus	stipe	52.6	16.3	29.3	1.3	41.5	1.7	24	10.8
Grifola frondosa	sporocarp	58.5	17.5	22.1	1.6	44.1	3.2	14	0.5
Hygrocybe punicea	stipe	65.6	19.4	13	1.6	41.7	3.6	12	3.4
Hygrophorus paludosoides	stipe	68.1	19.2	11.1	1.2	42.4	1.9	22	9.7
Laccaria spp.	stipe	57.7	20.8	13	8.1	40.6	2.2	19	3.4
Lactarius chelodonius	stipe	55.5	24.9	18.5	0.7	43.0	2.7	16	4.4
Lactarius chelodonius	cap	55.9	20	19.3	4.5	44.2	4	11	4.9
Lactarius vinaceorufescens	stipe	34.4	30.5	30.2	4.6	42.0	2.2	19	1.7
Laetiporus sulphureus	sporocarp	45.9	28.1	25.2	0.4	43.7	3.5	12	3.5
Leccinum spp.	stipe	64.3	14	20.9	0.4	41.7	1.5	28	7.9
Macrolepiota procera	stipe	61.3	14.3	17.6	6.6	42.3	4.5	9	3.3
Macrolepiota procera	cap	57.8	18.3	20	3.6	44.0	6.6	7	1.3
Polyporus squamosus	sporocarp	60	20.1	17.3	2.4	43.9	5.3	8	2.4
Rhizopogon ochraceorubens	sporocarp	55.4	16.2	26.7	1.3	45.0	2.9	16	4.5
Russula spp.	stipe	53.2	27.4	18.3	0.7	43.1	3.2	13	0.6
Russula spp.	cap	50	25.2	23.7	0.7	44.3	3.7	12	2.5
Scleroderma spp.	sporocarp	41.2	22.9	28	7.5	44.8	5	9	8.6
Suillus grisellus	stipe	52.7	25.4	20.4	1.2	44.7	1.4	33	9.4
Suillus spectabilis	stipe	69	18.6	11.6	0.4	43.8	1.7	25	5.3
Suillus spectabilis	cap	76.7	9.4	12.9	0.7	46.9	3.9	12	8.8
Suillus viscidus	stipe	58.4	20.8	19.6	0.8	43.2	2.1	21	7.1
Tricholoma spp.	stipe	54.2	24	20.7	0.8	43.2	1.6	27	1.1

Appendix S3.1

Methods of and summarized data for calculations of hyphal length density estimates

Literature search and data inclusion criteria:

On January 25, 2021 we conducted literature searches using Web of Science and Google Scholar using the following search terms: "hypha* length density", "arbuscular mycorrhiza* length", "AMF length", "ectomycorrhiza length", "ECM length". From this, we included all field-based studies (i.e. excluded greenhouse or potted plant studies) that reported quantitative measurements of hyphal length density (HLD) per unit of soil mass or volume. Mass-based estimates were converted to volume using bulk density estimates when reported in the paper. When bulk density was not reported, we used site specific estimates from other papers, and if none were available, used an assumed density of 1.33. We further excluded measurements not taken in the top 30 cm of soil, and measurements that were explicitly collected to soil adhering to roots (i.e. rhizosphere soil). This resulted in 197 observations. We averaged all within-site observations (e.g. across depths, plots, seasons) resulting in 41site level-means across 40 published studies. We differentiated between studies which exclusively quantified AM hyphae, and those which quantified all hyphae present. We further classified the systems into woody (forest, shrubland), non-woody (grasslands/rangelands) and croplands. A summary of site-level means is presented in the table below.

	AMF hyphae only			All hyphae		
Data Source	Cropland systems	Woody systems	Non-woody systems	Cropland systems	Woody Systems *	Non-woody systems
Bardgett et al. 1993.						61809
Camenzind and Rillig 2013		330				
Chen et al. 2018			1296			
Chen et al. 2014			213			
Curaqueo et al. 2010	633					
Faghihinia et. al 2020			584			
Gryndler et al. 2006.	110					
Li et al. 2015			337			
Li et al. 2017	147					
Liu et al. 2006					1800 1650	
Liu et al. 2014	224					
	493					
Miller et al. 1995			11100			
			8100			

Nilsson and Rulcker 1992					71250	
Querejeta et al. 2007					13600	3850
Ren et al. 2018			519			
Soderstrom 1978					857500	
Stahl and Parkin 1996				2000 3100 4800	8300 9800	6400 23900
Tian et al. 2011	172					
Wang et al. 2012		106				
Wang et al. 2015		128				
Wang et al. 2018			754			
Wang et al. 2011		619				
Xiang et al. 2014	265		353			
Yang et al. 2017		9113				
Zhang et al. 2016a			1476 1488 776 551 524			
Zhang et al. 2016b			1530			
Mean	29202	205939	197332	330000	13770000	2398986
Standard deviation	19613	394865	317878	141067	31833149	2674163

*Estimates of total hyphae in woody systems are from ingrowth cores which predominantly measure ectomycorrhizal fungi. These systematically underestimate total hyphal length density due to underrepresentation of saprotrophs.

Appendix S3.2

Global estimates of fine root turnover from the Fine Root Ecology Database (FRED) classified by growth form according to the TRY plant trait database (mean ± s.d.).

Woody species		Non-woody species	
Growth Form	Turnover (yr^{-1})	Growth Form	Turnover (yr^{-1})
shrub	0.93 ± 1.13	graminoid	0.61 ± 0.54
shrub/tree	2.16 ± 1.46	herb	0.26 ± 0.16
tree	0.81 ± 1.19		
mean	0.89 ± 1.23	mean	0.58 ± 0.52
Mean across all species = 0.82 ± 1.11			